IMPACT OF CLIMATE CHANGE ON SURFACE WATER AVAILABILITY IN THE MOJO RIVER CATCHMENT

ERGETIE TILAYE WONDMAGEGN

IN PARTIAL FULFILMENT OF THE REQUIRMENTS FOR THE DEGREE OF MASTER OF SCIENCE SPECIALIZATION IN IRRIGATION AND DRAINAGE ENGINEERING

February, 2018

IMPACT OF CLIMATE CHANGE ON SURFACE WATER AVAILABILITY IN THE MOJO RIVER CATCHMENT

A THESIS SUMMITED TO THE

SCHOOL OF WATER RESOURES ENGINEERING,

INSTITUTE OF TECNOLOGY

HAWASSA UNIVERSITY

HAWASSA, ETHIOPIA

February-2018

HAWASSA, ETHIOPIA

DECLARATION AND COPY RIGHT

I, Ergetie Tilaye Wondmagegn, declare this M.Sc. thesis is my original work and that it has not been presented to any other university and all sources of materials used in this thesis has been duly acknowledge.

Ergetie Tilaye Wondmagegn	_____	_____
Name of Candidate	Signature	Date

ADVISOR"S APPROVAL SHEET

This is to certify that the thesis entitled "IMPACT OF CLIMATE CHANGE ON SURFACE WATER AVAILABILITY AT MOJO RIVER CACHMENT**"** submitted in partial fulfillment of the requirements for the degree of master's with specialization in Irrigation and Drainage Engineering, the Graduate Program of the School Of Water Resources Engineering Institute of Technology School of Graduate Studies, Hawassa University and has been carried out by Ergetie Tilaye Wondmagegn ID.NO PGIDE/011/08, under my supervision. Therefore, I/We recommend that the student has fulfilled the requirements and hence here by can submit the thesis to the department.

Shemelies Asseffa (PhD)	_____	_____
Name of major advisor	Signature	Date
Moltot Zewude (PhD)	_____	_____
Name of co- advisor	Signature	Date

SCHOOL OF GRADUATE STUDIES HAWASSA UNIVERSITY

EXAMINERS' APPROVAL SHEET-2 (Submission Sheet-2)

We, the undersigned, members of the Board of Examiners of the final open defense by **Ergetie Tilaye Wondmagegn** have read and evaluated his/her thesis entitled *"Impact of Climate Change on Surface Water Availability in the Mojo River Catchment"* and examined the candidate. This is therefore to certify that the thesis has been accepted in partial fulfillment of the requirements for the degree of masters' of science

Teshale Tadesse		
Name of the Chairperson	Signature	Date
Shemelies Asseffa (PhD)		
Name of Major Advisor	Signature	Date
Sirak Tekleab (PhD)		
Name of Internal Examiner	Signature	Date
Samuel Dagalo (PhD)		16/06/2018
Name of External examiner	Signature	Date
SGS Approval	Signature	Date

Final approval and acceptance of the thesis is contingent upon the submission of the final copy of the thesis to the School of Graduate Studies (SGS) through the Department/School Graduate Committee (DGC/SGC) of the Candidates' department.

Stamp of SGS

Date:_____

Remark

☐ Use this form to submit the thesis with minor correction suggested by the examining board

Abstract

Climate change is likely to have severe effects on water availability in Ethiopia. The aim of the present study was to assess the impact of climate change in the Modjo River, Upper Awash Basin. The Statistical Downscaling Tool (SDSM) was used to downscale the HadCM3 (Hadley centre Climate Model 3) Global Circulation Model (GCM) scenario data into finer scale resolution. The Soil and Water Assessment Tool (SWAT) was set up, calibrated and validated. SDSM downscaled climate outputs were used as an input to the SWAT model. The climate projection analysis was done by dividing the period 2011-2099 into three time windows with each 30 years of data. The period 1980-2010 was taken as the baseline period against which comparison was made. Results showed that flow volume may decrease in the 90-year period (2020, 2050 and 2080) this decrease may. in seasons .Kiremit(2020,2050 and 2080) -94.36%,-43.38% and -49.31% in A2a respectively and -97.21% (2020) and -97.51% (2080) and negligible in 2050 for B2a scenario and Belg seasons should a decrease and is -92.12% and -80.035 in 2020 for A2a and B2a scenario respectively. In 2050 it should an increase is+3.87% for A2a and negligible for B2a and for 2080 it is -55.54% and -64.94% for A2a and B2a respectively that expected to show the larger share in decreased flow volume for both scenario and in Bega season may a decrease in 2080 for A2a by -54.46% , in B2a may decrease by -67.33% in 2020 and negligible for 2080s while for A2a in 2020 and 2050 it may increase by +43.29% and +13.995 respectively when one observe annual flow for both scenarios (2020,2050 2080) it may decrease by-47.73,-8.51% and-53.10 %respectively in A2a scenario and -81.52%,thechange negligible and -30.33% respectively in B2a scenario. Overall, it appears that climate change will result in an annual decrease in flow volume, ranges for A2a -8.51%-to -47.73% and from -30.33% to-81.52% for B2a scenarios.

Key Words: Climate Change, SDSM. Modjo, GCM. SWAT

Acknowledgement

First of all I would like to thank the almighty God for giving me the audacity and wisdom to reach this point in life. I am very grateful to Hawassa University, Department of Water Resources Engineering for allowing me to take part in the Master Program for Irrigation and Drainage Engineering and Awash Basin Authority and Ministry of Water Resource, Irrigation and Electric city for granting me to learn Thank you made my dream come true. I would like to express my sincere gratitude to my advisor, Dr. Shiemelies Asseffa for giving me deepest valuable guidance, technical advice, material support, suggestion and constructive ideas and support throughout my research. I am also indebted to my co-advisor, Dr. Moltot Zewude, who helped me in assisting and. commenting I will also like to extend. I am very grateful to all my teachers who taught me from grass root to this level. I will also like to thank the Ethiopian Ministry of Water Resources, National Meteorological Services Agency and Awash basin authority Office members for the data and keen assistance they gave me during field work. I like to thank Mikal Birhane for the SWAT, hydrological model, who solved my problems when I got stuck at some critical points and priceless comments he gave me at my modeling work. I will also like to thank Goitom and Yitbarek for the data, comments and helpful documents they gave me .for climate part Thanks to God, I have lots of exciting friends and my classmates whom I met in my walk of life. Letters and words limit me to list your names. You all were great. I learnt a lot from you. Those of you I met you in Hawassa University, thank you for those beautiful days we spent together and for our chats and discussions made my stay very easy. Friends back home, thank you. You were my courage to go forward. At last but not least, I would like to extend my deepest gratitude to my son Fitsum. Ergetie and his grandmother W/ro Beltu Dessalgn, for caring my son, without your encouragement and care this would not have happened.

Acronyms

A_2	Storyline is referred as the medium-high emissions scenario
AGCM	Atmospheric General Circulation Model
ANN	Artificial neural Networks
Arc SWAT	SWAT Integrated with ArcGIS
ARS	Agricultural Research Service
AOGCM	Coupled Atmospheric-Ocean general Circulation Model
B_2	Storyline is referred as the medium-low emissions scenario
CCA	Canonical Correlation Analysis
CGLAR	Consultative group on Agricultural Research
CICS	Canadian Institute for climate studies
CN	Curve Number
Co_2	Carbon dioxide
DEM	Digital Elevation Model
ESCO	Soil Evaporation Compensation Factor
FOA	Food and Agricultural Organization of the United Nation
GCM	General Circulation Model
GHG	Green House Gas
GIS	Geographic Information System
GW Delay	Groundwater Delay time
GW Revamp	Groundwater Revamp Coefficient
GWOMN	Threshold water Depth in the shallow aquifer for flow
HADCMB	Hadley Center compiled model version 3

HADCMBA2u	Hadley center Coupled Model version 3 for the A2a emission
HADCM3B2A	Hadley center coupled model, version, for the B2a Emission
HRU	Hydrological Response unit
IPCC	International panel on climate charge
ITCZ	Inter- tropical convergence zone
LULC	Land use land cover
LUPSA	Land use update and soil Assessment
m.a.s.l	Meters above sea level
MOA	Ministry of Agriculture
MOWRIE	Ministry of Water Recourse Irrigation and Electric city
NASA	National Aeronautics and space Administration
NCEP	National center for Environmental Predication
NMSA	National Metrological Services Agency
NSE	Nash- Sutcliff efficiency
PBIAS	Percent Bias
PET	Potential Evapotranspiration
R^2	Coefficient of Determination
ROTO S	Routing outputs to outlet
SCS	Soil Conservation system
SDSM	Statistical Down Scaling Model
SRES	Special Report on emission Scenarios
SWAT	Soil and water Assessment Tool
SWRRB	Simulator for water Resources in rural Basins

TGSCIA	Task group on scenarios for climate and impact Assessment
UNEP	United Nations Environment program
USDA	United States Department of Agriculture
WGEN	Weather Generator
WHAT	Web Based Hydrograph Analysis Tool
WMO	World Metrological Organization

Contents

Lists of TABLES

Lists of Figures

1. Introduction

The environment has been influenced by human beings for centuries. However, it is only since the beginning of the industrial revolution that the impact of human activities has begun to extend to a global scale. Today, environmental issue becomes the biggest concern of mankind as a consequence of scientific evidence about the increasing concentration of greenhouse gases in the atmosphere and the changing climate of the Earth. Globally, temperature is increasing and the amount and distribution of rainfall is being altered (Cubasch et al, 2001). According to the International Panel on Climate Change (IPCC) Scientific Assessment Report, global average temperature would rise between 1.4 and 5.8°C by 2100 with the doubling of the CO2 concentration in the atmosphere. Sea level rise, change in precipitation pattern (up to ±20%), and change in other local climate conditions are expected to occur as a consequence of rising global temperature (Cubasch et al., 2001). This is expected to have a potential impact on different socio-economic sectors (IPCC, 2001).

Scientists have made estimates of the potential direct impacts on various socio-economic sectors, but in reality the full consequences would be more complicated as impacts on different sectors are indirectly interrelated to one another (UNEP, 2005) Projections of climate change in semi-arid regions, such as Ethiopia, show that temperatures will rise, and droughts will occur more frequently (Rockstrom et al.2007). Precipitation will become more intense, and will occur during shorter periods (IPCC, 2012). Year-to-year rainfall records in Ethiopia show that rainfall is seasonal and already highly erratic, hampering the socio-economic development of these areas. Since 95 % of the agricultural area in Ethiopia relies on rain-fed farming systems (Dixon et al. 2003; World Bank 2006), climate changes may have a negative impact on the productivity of major crops (e.g. Knox et al., 2012, Hayashi et al. 2012 and Rockstrom et al., 2009). In addition, achieving Millennium Development Goal 7, which aims to provide world wide access to clean drinking water for all communities, will be more challenging because of these future changes (World Bank, 2010). Being one of the very sensitive sectors, climate change can cause significant impacts on water resources by resulting changes in the hydrological cycle. The change on temperature and precipitation components of the cycle can have a direct consequence on the quantity of Evapotranspiration component, and on both quality and quantity of the runoff component. Consequently, the spatial and temporal water resource availability, or in general the

water balance, can be significantly affected, which clearly amplifies its impact on sectors like agriculture, industry and urban development (Hailemariam, 1999).

Due to climate change, water and its availability and quality will be the main pressures on, and issues for, societies and the environment, Climate change also increase the vulnerability of ecosystems due to temperature increases, changes in precipitation patterns, frequent severe weather events such as flooding and prolonged droughts (IPCC, 2007). Climate change will have a profound impact on natural resources, of which water is one of the most important. With climate change the amount of rainfall in many parts of Africa is expected to decline while variability may increase dramatically (IPCC, 2007). With climate change and increases in climate variability, the need for managing water resources requires immediate action or attention.

Due to climate change and variability there is an increase in severity of extreme events which results in fluctuation of storages. Ethiopia is highly sensitive to climate change and variability .Dile. et, al (2013)This may lead to an increase in floods and droughts. Due to underdevelopment of the water resources, the people of Ethiopia have been exposed to major problems such as impacts of drought and flood; shortage of clean water supply and inadequate energy supply (Hailemariam, 1999). Ethiopia is highly vulnerable to climate change because of the fact that the economic structure of the country largely depends on agriculture. Most of GHG emissions are dominated, which contributes 80% of the total GHG emissions.. Total greenhouse gas emissions by sectors in 1994, (First, 2001). This change causes a significant impact on the water resources by disturbing the normal hydrological processes.

One of the most significant potential consequences of changes in climates may be alterations in regional hydrological cycles and subsequent changes in river flow regimes. Climate change can affect multiple features of water resources (e.g., quantity and quality, high and low flow extremes, timing of events, water temperature, etc.) (Kim et al, 2008).Appropriate adaptation strategies are important policy options to limit the unprecedented impact of climate change for the livelihoods of the rural Ethiopian poor (Fischer et, al 2005 and Deressa et ,al 2009) While the focus on considering global impact of climate change is primarily on societal responses to the local and regional consequences of large-scale changes (Xu CY 2000) most climate change studies in Ethiopia have been done either at country or river basin scale (Dile , et, al 2013).Therefore, results from these studies (e.g. Conway and Hulme 1996 , Gleick P 1991, Hailemariam 1999,Kim . et, al 2008, Beyene et al l2010 and Abdela. 2013) are highly aggregated and have little importance in informing the impact of climate change at smaller scale. Gibson et, al 2000 and Wilbanks et, al

(1999). The impact of climate change at mojo river catchment on surface water resources availability has be studied. The present research assesses the impact of climate change for the Modjo sub basin, Modjo River which-h is found in A wash Basin is one of the contributors of water for the koka dam, main water supply for different water use sectors, like domestic water supply of towns and rural area, irrigation, hydropower, industries, and livestock.

1.1 Statement of the Problem

As most climatic change studies made in Ethiopia is in river basin scale and their result do not show the impact of climate change in small scale and Impact of climate change at mojo river catchment on surface water resources availability has be studied for feature water allocation and water resource planning and decisions, therefore this study aims to fulfill this gap

1.2 General objective

To assess the impact of climate change on surface water resources availability at Mojo river catchment (upper koka) using the General Circulation (climate) Model and Soil and Water Assessment Tool (SWAT) model.

1.2.1 Specific objectives**;**

The specific objectives of this study are

- to evaluate climate scenario data using maximum and, minimum temperature and precipitation based on a General Circulation Model and a Statistical Down Scaling Model for Modjo River catchment,
- to quantify possible effects of climate change on the surface water quantity of Modjo river based on the down scaled climate scenario data using hydrological model (SWAT)

1.3 Research Questions

In order to meet the above objectives the research questions for this study are.

i. What will be the future general trends of precipitation, maximum and minimum temperature of the area?

ii. How this trend is reflected on surface water availability of Modjo River.

1.4 Hypothesis

Climate change doesn’t have any/ significant impact on river flow

1.5 The scope of the study

The scope of the study is concentrated on the Mojo sub basin area of the Awash River Basin This research therefore extends the integration of a hydrologic model SWAT with a newly developed climate downscaling methodology for the purpose of determining future water availability .

1.6 The Significance of the study

The significance of investigating climate change and their impacts on hydrology has been highlighted by many researchers for planning and sustainable management of natural resources in many parts of the world. Mojo River is the source of water for Koka dam, which is the source of hydro power, irrigation and domestic use in the area. Therefore, the contribution of this research is to assess a future available water resource which has different uses Understanding the types and impacts of climate change is an essential indicator for resource base analysis and development of effective and appropriate use for sustainable management of water resources in the basin in general and at the study area in particular.

2. LITERATURE REVIEW

2.1 Climate change

The environment has been influenced by human beings for centuries. However, it is only since the beginning of the industrial revolution that the impact of human activities has begun to extend to a global scale (Baede et al., 2001). Today, environmental issue becomes the biggest concern of mankind as a consequence of scientific evidence about the increasing concentration of greenhouse gases in the atmosphere and the changing climate of the Earth. Globally, temperature is increasing and the amount and distribution of rainfall is being altered (Cubasch et al., 2001).

Climate change has impacts on water resources as it may alter seasonal temperature and precipitation, shift the timing of stream flow, and reduce the ability of existing supplies to meet the water demands. The only means available to quantify the non-linear climate response impacts is by using numerical models of the climate system based on well-established physical, chemical and biological principles, possibly combined with empirical statistical methods. These are designed mainly for studying climate processes and natural climate variability, and for projecting the response of the climate to human-induced forcing (Baede et al., 2001).

2.2 Climate Change and Water Resources

Potential impacts of climate change on water resources may include changes in hydrological processes such evapotranspiration, soil moistures, water temperature, stream flow volume, timing and magnitude of runoff, and frequency and severity of floods, all of which would cause changes in other environmental variables such as plant growth and sediment and nutrient flow into water bodies. Such hydrologic changes will affect almost every aspect of human well-being, from agricultural productivity and energy use to flood control, municipal and industrial water supplies, and fish and wild life management (Xu, 2000).

Studies in recent years have been shown important regional water resource vulnerabilities to changes in both temperature and precipitation patterns (Lahmer et al., 2001). Climate change: Temperature: For the past four decades, the average annual temperature in Ethiopia has been increasing by 0.37ºC every ten years, which is slightly lower than the average global temperature rise. The majority of the temperature rise was observed during the second half of the 1990s (EEA, 2008).

Temperature rise is more pronounced in the dry and hot spots of the country, which are located in the northern, northeastern, and eastern parts of the country. The lowland areas are the most affected, as these areas are largely dry and exposed to flooding during period of extreme precipitation in the highlands. Future temperature projections of the IPCC mid-range scenario show that the mean annual temperature will increase in the range of 0.9 to 1.1ºC by 2030, in the range of 1.7 to 2.1ºC by 2050, and in the range of 2.7 to 3.4ºC by 2080 in Ethiopia compared to the 1961 to 1990 normal posing a sustained threat to the economy (EEA, 2008).

Agriculture is the source of livelihood to an overwhelming majority of the Ethiopian population (it employees more than 80% of the lab our force) and is the basis of the national economy. A decrease in seasonal rainfall has devastating implications on agricultural production leading to food insecurity, malnutrition and famine. The frequency and intensity of drought is likely to increase over the coming decades, which will present a serious threat to biodiversity, ecosystems, water, agricultural and human health. Impacts of increased climate variability and change include (i) increased food insecurity; (ii) outbreaks of diseases such as malaria, dengue fever and water borne diseases such as cholera and dysentery due to floods, and (iii) respiratory diseases associated with droughts; (iv) heavy rainfalls which tend to accelerate land degradation and damage to communication infrastructure (World Bank,2012).

2.3 Climate Models

Global Climate Models (GCMs) are the best tools to estimate future global climate changes resulting from the continuous increase of greenhouse gas concentration in the atmospheres (Busuioc et al., 2001; Dibike and Coulibaly, 2005).

However, due to their coarse spatial resolution, the outputs from these models may not be used directly in climate change impact studies. Hydrological models, for instance, deal with small or sub catchment scale whereas GCMs simulate large scale and parameterize many regional processes. Therefore, downscaling techniques are emerged as a means to relate the scale mismatch between the GCMs results and the increasingly small scales required by impact community (Dibike and Coulibaly, 2005; Wilby and Wigley, 1999).

2.3.1. Global Circulation Models (GCM)

GCM describes the global climate system, representing the complex dynamics of the atmosphere, oceans, and land with mathematical equations that balance mass and energy. By simulating interactions among sea ice, land surface, atmospheric chemistry, vegetation, and the oceans, they predict future climates characterized by temperature, perception, air pressure, and wind speed. since these models are computationally so intensive, they can only be run on supercomputers at large research institutes. However, the results are made available to the general scientific community and have so far been used for studies of climate change and its impacts on natural, social, and economic systems (IPCC AR4, 2007).

GCMs are referred to as "coupled models" because they are comprised of linked components which model physical processes in the atmosphere, oceans, land surfaces and sea ice. Atmospheric and ocean components are represented as grid cells in all GCMs while the representation of land surfaces and sea ice vary more. HadCM3 is a coupled atmospheric-ocean GCM developed at Hadley Centre for Climate Prediction, detection, attribution and other climate sensitivity studies and research in the UK. The atmospheric part of HadCM3 have a horizontal resolution of 2.5º latitude x 3.75º longitude which is almost (228 km x 417 km) and has 19 vertical levels. The ocean component of the model has 20 vertical levels with horizontal resolution of1.25º latitude x 1.25º longitude (IPCC, 2001).

HadCM3 was applied in this study because this model is widely applied in many climate change impact studies, HadCM3 is also in a public domain and it provides daily predictor variables which can be used for the Statistical Downscaling Model. The model has been applied in many parts of Ethiopia, like.

i. Assessment of Climate Change; Impact on Water Availability of Bilate Watershed, Ethiopian Rift Valley Basin. To project the probable impact of climate change on the available water, HadCM3 coupled atmosphere-ocean GCM model was used since it is the only GCM model that has grid box containing the study area for SDSM. The output of HadCM3 coupled atmosphere – ocean GCM model for the A2a and B2a SRES emission scenarios were used to produce future scenarios of precipitation and temperature. The SWAT simulation of future average annual flow shows a decreasing trend in 2011-2040 periods and an increasing trend in 2041-2070 periods. The average total annual flow at outlet of the watershed might decrease up to 3.7% for A2a scenario

and1.5% for B2a scenario for the 2011-2040 periods but for 2041-2070 periods it might increase up to 2.6% for A2ascenario and 3.7% for B2a scenario. The decrease in the future flow of 2011-2040 periods might be insufficient in some months to meet future demands for water of the ever increasing population with in and around the watershed. Adopting water storage options to store the excess water flowing during the rainy period is crucial (Abadi and Kassa, 2014)

ii. Study Climate Change Impact on Lake Ziway Watershed Water Availability; to estimate the level of impact of climate change on the watershed's water availability, climate change scenarios of precipitation and temperature were developed for four future periods of 25 years from the year 2001 until 2099... Generally, both precipitation and temperature show an increasing trend from the 1981-2000 (base period) level. It is estimated that the average monthly and annual precipitation in the watershed might increase up to 29% and 9.4%, respectively.

Besides, the average maximum temperature might rise up to 3.6°C, and1.95°C; and the average minimum temperature 4.2°C and 2°C monthly and annually, respectively. These changes of the climate variables were applied to SWAT hydrological model to simulate future flows. The simulation result revealed that, except during the 2001-2025 periods, the total average annual inflow volume into Lake Ziway might decline significantly up to 19.47% for A2a- and 27.43% for B2a-scenarios. This inflow volume reduction is likely to drop the lake level up to two third of a meter. Consequently, the surface area might also shrink by 25.3 km2, which is about 6% of the base period lake surface area. This shows a worsening trend of the recent lake level fluctuation and aerial coverage contraction. This combined with the unbalanced supply-demand equation in the watershed is expected to have significant impact on the lake water balance. Hence, in Lake Ziway Watershed, runoff is likely to decrease in the future and be insufficient to meet future demands for water of the ever increasing population in the region (Zeray, 2006).

iii. According to Henok (2013) the time series generated by GCM of HadCM3 A2a and B2a and Statistical Downscaling Model (SDSM) indicate a significant increasing trend in maximum and minimum temperature values and a slight increasing trend and decreasing and underestimation in precipitation for both A2a and B2a emission scenarios in both Mekelle and Wukro stations. And the SWAT model output shows that there will be an annual decrease reduction in surface runoff volume in Agula watershed for A2a and B2a emissions scenarios, by 2.85.7% for the next 90 years

for both A2a and B2a emission scenarios, the future. Potential evapotranspiration will be10 to 166 mm per year for the future time (2012-2099) (Henok, 2013)

The detail for a general circulation model is defined by the number of layers it uses to model the atmosphere and the ocean and its spatial resolution, i.e. the size of the cells in its discretization of those layers (IPCC, 1996).Baseline period is needed to compare the observed climate variables with the model computed climatic in climate change the climate change. When using climate model results for scenario construction, the baseline also serves as the reference period from which the modeled future climate change is calculated. Climate scenario is a plausible indication of what the future could be like over the decades or centuries, given a specific set of assumptions. These assumptions include future trends in energy demand, emissions of greenhouse gases, land use change as well as assumptions about the behavior of the climate system over long time scales. It is largely the uncertainty surrounding these assumptions which determine the range of possible scenarios (Carter, 2007).

2.4. Emission Scenarios

Four different narrative storylines where developed to describe the relationship between the forces driving emission and there evaluation and to add context for the scenario quantification. The resulting set of scenarios cover the wide range of the main demographic, economic and technological driving forces of the future greenhouse gas. Each scenario represents the specific quantification of one of the four storylines. All the scenarios based on the same storyline constitute a scenario 'family' which briefly describe the main characteristics of the four SRES storylines and scenario family (IPCC-TGICA, 2007). The A1 storyline and scenario family describe a future world of very rapid economic growth, global population that peaks in mid-century and declines the rapid introduction of new and more efficient technologies. Major underlying themes are convergence among regions, capacity building and increased cultural and social interactions, with a substantial reduction in regional differences in per capita income. The A1 scenario family develops into three groups that describe alternative directions of technological change in the energy system. The three A1 groups are distinguished by their technological emphasis: (*IPCC-TGICA, 2007*) Fossil intensive (A1FI) Non-fossil energy sources (A1T), or - Balance across all sources (A1B) (balanced is defined as not relying too heavily on one particular energy source, on

the assumption that similar improvement rates apply to all energy supply and end use technologies).

The A2 storyline and scenario family describe a very heterogeneous world. The underlying theme is self-reliance and preservation of local identities. Economic development is primarily regionally oriented and per capita economic growth and technological changes are more fragmented and lower than other storylines. (*IPCC-TGICA, 2007*).The B1 storyline and scenario family describes a convergent world with the same global population, that peaks in mid-century and declines thereafter, as in the A1 storyline, but with rapid change in economic structures toward a service and information economy, with reductions in material intensity and the introduction of clean and resource-efficient technologies. The emphasis is on global solutions to economic, social and environmental sustainability, including improved equity, but without additional climate initiatives. (*IPCC-TGICA, 2007*).The B2 storyline and scenario family describe a world in which the emphasis is on local solutions to economic, social and environmental sustainability. It is a world with continuously increasing global population at a rate lower than A2, intermediate levels of economic development, and less rapid and more diverse technological change than in the B1 and A1 storylines. The scenario is also oriented towards environmental protection. (*IPCC-TGICA, 2007*) Overall the above story line can be summarized by the tree graph of the scenarios as indicated in figure 2.1. GCMs have been used to predict future changes in climate until the end of the 21st century by various institutions specializing in climate research. More information on these institutions, their models and analyses data can be obtained from the IPCC Data Distribution Centre at http://www.ipcc-data.org

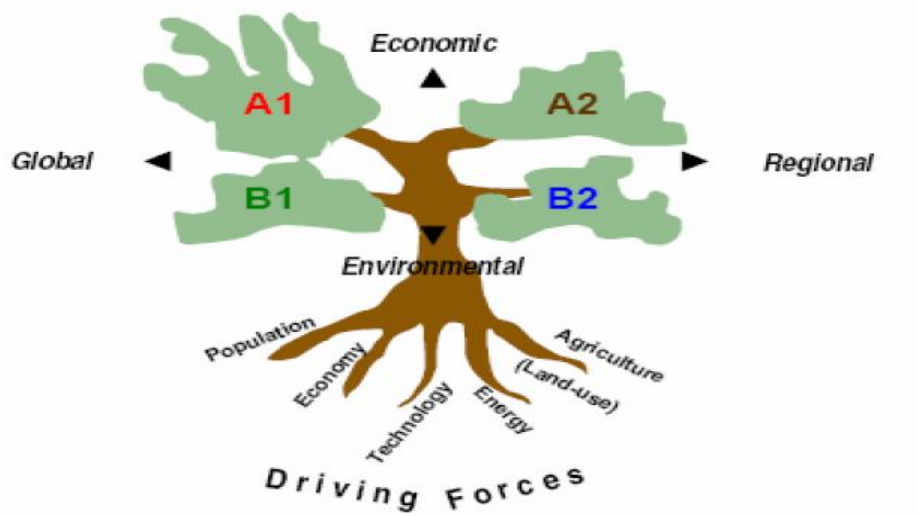

Figure 2.1 Four IPCC SRES scenario storylines (IPCC-TGICA 2007)

2.5. Downscaling methods and tools

The various downscaling methods available in literature can be broadly classified as dynamic downscaling and statistical downscaling (Figure 2.2). In the dynamic downscaling method, a Regional Climate Model (RCM) is embedded into GCM. There are two types of dynamic downscaling based on the types of nesting: one-way nesting and two-way nesting (Wang et al. 2004). One-way nesting consists of driving a limited-area high-resolution RCM with low-resolution data obtained previously by a GCM or by analyses of atmospheric observations. The one-way nesting technique does not allow feedback from the RCM to the driving data. In two-way nesting, the RCM is run simultaneously with the host GCM, and it regularly updates the host GCM in the RCM region. Models of this type are typically developed using different numeric and physical parameterizations. They are no presently in use as they are cumbersome. Benefits similar to ‘‘two-way nesting’’ can be derived from the use of a variable-resolution GCM Statistical downscaling involves developing quantitative relationships between large-scale atmospheric variables (predictors) and local surface variables (predictands).Among the widely applied statistical downscaling techniques the universally multiple linear regression models called Statistical Down-Scaling Model (SDSM)are often used. When GCMs come to quantifying the potential impacts of climate change on water resources, more problems arise.

GCMs generally operate at coarse resolutions across the continents, but much smaller scales (in both in time and space) and are required for catchment hydrological modeling (Bergkamp et al. 2003).Even though, GCMs have the above main limitations, they represent reasonably well the main futures of global distribution of the basic climate parameters (Gates et al., 1999). In order to decrease the uncertainty related to coarse resolution of GCMs, usually, most climate impact assessment researches use different downscaling methods such as dynamic downscaling method and/or statistical downscaling method. Downscaling is the term given to the process of deriving finer resolution data (e.g., for a particular site) from coarser resolution GCM data. It may be possible to define a relationship, between site climate and large-scale (i.e., GCM grid box scale) climate which can then be used to derive more realistic values of the future climate at the site scale (IPCC-TGICA, 2007).The approach is shown by figure 2.3.

2.5.1. Empirical (statistical) downscaling

General circulation models (GCMs) indicate that rising concentrations of greenhouse gases will have significant implications on the climate at global and regional scales (Wilby and Dawson 2007). Due to their coarse spatial resolution and inability to resolve important sub-grid scale features such as clouds and topography, GCMs are restricted in their usefulness for local impact (for small area) studies by their coarse spatial resolution GCMs depict the climate using a three-dimensional grid over the globe, typically having a horizontal resolution of between 250 and 600 km, 10–20 vertical layers in the atmosphere, and sometimes as many as 30 layers in the oceans (Nakicenovic et al. 2000). Their resolution is thus quite coarse relative to the scale of exposure units in most impact assessments. Several methods have been adopted for developing regional GCM-based scenarios at the sub-grid scale, a procedure known as “regionalization” or “downscaling.”

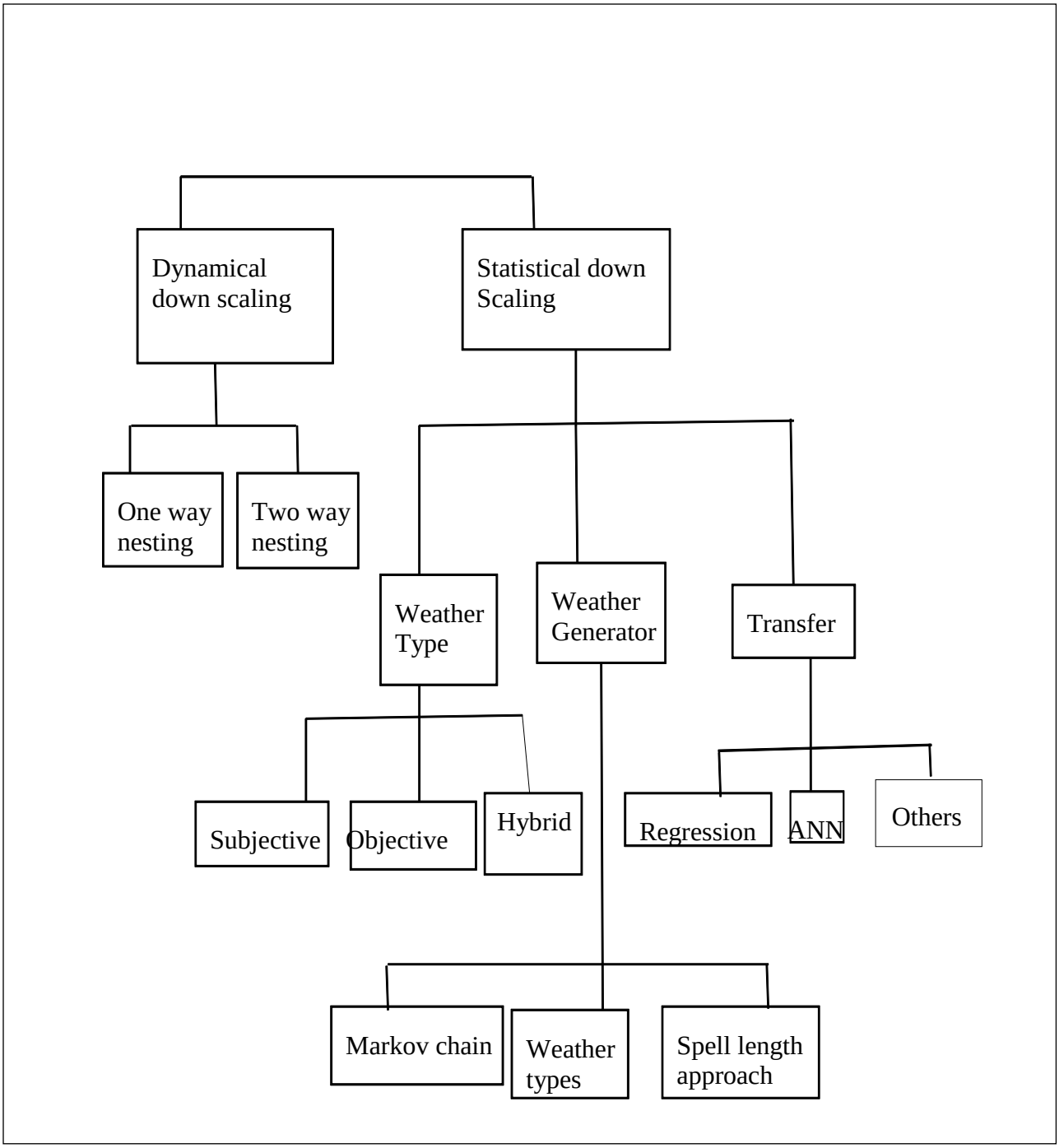

Figure 2.2 Methods of downscaling

Two different approaches to downscaling are possible which are dynamical and statistical (Hewitson and Crane,1996).

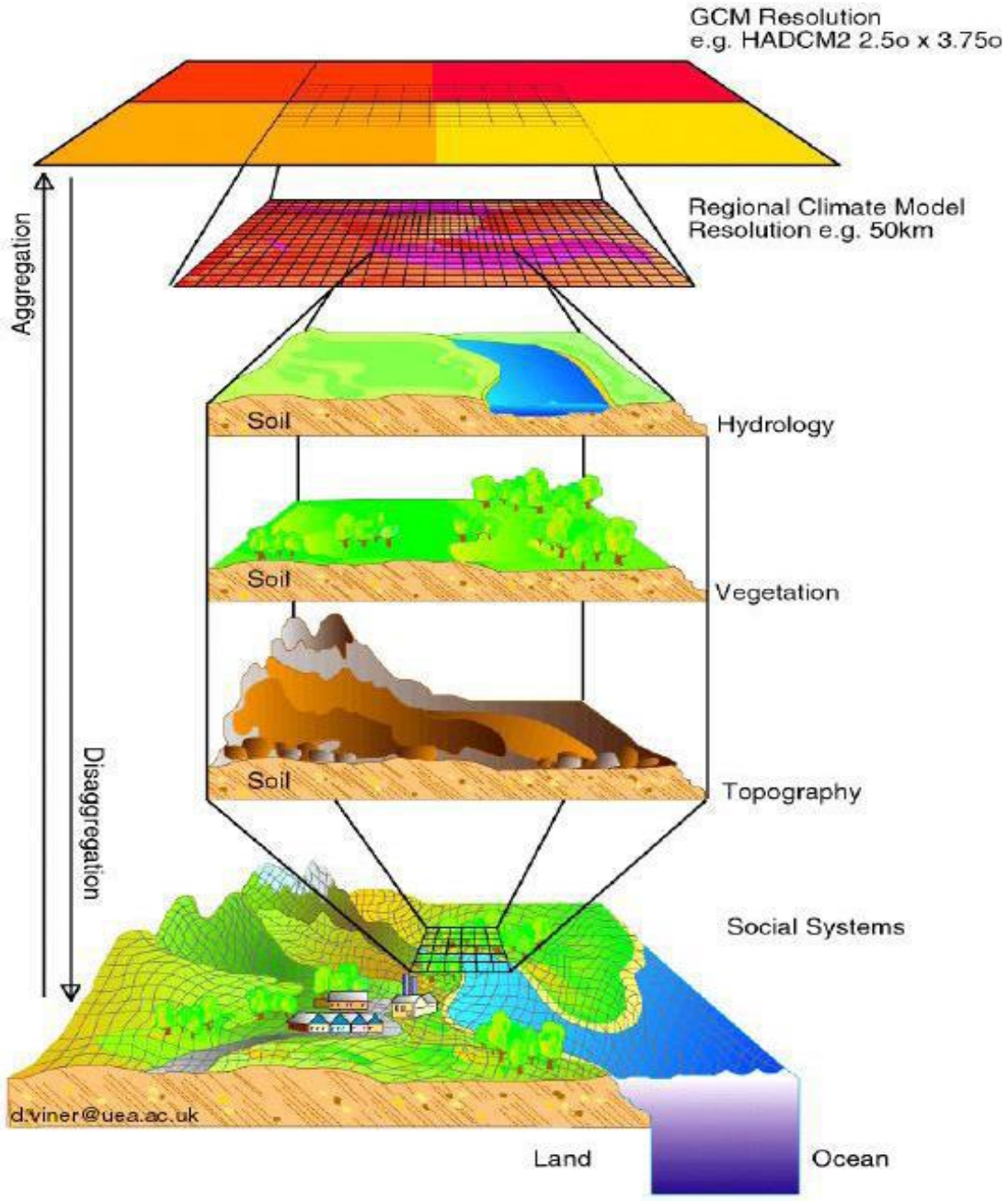

Figure 2.3 Schematic illustration of the general approach for down Scaling (IPCC-TGIC2007)

The typical application in dynamic (nested model) downscaling is to drive a regional dynamic model at meso scale or finer resolutions with the synoptic-scale and larger scale information from a GCM (Giorgi and Mearns 1991; Jenkins and Barron 1997).

Detailed information at spatial scales down to 10–20 km, and at temporal scales of hours or less, may be achieved in such applications (Hewitson and Crane 1996).Such models are

computationally demanding and are not easily accessible, but in the long term, this technique is likely to be the best approach that needs to be encouraged, whereas statistical (empirical) downscaling is computationally efficient in comparison to the dynamical downscaling. It is a practical approach for addressing current needs in the climate change research community especially in many of the countries liable to be most sensitive to climate change impacts (Hewitson and Crane 1996).

From the two approaches of downscaling, the common approach is the statistical downscaling method. As described by (Palmer et al., 2004), this method is advantageous as it is easy to implement, and generation of the downscaled values involves observed historic daily data and applicable to 'exotic' predictands such as air quality and wave heights. In addition the statistical down scaling methods ensures the maintenance of local spatial and temporal variability in generating realistic time series data. Many of the processes, which control local climate as topography, vegetation, and hydrology, are not included in coarse resolution GCMs. The development of statistical relationships between the local scale and large scale may include some of these processes implicitly. Under the broad empirical/statistical downscaling techniques, the following three major techniques have been developed. These are weather classification or typing schemes, transfer function or regression models, and stochastic weather generator methods. Regression models are conceptually simple means of representing linear or nonlinear relationships between local climate variables (predict ands) and the large-scale atmospheric forcing predictors, (Wilby et al., 2004).

Commonly applied methods include canonical correlation analysis (CCA) (von Storch et al. 1993),artificial neural networks (ANN) which are skin to nonlinear regression (Crane and Hewitson 1998), and multiple regression (Murphy 1999).In this study, a regression model, SDSM, was used. SDSM is widely applied in many regions of the world over a range of different climatic conditions. It permits the spatial downscaling of daily predictor–predict and relationships using multiple linear regression techniques. The predictor variables provide daily information concerning the large-scale state of the atmosphere, while the predictand describes conditions at the site scale (CCIS 2008).

SDSM is a decision support tool that facilitates the assessment of regional impacts of global warming by allowing the process of spatial scale reduction of data provided by large-scale GCMs

(Wilby et al. 2002). It is best described as a hybrid of the stochastic weather generator and regression based methods. This is because large-scale circulation patterns and atmospheric moisture variables are used to linearly condition local-scale weather generator parameters as precipitation occurrence and intensity (Wilby et al. 2002) Statistical downscaling methods involve developing quantitative relationships between large-scale atmospheric variables (predictors) and local scale surface variables (predictand) through the transfer functions (Wilby et al., 2004).

The two frequently used terms in statistical downscaling are defined as follows. The predictor is the input data used in statistical models, typically a large scale variable describing the circulation regime over a region. The predictor is also known as 'independent variable', or simply as the 'input variable', usually written as Predictand = f (predictors) (Taylor and Francis, 2014) .The predictand is the output data, typically the small-scale variable representing the temperature or rainfall at a weather/climate station. The predictand is also known as 'dependent variable' or response variable' (Taylor and Francis, 2014).

2.5.2 Uncertainties in Climate Change Studies

There are several sources of uncertainty in the generation of climate change information.

There is uncertainty associated with alternative scenarios of future emissions and their radiative effects. Uncertainties in the climatic effects of manmade aerosols (liquid and solid particles suspended in the atmosphere) constitute a major hesitation in quantitative studies.(Bader et al., 2008) stated that we do not know how much warming due to greenhouse gases has been cancelled by cooling due to aerosols. Uncertainties related to clouds increase the difficulty in simulating the climatic effects of aerosols, since these aerosols are known to interact with clouds and potentially can change cloud radiative properties and cloud cover (Bader et al, 2008).

The numerical models also may introduce uncertainties because of the finite approximation to the continuous equations. This approximation has two related aspects: one that there is a truncation error because of the numerical method and the other because of the effects of scales of motion smaller than the grid resolution on the resolved scale flow must be included (Thorpe, 2005)

2.6 Hydrological models

Hydrologic models are simplified, conceptual representations of a part of the hydrologic cycle. They are primarily used for hydrologic prediction and for understanding of the hydrologic processes. Without going into too much detail, deterministic hydrologic models (Cunderlik, 2003).

i. Lumped models: Parameters of lumped hydrologic models do not vary spatially within the basin and thus, basin response is evaluated only at the outlet, without explicitly accounting for the response of individual sub-basins. The impact of spatial variability of model parameters is evaluated by using certain procedures for calculating effective values for the entire basin. The most commonly employed procedure is an area-weighted average (Haan et al., 1982).

ii. Semi-distributed models**:** Parameters of semi-distributed (simplified distributed) models are partially allowed to vary in space by dividing the basin into a number of smaller sub-basins (Cunderlik, 2003).

iii Distributed models: Parameters of distributed models are fully allowed to vary in space at a resolution usually chosen by the user. Distributed modeling approach attempts to incorporate data concerning the spatial distribution of parameter variations together with computational algorithms to evaluate the influence of this distribution on simulated precipitation-runoff behavior. Distributed models generally require large amounts of (often unavailable) data for parameterization in each grid cell. However, the governing physical processes are modeled in detail, and if properly applied, they can provide the highest degree of accuracy (Cunderlik 2003).

2.6.1. Hydrological Model Selection Criteria

There are a number of criteria which can be used for choosing the right hydrologic model. These criteria are mainly dependent on the use of the model. Furthermore, some criteria are also user dependent such as: personal preference; computer operation system; input/output management and structure etc. (Cunderlik, 2003) suggested four criteria for the selection of hydrological models. These are: (1) required model outputs for the needed purpose, (2) different hydrological processes that are required to be modeled for the desired purpose, (3) availability of input data and (4) cost of readymade packages. Depending upon the above selection criteria for the Soil and Water Assessment Tool (SWAT) was selected in this study: SWAT is selected since;

i) SWAT is public or open source domain software actively supported by the USDA (United States Department of Agriculture) ARS (Agricultural Research Service) at the Grass-land, Soil and Water Research Laboratory in Temple, Texas, USA.

ii) SWAT performs for well a river basin scale, for a continuous time period and is, a spatially distributed model developed to predict the impact of land management practices on water, sediment and agricultural chemical yields in large complex watersheds with varying soils, land use and management conditions over long periods of time (Neitsch et al., 2005).

iii) SWAT can analyze both small and large watersheds by subdividing the area into homogenous parts. SWAT uses hydrologic response units (HRUs) to describe spatial heterogeneity in terms of land cover, soil type and slope within watershed. The SWAT system embedded within geographic information system (GIS) can integrate various spatial environmental data including soil, land cover, climate and topographic features. (Lenhart et al, 2002).

2.7 Hydrological Models used in Ethiopia and in Awash Basin

i. The effects of land use change on hydrological responses in the Choke Mountain Range (Ethiopia) A new Approach Addressing Land Use Dynamics in the Model SWAT A catchment in the Choke Mountain Range (Ethiopia) was selected as test case where significant land use change occurred during the last decades. The impact of land dynamics on the hydrological response was observed and shown at the daily discharge, the total annual runoff and the peak flow. Also a higher proportion of low flow rates was found and caused more water stress. Considering the high uncertainties, SWAT was not able to produce reliable results due to the bad data quality. Nevertheless, the implementation of land cover dynamics in SWAT led to a significant change in the model outputs and demonstrated improved capabilities to handle their impacts on water resources. Further model testing is strongly recommended (Koch et al, 2012).

ii. Predicting runoff yield using SWAT model and evaluation of Boru dodota Spate Irrigation Scheme, Arsi Zone, Southeastern Ethiopia (upper Awash basin);The result of model performance analysis demonstrated a good agreement between the average monthly simulated and measured values: Nash-Sutcliffe model efficiencies (NSE) of 0.71 for calibration and 0.73 for validation periods. Moreover, the coefficients of determination (R^2), 0.73 and 0.76, were obtained during the same period. The calibrated parameter on the gauged catchment was in turn used to estimate runoff

yield of the un gagged catchment. The simulated mean monthly and average annual water yields of the Boru River Watershed were found to be 0.53 and 6.4m^3/s respectively.The70% dependable wet season water yield of the catchment was 3.4m^3/s and crop water requirement of the command area was 1.2l/s/ha. The water yield from the catchment can irrigate only 2,842ha of land out of the pre-designed 5,000 ha of land of the BoruDodota spate irrigation scheme .In conclusion the SWAT model can be used to analyze ungagged watershed runoff yield in areas that have similar hydro meteorological characteristics as those of the Keleta Watershed in the region. The information obtained can then be used to redesign the spate system or a conventional irrigation system (Teso et al, 2014).

2.8 Hydrological component of SWAT

The simulation of the hydrology of a watershed is done in two separate divisions. One is the land phase of the loadings hydrological cycle that controls the amount of water, sediment, nutrient and pesticide to the main channel in each sub-basin. Hydrological components simulated in land phase of the hydrological cycle are canopy storage, infiltration, redistribution, evapotranspiration, lateral flow, surface runoff, ponds, tributary channels and return flow. The second division is routing phase of the hydrologic cycle that can be defined as the movement of water, sediments, nutrients and organic chemicals through the channel network of the watershed to the outlet. In the land phase of hydrological cycle, SWAT simulates the hydrological cycle based on the water balance equation. (SWAT manual, 2005)

$$S_{Wt} = S_{WO} + \Sigma\left(R_{day} - Q_{surf} - E_a - W_{seep} - Q_{gw}\right) \quad (2.1)$$

where : S_{Wt} is the final soil water content (mm),S_{WO} is the initial soil water content on day i (mm), t is the time (days), R_{day} is the amount of precipitation on day i (mm) ,*Qsurf* is the amount of surface runoff on day i (mm) , E_a is the amount of evapotranspiration on day i (mm), $W_{seep}$is the amount of water entering the vadose zone from the soil profile on day i (mm) ,and Q_{gw} is the amount of return flow on day i (mm).Using the above equation the soil moisture content for the given area is simulated. The brief description of some of the key model components only provided in this proposal. More detailed descriptions of the different model components are listed in (Neitsch et al., 2005).Soil water may follow different paths of movement: vertically upward (plant uptake), vertically downward (percolation), or laterally-contributing to stream flow. The vertical movement also describes the plant uptake that removes the largest portion of water that enters the

soil profile. Surface runoff**:** occurs whenever the rate of precipitation exceeds the rate of infiltration. SWAT offers two methods for estimating surface runoff: the SCS curve number procedure and the Green &Ampt infiltration method (Green and Ampt, 1911).

SWAT incorporates a kinematic storage model for subsurface flow (Neitsch et al., 2002).The peak surface runoff rate is the maximum volume flow rate passing a particular location during a storm event. SWAT calculates the peak runoff rate with a modified rational method. In rational method, it is assumed that a rainfall of intensity I begins at time t = 0 and continues indefinitely, the rate of runoff will increase until the time of concentration, t = t_{conc}. The modified rational method is used in the current version SWAT witch is expressed as:

$$q_{peak} = \frac{\alpha t_c * Q_{surf} * A}{3.6 * t_{conc}} \quad (2.2)$$

Where *q peak* is the peak runoff rate (m^3/s), αt_c is the fraction of daily rainfall that occurs during the time of concentration, Q_{surf} is the surface runoff (mm), A the sub-basin area (km²), t_{conc} is the time of concentration (hr), and 3.6 is a conversion factor.

Potential evapotranspiration**:** there are many methods that are developed to estimate potential evapotranspiration (PET).Three methods are incorporated into SWAT: the Penman-Monteith method (Monteith, 1965), the Priestley-Taylor method (Priestley and Taylor, 1972) and the Hargreaves method (Hargreaves et al., 1985. Groundwater: the simulation of groundwater is partitioned into two aquifer systems i.e. an unconfined aquifer (shallow) and a deep-confined aquifer in each sub basin. The unconfined aquifer contributes to flow in the main channel or reach of the sub basin. Water that enters the deep aquifer is assumed to contribute to stream flow outside the watershed (Arnold et al, 1993). In SWAT the water balance for a shallow aquifer is calculate with equation

$$aq_{shi} = aq_{shi-1} + W_{rchrg} - Q_{gw} - w_{revap} - W_{deep} - W_{pump.sh} \quad (2.3)$$

Where: aqsh,i; is the amount of water stored in the shallow aquifer on day i (mm).

aq_{shi-1}, is the amount of water stored in the shallow aquifer on day i-1 (mm), $W_{rchrg;}$ is the amount of recharge entering the aquifer on day i (mm) , Q_{gw} ; is the groundwater flow, or base flow, into the main channel on day i (mm), w_{revap}; is the amount of water moving into the soil zone in response to water deficiencies on day i (mm), W_{deep} *;* is the amount of water percolating

from the shallow aquifer into the deep aquifer on day i (mm), and $W_{pump.sh}$; *is* the amount of water removed from the shallow aquifer by pumping on day i (mm).

SWAT is a physically based river basin scale model developed to predict the impact of land management practices on water, sediment and agricultural chemical yields in large complex watersheds with varying soils, land use and management conditions over long periods of time (Neitsch et al., 2005). SWAT is separated into two major divisions, the first division is the land phase of the hydrological cycle as depicted in Figure 2.4which controls the amount of water, sediment, nutrient and pesticide loadings to the main channel in each sub-basin. The land phase of the hydrological cycle is simulated by SWAT based on the water balance equation:

The second division is the water or routing phase of the hydrological cycle which is the movement of water, nutrients, sediment and pesticides through the channel network of the watershed into the outlet. SWAT requires daily values of precipitation, maximum and minimum temperature, solar radiation, relative humidity and wind speed. These files may be given as an input to the model or can be generated from the monthly average data summarized over a number of years using WXGEN (an in-built weather generator model). These climatic variables are central in the determination of hydrological cycle of the drainage sub basin besides land use, soil and management practices inputs. It might be vital to discuss the most important hydrological cycle components and their estimation by SWAT model for this study; for further detailed explanation the author recommends referring the SWAT2005 theoretical documentations.

. SWAT uses three methods Penman-Monteith, the Priestley-Taylor, and the Hargreaves method for the estimation of potential evapotranspiration. Three of the methods have different input data requirements. The Penman-Monteith method requires solar radiation, air temperature, relative humidity and wind speed. The Priestley-Taylor method requires solar radiation, air temperature, and relative humidity. The Hargreaves method requires only air temperature. For this study due to availability of precipitation and temperature data, the Hargreaves method was used for the determination of the potential Evapo transpiration.

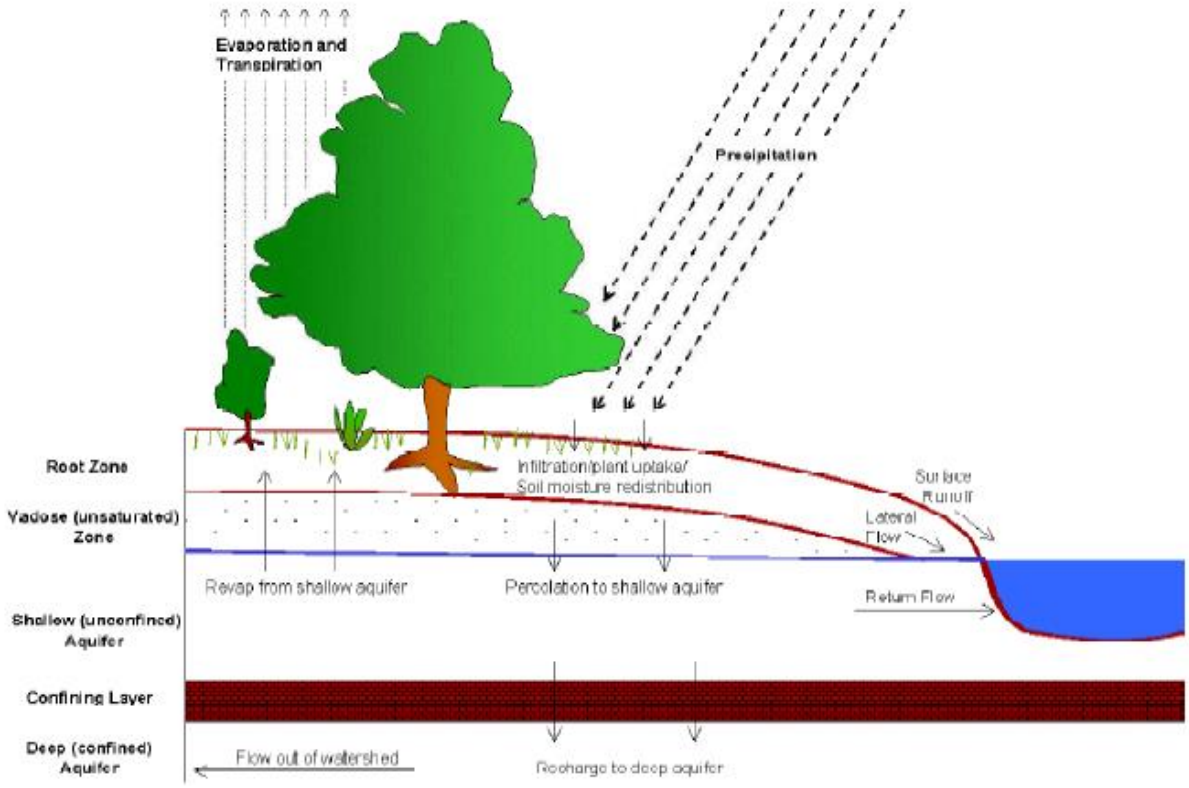

Figure 2.4 Schematic representation of the hydrological cycle (Neitsch, et.al, 2005)

The Hargreaves method was developed in 1975 but several improvements were made to the original equation. The form used in SWAT (Eqn 2.4) was published in 1985 (Neitsch et al., 2005).

$\lambda E_o = 0.0023 * H_O * (T_{max} - T_{min})^{0.5} (T_{ave} + 17.8)$ ---------- Eqn 2.4

Where $\lambda\ is\ the\ latent\ heat\ of\ vaporzation (MJK^{-1})$, E_o is the potential evapotranspiration (mmd^{-1}), H_O is the extraterrestrial radiation ($MJm^{-1}d^{-1}$), T_{max} is the maximum air temperature for a given day(℃), T_{min} is the minimum air temperature for a given day(℃) and T_{ave} is the mean air temperature for a given day(℃)

. The Green & Ampt infiltration method assumes that there will be excess water at the surface at all times which was invalid assumption in the study area. Besides, the Green and Ampt infiltration method requires sub-daily precipitation data which was other limitation to use this method.

The SCS curve number method is simple, widely used and efficient for determining the approximate amount of runoff from a rainfall event under a varying land use and soil types. The 1972 SCS curve number equation (Eqn 2.5) is used in SWAT model.

$$Q_{surf} = \frac{(R_{day}-l_a)^2}{R_{day}-l_a+S}$$----------Eqn 2.5

Where;Q_{surf} is the accumulated rainfall excess mm (H_2o), Ia is the initial abstraction which includes surface storage, infiltration and infiltration prior to runoff (H_2o) and S is the retantion parameter(H_2O) The retention parameter varies spatially due to changes in soils, land use, management and slope and temporarily due to changes in the soil water content. The retention parameter is defined as in.

$$S=25.4+ (\frac{1000}{CN} -10)$$ ----------Eqn 2 6

where, CN is the curve number for the day. The curve number is based on the area's hydrologic soil group, land use and hydrologic condition. The initial abstractions, is commonly approximated as 0.2S and Eqn 2.5 becomes:

$$Q_{surf}= \frac{(R_{day}-0.2S)^2}{R_{day}+0.8S}$$ ----------Eqn 2.7

The other component of the hydrological cycle which contributes to the stream flow is the groundwater. SWAT simulates two aquifers in each sub-basin: shallow and deep. The shallow aquifer is an unconfined aquifer and deep aquifer is the confined aquifer. Water that moves past the lowest depth of the soil profile by percolation or bypass flow enters and flows through the vadose zone before becoming shallow and/or deep aquifer recharge. The lag between the time that water exits the soil profile and enters the shallow aquifer will depend on the depth to the water table and the hydraulic properties of the geologic formations in the vadose zone and groundwater zones.

SWAT utilizes an exponential decay weighing function proposed by Venetis (1969). In a precipitation/groundwater response model to estimate the time delay in aquifer recharge once the water exits the soil profile (Neitsch et al., 2005). The recharge to both aquifers on a given day is calculated using Eqn 2.8.

$W_{rchrgi} = (1-\exp[-1/\sigma_{gw}])*W_{seep} +\exp[-1/\sigma_{gw}]*W_{rchrgi-1}$----------Eqn2.8

Where; W_{rchrgi} is the amount or recharge entering the aquifer on day i (mmH_2o) ,σ_{gw} is the delay time of the overlying geologic formations (days) and W_{seep} is the total amount of water exiting the

bottom of the soil profile on day i-1.The total amount of water exiting the bottom of the soil profile on a day is calculated using Eqn 2.9.

W_{seep}=W_{percly}=n+$W_{crk,btm}$, ----------Eqn 2.9

Where W_{percly} is the amount of water percolating out of the lowest layers n, in the soil profile on day i (mm H_2o), $W_{crk,btm}$ is the amount of water flow past the lower boundary of the soil

The shallow aquifer contributes to base flow in to the main channel or reaches within the sub-basin. Base flow is allowed to enter the reach only if the amount of water stored in the shallow aquifer exceeds a threshold value specified by the user; SWAT uses the Hooghoudt (1940) equation (Eqn 2.10) to determine the steady-state response of groundwater flow recharge.

Q_{gw}=$\frac{8000*K_{sat}}{L_{gw}^2}$* h_{wtbi} ----------Eqn 2.10

Where: K_{sat} is the hydraulic conductivity of the aquifer (mm/day), L_{gw} is the distance from the ridge or sub − basin divide for the ground water system to the main channel (m) and h_{wtbi} is the water table height; SWAT to know the water level fluctuations due to non-steady-state response of groundwater flow to periodic recharge using Eqn 2.11 (Smedema and Rycroft, 1983).

$\frac{d_{hiw}}{d_t} = W_{rchrg} - \frac{Q_w}{800-\mu}$ ----------Eqn 2.11

Where; $\frac{d_{hiw}}{d_t}$ is the change in water table height with time and μ is the specific yield of the shallow aquifer($\frac{m}{m}$)

Assuming that variation in groundwater flow is linearly related to the rate of recharge in water table height, Eqn 2.10 & 2.11 can be combined to obtain Eqn 2.12.

$\frac{dQ_{gw}}{d_t}$=10*$\frac{K_{sat}}{\mu-L_{gw}^2}$*($W_{rchrg}$-$Q_{gw}$)= $\alpha_{gw} * - Eqn$ 2.12

Where; α_{gw} is the base flow recession constant and all the other terms are as defined before

Integration and rearranging of Eqn 2.12 yields Eqn 2.13 & 3.14 which is used to calculate the groundwater flow.

Q_{gwi}=Q_{gwi}-1*exp [-$\alpha_{gw} * \Delta t$] + $W_{rchrg} * (1 - \exp[-\alpha_{gw} * \Delta t)$

If $aq_{sh} > a_{qshtr,q} - Eqn$ 2.13

Q_{gwi}=0 if $aq_{sh} < a_{qshtr,q}$ ---- --Eqn 2.14

Where; Q_{gwi} is the groundwater flow in to the main channel on day i (mmH_2o), Q_{gwi}-1 is the ground water flow in to the main channel on day i-1 (mmH_2O), Δt is the time step (1day) and $a_{qshtr,q}$ is the threshold water level in the shallow aquifer for ground water contribution to the main channel to occur (mmH_2o) and all the other terms are as defined above Water may move from the shallow aquifer into the overlaying unsaturated zone.

SWAT models the movement of water into the underlying unsaturated layers as a function of water demand for evapotranspiration. When the material overlying the aquifer is dry, water in the capillary fringe evaporate and diffused upward. As water is removed from the capillary fringe by evaporation, it will be replaced from the underlying aquifer. This process is termed as 'revap'. 'Revap' is allowed to occur only if the amount of water stored in the shallow aquifer exceeds a threshold value, ,. The maximum amount of water that will be removed from the aquifer via 'revap' on a given day is as in Eqn 2.15.

$$W_{revap,mx}=\beta_{rev} + E_o - Eqn\ 2.15$$

Where $W_{revap,mx}$ is the maximum amount of water moving into the soil zone in response to water deficiencies (mmH_2o), β_{rev} is the revap coefficient and E_O is the potential evapotranspiration for the day (mmH_2O).The water balance for the deep aquifer is calculated by Eqn 2.16.

$aq_{dp,i} = aq_{dp,i} - 1 + W_{deep} - W_{pump,dp}$--Eqn 2.16

Where; $aq_{dp,i}$ is the amount of water stored in the deep aquifer on day i (mmH_2o), $aq_{dp,i} - 1$ is the amount of water stored in the deep aquifer on day i-1 (mmH_2o), W_{deep} is the amount of percolating from the shallow aquifer in to the deep aquifer on day i (mmH_2o) and $W_{pump,dp}$ is the amount of water removed from the deep aquifer by pumping on day i (H_2O).

In SWAT, the amount of water entering to the deep aquifer is not considered in water budget calculations and can be considered to be lost from the system. SWAT uses manning's equation to define the rate and velocity of flow. Water is routed through the channel network using the variable storage routing method or the Muskingum river routing method. Both of the methods are variations of the kinematic wave model. In this study due to its simplicity, the variable storage model was selected. SWAT assumes the main channels are a trapezoidal shape.

$V_{in-V_{out}} = \Delta V_{stored}$ ----------2.17

Where; Vin is the volume of inflow during the time step (m^3H2O), Vout is the volume of out flow during the time step (m^3H2O),$\Delta Vstorage$ is the change in the volume of storage during time step (m^3H2O),The Eqn 2.17 can be written as:

$\Delta t * (\frac{q_{in,1}+q_{in,2}}{2})$- $\Delta t * (\frac{q_{out,1}+q_{out,2}}{2}) = V_{stored,1}$-$V_{stored,2}$ - - - - - - - - - - ----------Eqn 2.18

Where; $\Delta t\ is\ the\ time\ step(s)$, $q_{in,1}$ is the inflow rate at the beginning of the flow rate ($\frac{m^3}{s}$ $q_{in,2}\ is\ the\ inflow\ rate\ at\ the\ end\ of\ the\ flow\ rate$ ($\frac{m^3}{s}$), $q_{out,1}$ is the outflow rate at the beginning of flow rate($\frac{m^3}{s}$), $q_{out,2}$ is the outflow rate at the end of flow rate ($\frac{m^3}{s}$), $V_{stored,1}$ is the storage volume at the beginning of time step (H_2O) and $V_{stored,2}$ is the storage volume at the end of time step (H_2O)

Rearranging Eqn 2.18, all the known variable are on the left side of the equation, $\bar{q}_{in} + \frac{V_{stored,1}}{\Delta t} - \frac{q_{out}}{2} = \frac{V_{stored,2}}{\Delta t} + \frac{q_{out}}{2}$ ---------- ----------Eqn 2.19

Where: $\bar{q}_{in}$ is the average inflow rate during the time step.

$TT = \frac{V_{Sstored}}{q_{out}} = \frac{V_{stored,1}}{q_{out,1}} = \frac{V_{stored}}{q_{out,2}}$----------Eqn.2.20

Where: TT is the travel time and others are as defined before

By substituting Eqn 2.20 is substituted into Eqn 2.19 to develop a relationship between travel time and storage coefficient

$\bar{q}_{in} + \frac{V_{stored}}{(\frac{\Delta t}{TT})*(\frac{V_{stored,1}}{q_{out,1}})} - \frac{q_{out,1}}{2} = \frac{V_{stored}}{(\frac{\Delta t}{TT})*(\frac{V_{stored,2}}{q_{out,2}})} + \frac{q_{out,2}}{2}$ ----------Eqn 2.21

This simplifies to

$q_{out,2} = (\frac{2*\Delta t}{2*TT+\Delta t})*\bar{q}_{in} + (1 - \frac{2*\Delta t}{2*TT+\Delta t})*q_{out,1}$ ----------Eqn 2.22

This equation is similar to the coefficient method equation ,

$q_{out,2}$ = SC*$\bar{q}_{in}$+(1-SC)*$q_{out,1}$----------Eqn 2.23

Where: SC is the storage coefficient. Eqn 2.23 is the basis for the SCS convex routing method and the Muskingum method. From equation Eqn 2.22 the storage coefficient in Eqn 2.23 is defined as

$SC=\frac{2*\Delta t}{2*TT+\Delta t}$ ----------Eqn 2.24

It can be shown that

(1-sc)* q_{out}=SC*$\frac{V_{stored}}{\Delta t}$ ----------Eqn 2.25

Substituting Eqn 2.24 into Eqn 2.23 gives

$q_{out,2}$=SC*(q_{in}+$\frac{\mathrm{V_{stored}}}{\Delta t}$) ----------Eqn 2.26

To express all values in units of volume, both sides of the equation are multiplied by the time step and Eqn 2.27 obtained.

$q_{out,2}$=SC*(V_{in} +V_{stored}) ----------Eqn 227.

3. MATERIAL AND METHODS

3.1. Description of Study Area

3.1. 1. Location /Topography

Awash River Basin is one of the significant river basins among the twelve River Basins in Ethiopia. This basin covers a total land area of 110,000 km^2. The river rises on the high plateau near Ginchi town west of Addis Ababa in Ethiopia and flows along the rift valley into the Afar triangle, and terminates in salty Lake Abbe on the border with Djibouti (Dilnesaw, 2006). This study was conducted on the upper most part of Awash River Basin, which is located between latitude 8° 30‘ N and 9° 5‘ N and longitude 38° 7‘ E and 39° 18‘ E. with the outlet at Modjo gauging station. The areal coverage of the watershed is about 1702.15km^2.

Generally highlands and lowlands characterize the topography of Modjo watershed. The highlands with an elevation range of 1790-3060 m.a.s.l occupy the northern and western part of the study area. The lowlands on the southern and eastern have an altitude range of 1550-1800 m.a.s.l. Northern part of the basin has a steeper slope of more than 15% (Dilnesaw, 2006).

3.1.2. Climate and Hydrology

The climate of the Awash basin is humid to sub-humid in the highlands and semi-arid to arid in the rift valley and it is under the influence of the Inter-Tropical Convergence Zone (ITCZ). This Zone of low pressure marks the convergence of dry tropical easterlies and moist equatorial westerly. The explanation of the seasonal rainfall distribution within the basin lies in the annual migration of the ITCZ across the basin. The ITCZ starts its advance across the basin from south in March, bringing the small- or spring – rains. In June and July it reaches it’s most northerly location beyond the basin, which it experiences the heavy summer rains throughout. The ITCZ returns southwards during August, September and October, restoring a drier, easterly air stream that prevails until the ITCZ resumes its northward migration in March. The distribution of rainfall over the highland areas tends to be modified by orographic effects. (Dilnesaw, 2006)

As it is described above the major rainy season is between June and mid-September with a short monsoon rain in March to April. The Modjo catchment has an annual average rainfall of 1069 mm unevenly distributed throughout the year. Mean annual temperature is about around 20°C. The

lowest temperature occurs during the main rainy season; seasonal temperature variation is not pronounced. The rainfall shows strong altitudinal variations (Dilnesaw, 2006).

3.1.3. Soils of the study area

Soils of the study area are classified by the FAO (1990) soil classification system. There are four major soil types in the upper basin of Awash river: the deep red clay soil, Nitosols, the dark clay soil, Vertisol, Luvisol, and Cambisol. The Nitosols are found in the upland areas, whereas the Cambisols and Luvisols are found in the escarpment and Vertisols are found in lowland areas with slopes ranging from 2 to 8%..The Vertisols are by far the dominant soil classes, accounting for about 60% of the study area, and including the upland plains, all the seasonal swamps, and most of the alluvial cover flood plains and terraces (Dilnesaw, 2006).

3.1.4 Land use and Land cover

Soil type, mineral resources, vegetation, topography, climate and location influence the potential use of a piece of land. Based on these factors land can be used for urban development, small and large scale agricultural activities, and forestry, mining or solid waste disposal. Open bushy woodland being the dominant, open bushy wood lands, dense wood lands, grass land, and open shrub are the prominent types of vegetation that are found in the study area. The main land use categories are cultivation of annual crops and livestock grazing and urban centers.

There is a significant difference in the extent and intensity of utilization within each land use type and each activity has not been equally practiced. Crop production has got a lion share of the existing land use than livestock rearing; this is considered as a secondary activity. Nevertheless it is an essential part of agricultural practices to back up the crop production. Cereal crops are entirely based on rainfall (rain fed cropping) but root crops, and vegetables are produced along Mojo River using irrigation.

3.2 Climate projections

3.2.1 Climate Scenario

GCM derived scenarios of climate change were used for predicting the plausible future climate of the study area as they conform to most of the criteria proposed by the IPCC task group on data and scenario support for impact and climate assessment (IPCC-TGICA). IPCC recommends using multiple scenarios. At minimum scenarios constructed from two different GCMs should be used in

impacts assessments. Despite the advances in computing technology that have enabled large increases in the resolution of GCMs over the last few years, climate model results are still not sufficiently accurate at regional scales to be used directly in impacts studies (Mearns et al., 1991).

In this study due to availability of limited public domain of GCM data and time constraint, only the GCM data from UK Hadley Center (HadCM3) was used. Further, it was also for this GCM data a freely available downscaling tool was obtained and used to bridge the spatial and temporal resolution gaps between what climate modelers are currently able to provide (Wilby & Dawson, 2007). Statistical Down Scaling Model was used.

3.2.2 Statistical Down Scaling Model

Statistical Down Scaling Model (SDSM) is a decision support tool for assessing local climate change impacts using a robust statistical downscaling technique. SDSM facilitates the rapid development of multiple, low cost, single site scenarios of daily surface weather variables under present and future climate forcing. SDSM calculates statistical relationships, based on multiple linear regression techniques, between large-scale (the predictors) and local (the predictand) climate. These relationships were developed using observed weather data and, remain valid in the future. SDSM used to obtain downscaled local information for future time period by driving the relationships with GCM-derived predictors.

3.2.3 Statistical Down Scaling Model Input

The predictor variables provide daily information concerning the large-scale state of the atmosphere, while the predictand describes conditions at the site scale (i.e. temperature or precipitation observed at a station). Large-scale predictor variable information was obtained from the National Center for Environmental Prediction (NCEP) reanalysis data set (for the calibration and validation) and HadCM3 GCM data were used for the baseline and climate scenario periods.

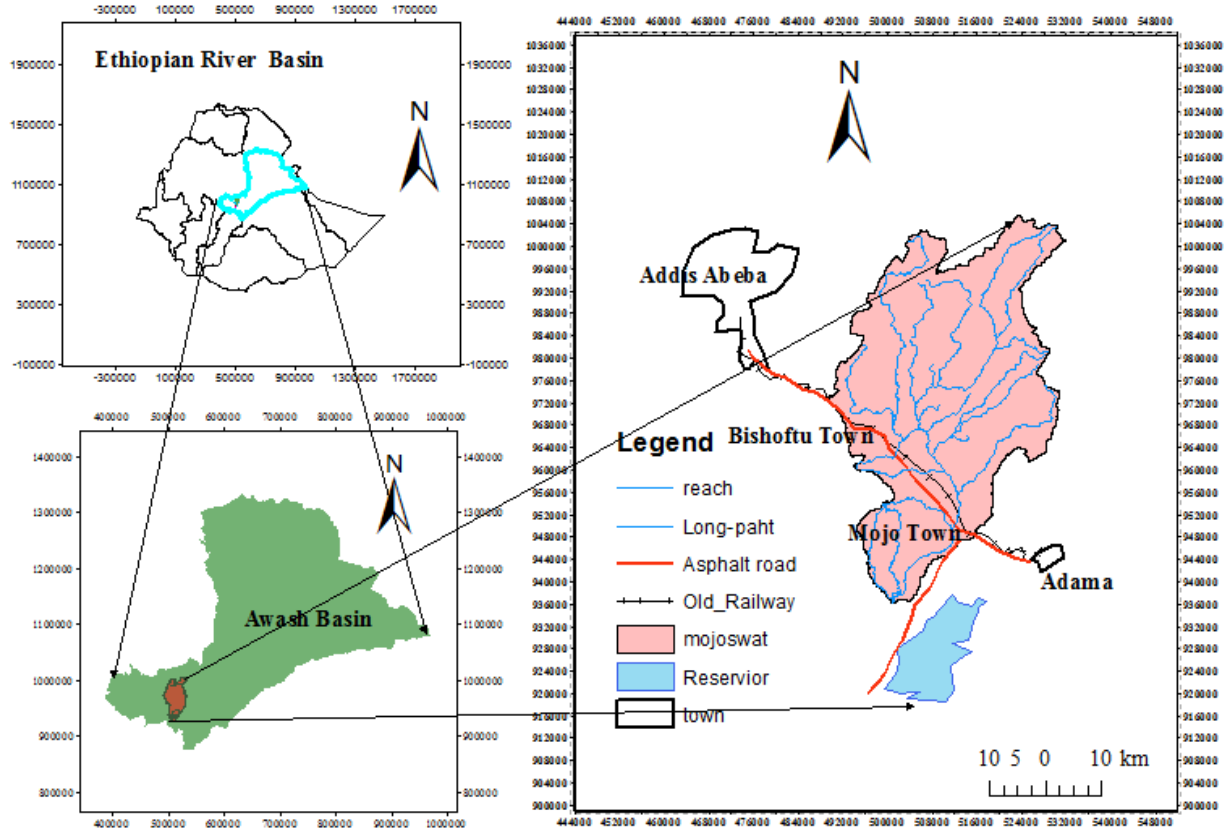

Figure3.**1 Location Map of Modjo sub basin**

The HadCM3 predictor variables were available for the A2a and B2a experiments and were downloaded from the Environment Canada website. The predictor variables were supplied on a grid by grid box basis on entering the location of the site. For the study latitude :(8^0 61 '-8^0 97'N and Longitude: 38^0 95 '-39^0 26 'E) the correct grid box calculated and a zipped file was downloaded. The downloaded data consists of three data files as listed below and represents resolution of2.50 latitude by 3.750 longitudes.

NCEP_1961-2001: This directory contains 41 years of daily observed predictor data, derived from the NCEP reanalysis, normalized over the complete 1961-1990 period

H3A2a_1961-2099: This directory contains 139 years of daily GCM predictor data ,derived from the HadCM3 A2(a) experiment, normalized over the 1961-1990 period

H3B2a_1961-2099: This directory contains 139 years of daily GCM predictor data, derived from the HadCM3 B2 (a) experiment, normalized over the 1961-1990 period

The predictors of the NCEP and HadCM3 GCM experiment were listed in the Table 3.1 with their descriptions. The predictand variables used in this study were precipitation, maximum and

minimum temperature. The stations in the study area, Debrezeyit, Modjo, Ejere & Chefedensa which were taken for downscaling. All of the stations in the drainage basin lay in the same grid box in the African window.

3.2.4 SDSM Modeling Approach

The downscaling of the GCMs data using SDSM was done following the procedures in the flow chart (Figure 3. 1). Before starting the main SDSM downscaling operation, quality control of the data was undertaken to check an input data file for missing and unreasonable values. Scatter plot analysis was performed and it was checked that all the predictands were normally distributed; hence transformation operation was found unimportant. The other operations performed for downscaling are dealt in detail in the following sections.

3.2.4.1 Screening of downscaling predictor variables

The screen variables option used to select the appropriate downscaling predictors for model calibration. The screening of variables was done by trial and error procedure and it was the most time consuming activity in the downscaling process. For maximum and minimum temperature downscaling an unconditional process was selected as the predictor-predict and process was not regulated by an intermediate process where as for the precipitation as the amount depends on wet-dry day occurrence, a conditional process was selected. The significance level which tests the significance of predictor-predictand correlation was set to the default ($P<0.05$). The correlation analysis was used to investigate inter-variable correlations for specified periods (monthly, seasonal, or annual). The correlation matrix gives a report for the partial correlations between the selected predictors and predict and which helped to identify the amount of explanatory power that was unique to each predictor. Using the partial correlations statistics, predictors which showed the strongest association with the predictand were selected. The scatter plot operation was also performed for visual inspection of inter-variable behavior for specified sub-periods (monthly, seasonal, or annual). The scatter plots were used to see the nature of association (linear, non-linear, etc) between the predictor and predictand which was important to decide whether or not data transformation was necessary.

Table 3.1 NCEP daily predictor variable and definitions

No	Predictor variable	Predictor Description	No	Predictor variable	Predictor Description
1	dswr	Direct shortwave radiation	17	p5th	Wind direction at 500 hPa
2	lftx	Surface lifted index	17	p5zh	Divergence at 500 hPa
3	mslp	Mean sea level pressure	18	p_zh	Divergence near the surface
4	p__f	Geostrophic airflow velocity near the surface	19	p8_f	Geostrophic airflow velocity at 850 hPa
5	p__u	Zonal velocity component near the surface	20	p8_u	Zonal velocity component at 850 hPa
6	p__v	Meridional velocity component near the surface	21	p8_v	Meridional velocity component at 850 hPa
7	p__z	Vorticity near the surface	22	p8_z	Vorticity at 850 hPa
8	p_th	Wind direction near the surface	23	p8th	Wind direction at 850 hPa
9	p_zh	Divergence near the surface	24	p8zh	Divergence at 850 hPa
10	p5_f	Geostrophic airflow velocity at 500 hPa	25	p500	500hPa geopotential height
11	p5_u	Zonal velocity component at 500 hPa	26	p850	850hPa geopotential height
12	p5_v	Meridional velocity component at 500 hPa	27	pottmp	Potential temperature
13	p5_z	Vorticity at 500 hPa	28	pr_wtr	Perceptible water
14	prec	Precipitation total	29	rhum	Near surface relative humidity
15	r500	Relative humidity at 500 hPa height	30	shum	Near surface specific humidity
16	r850	Relative humidity at 850 hPa height	31	temp	Near surface air temperature

**hpa – is a unit of pressure, 1 hPa = 1 mbar = 100 Pa = 0.1 kPa*

All variables are available from the SDSM portal: http: //copublic.lboro.ac.uk/cocwd /SDSM/data.html

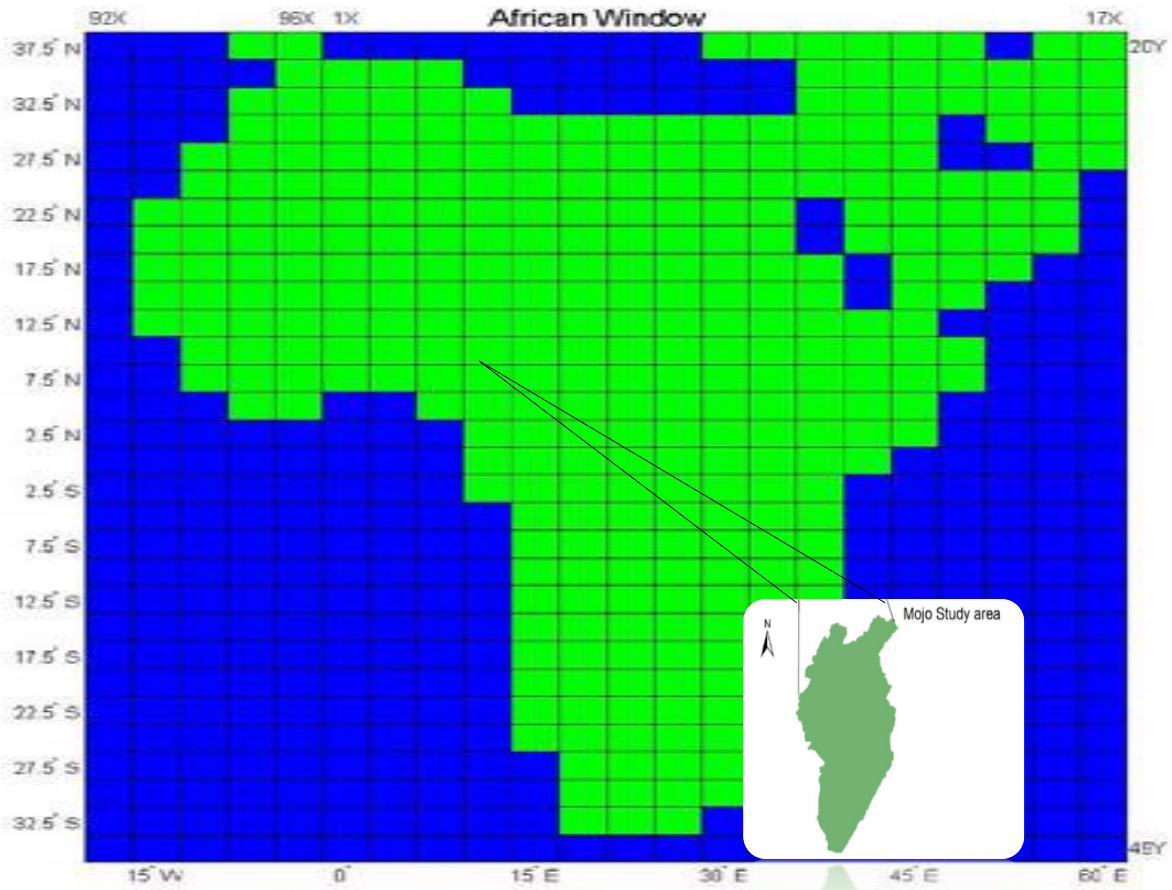

Figure **3**.2The African continent window with 2.5latitude and 3.750 Longitude grid size and location area of the study

3.2.4.2 Model Calibration

The observed data collected from the Ethiopian National Metrological Services Agency (NMSA) was from 1980-2010. Hence, the data from 1980-2001 was used for model calibration and from 2002-2010 was used for model validation. The calibrate model process constructed downscaling models based on multiple regression equations, given daily weather data (predictand) and regional scale, atmospheric (predictor) variables The ordinary least squares optimization technique was used the SDMS. An unconditional process was selected for the maximum and minimum temperature and conditional for the precipitation owing to the presence of intermediate processes (Wilby and Dawson, 2007)

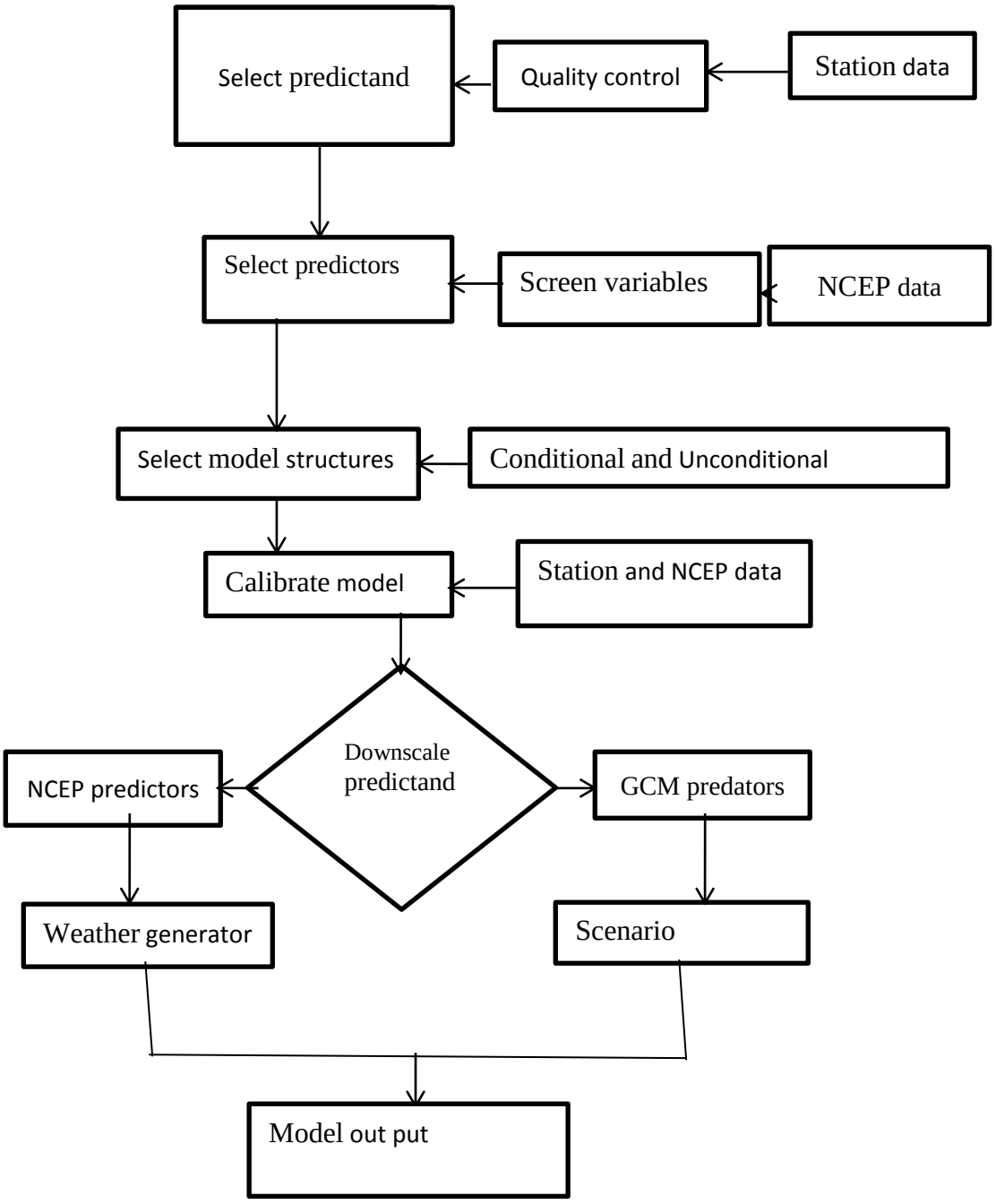

Figure 3.3 SDSM 4.1climate Scenario generation **flow chart (Wilby&Dawson, 2007)**

A monthly temporal resolution of the downscaling model was chosen to derive different model parameters for each month. Upon completion of the appropriate selections, the model was calibrated. The resultant model calibration parameter (*.par) file generated for the precipitation, maximum and minimum temperature values are shown in table 3.2.

Table 3.2 Large-scale predictor variables selected for SDMS

Station name	Precipitation	Maximum Temperature	Minimum Temperature
	ncepp500af.dat(r500)	ncepp500af.dat	ncepp500af.dat
	ncepp8_zaf.da t (p8_z)	ncepp850af.dat	ncepp850af.dat
	ncepp850af.dat (r850)	ncepshumaf.dat (shum)	ncepshumaf.dat
Modjo	nceptempaf.dat (temp)	nceptempaf.dat	nceptempaf.dat
	ncepmslpaf.dat	ncepmslpaf.dat (mslp)	ncepmslpaf.dat
	ncepp500af.dat	ncepp500af.dat	ncepp850af.dat
	ncepp850af.dat	ncepp850af.dat	ncepr850af.dat
Debrezeyit	ncepshumaf.dat	nceptempaf.dat	ncepshumaf.dat
	ncepp500af.dat	ncepp500af.dat	ncepmslpaf.dat
	ncepp850af.dat	ncepp850af.dat	ncepp500af.dat
	ncepshumaf.dat	nceptempaf.da	ncepp850af.dat
EJERE	nceptempaf.dat		ncepshumaf.dat
	ncepmslpaf.dat	ncepp500af.dat	ncepp500af.dat
	ncepp500af.dat	ncepp850af.dat	ncepp850af.dat
	ncepp5zhaf.dat	ncepr500af.dat	ncepshumaf.dat
	ncepp850af.dat	ncepshumaf.dat	
CHEFE		nceptempaf.dat	

3.2.4.3 Weather Generation

A synthetic ensembles of daily weather series were produced giving the observed (NCEP reanalysis) atmospheric predictor variables and regression model produced by the calibrate model operation. The generated weather was used for the verification of the calibrated model for an independent data set (2002-2010) withheld from the calibration process. An ensemble size of 20 (default) values was generated. Despite individual ensemble members are considered equally plausible, the mean of the 20 ensembles was used for the model validation process (Wilby and Dawson, 2007)

3.2.4.4 Scenario Generation

The calibrated and validated model was used for the generation of ensembles of synthetic daily weather series giving daily atmospheric predictor variables from the HadCM3 A2a and B2a experiment. The scenario generation produced 20 ensembles of synthetic weather data for 139 years (1961-2099), and the mean of the ensembles was calculated and used for impact assessment. According to Zeray 2006 it was adequate to consider the mean of the ensembles to see the general trend of climate change in the future, and to preserve inter-variable relationships

3.3 Hydrological Modeling

Physically based hydrological model was selected for the Modjo sub basin to assess the impact of climate change on the river .Soil and Water Assessment tool (SWAT) was selected as the best modeling tool owing to many reasons**.** SWAT is a public domain model and it is used for free. In addition in countries like Ethiopia, there is a shortage of long term observational data series to use sophisticated models; SWAT is computationally efficient and requires minimum data. SWAT was checked for the highlands of Ethiopia and gave satisfactory results (Setegn, 2008). SWAT model was developed to predict th**e** impact of land management practices on water, sediment, and agricultural chemical yields. However, this study concentrated on the hydrological aspect of the sub-basin. The description of the model, model inputs and model setup are discussed in detail in the subsequent sections.

3.3.1 SWAT Model Inputs

3 .3.1.1 Digital Elevation Model

The digital elevation model (DEM) data was used to delineate the sub-watersheds in the QSWAT interface. The DEM data was collected from the Ethiopian Ministry o of Water Resources, Irrigation and Electricity (MoWRIE), GIS department It had a resolution of 90.m*90m

3.3.1.2 Stream Network

The stream network data set was collected from the Ethiopian Ministry o of Water Resources, Irrigation and Electricity (MoWRIE), GIS department. The stream network was in a shape file format consisting of the major and minor river systems in the study area the stream network dataset was superimposed onto the DEM to define the location of the stream network. Burning-in stream network operation is most important in situations where the DEM does not provide enough detail to allow the interface to accurately predict t the location of the stream network.

3.3.1.3 Land Use/Land Cover

The land use/land cover map of the study area was collected from MoWRIE, (2014) GIS department which was obtained in shape file format. The land use/cover data reclassified according to the SWAT land use/cover type. Redefining was done based on the data collected from physical observation during field visit

Table 3.3 land use/Land cover types in the study area &redefinition according to SWAT code.

Land use/land cover types and area of watershed			
land use code	Area (ha)	Percentage of area	Description of code
TEFF	151861	89.22	EragrostisTeff
DWHT	9540.81	5.61	Durum Wheat
URBN	4890.68	2.87	Residential
WATR	6.71	0.000009	Water
WETN	328.87	0.19	Wetland- Non-Forested
RNGB	3587.9	2.11	Range-Brush
Total	170215	100	

and personal judgment A look up table that identifies the 4-letter SWAT code for the different categories of land cover/land use were prepared so as to relate the grid values to SWAT land cover/land use classes. SWAT calculated the area covered by each land use. The different land use/cover types are presented in Table.3.3

3.3.1.4 Soil Data

Soil data was also collected from the Ethiopian (MoWRIE), GIS department. However, this data was only in shape file format and the characteristics of the soils needed by the SWAT.

Table 3.4 Properties of soil

SOIL ID	Soil type	HSG	texture	KSat (mm/hr.)	BD (g/cm^2)	CB (%)	ECE (dS/m)	AWC (mm/m)
303	CMv	B	silt	7.58	1.33	2.23	1.00	0.20
305	LPq	C	loam	13.06	1.43	2.84	0.1	0.12
306	LVh	D	clay	3.17	1.23	5.54	0.09	0.09
307	LVx	D	clay	2.64	1.22	3.77	0.09	0.1
309	VRe	D	clay	1.77	1.19	3.59	0.11	0.07
316	ANm	C	loam	12.31	1.35	3.71	1.00	0.14
317	PHl	D	silt clay loam	3.03	1.25	2.54	0.04	0.14

NB,

1 HSG: hydrologic soil group
2. KSat: saturated hydraulic conductivity
3. BD: bulk density
4. CBO: organic carbon content
5 EC: electrical conductivity
6. AWC: Available soil water content

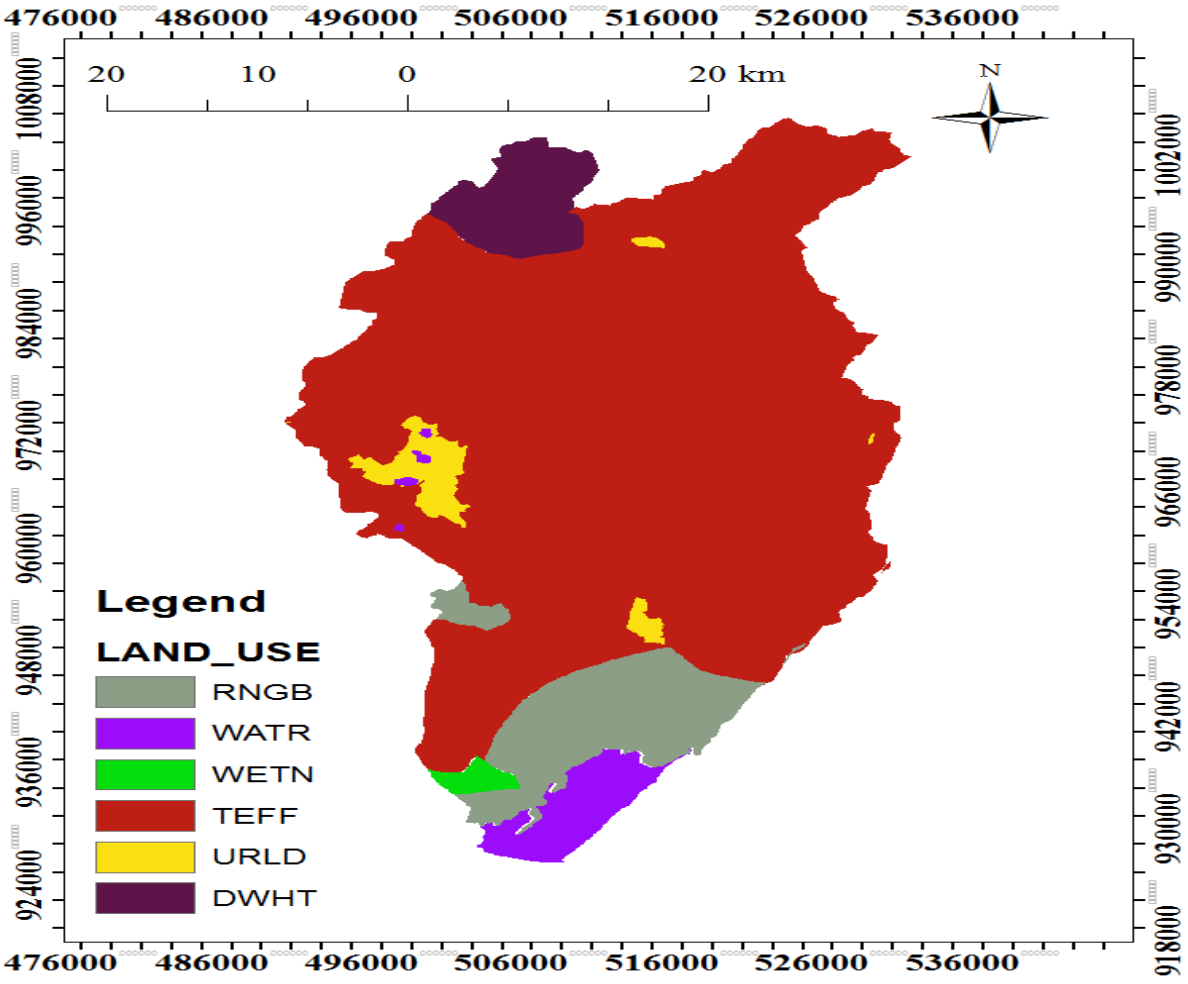

Figure 3.4 Land use/Land cover map of the study area (source shape file obtained from MOWIE)

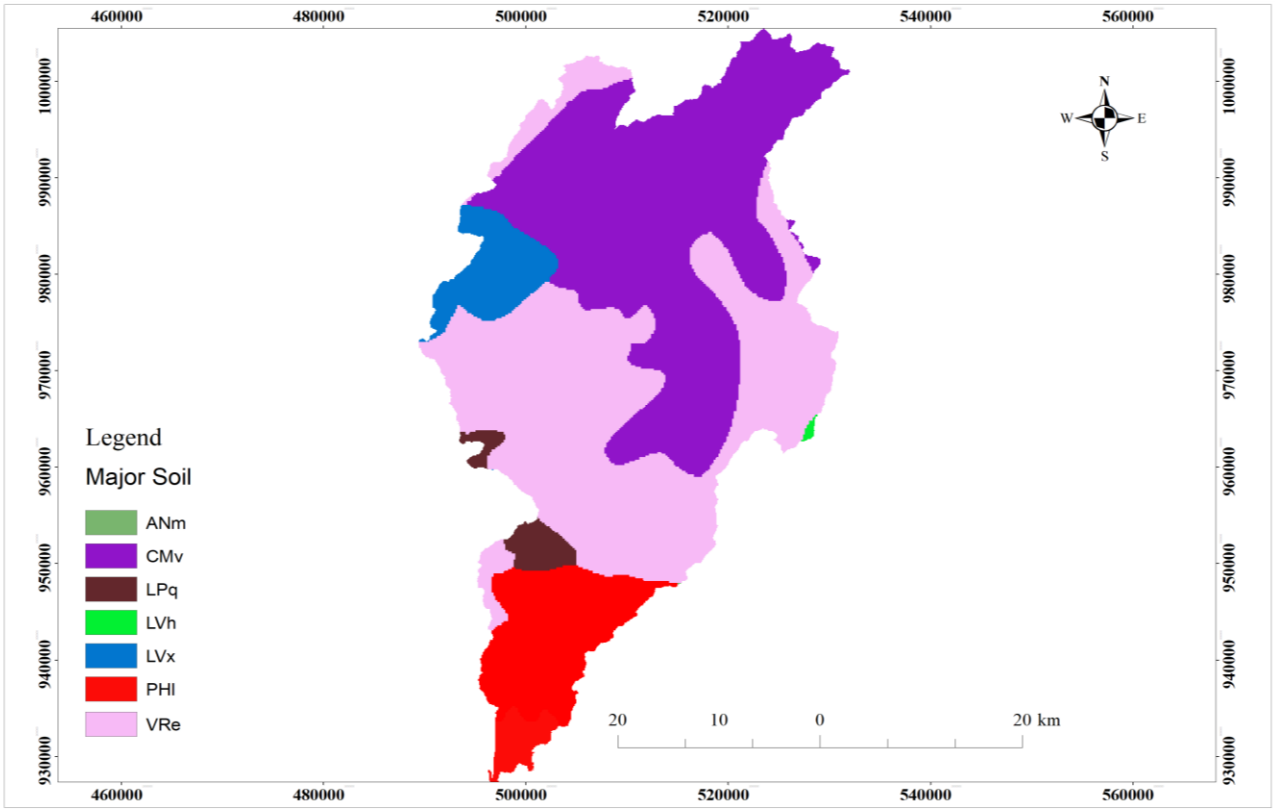

Figure 3.5 Soil map of the study area (source; shape file obtained from (MOWIE)

3.3.1.5 Meteorological Data

Meteorological data is needed by the SWAT model to simulate the hydrological conditions of the basin. The meteorological data required for this study were collected from the Ethiopian National Meteorological Services Agency (NMSA). The meteorological data collected were precipitation, maximum and minimum temperature, relative humidity, and wind speed and sunshine hours. , which were within the study area, was collected .Most the stations have missing data especially during 1963-1979 and 2011. The other problem in the weather data was inconsistency in the data record. In some periods there is a record for precipitation but there was a missing data for temperature, and vice versa. As the SWAT model requires data of the same periods of record, the weather data used for the study was set from 1980-2010 Data quality analysis was performed using SDSM quality control operation like missing data based on the SDSM quality control analysis and data availability.

The hydrological (flow) data was required for performing sensitivity analysis, calibration and uncertainty analysis and validation of the SWAT model. The hydrological data was also collected from the Ethiopian MoWRIE, hydrology section. The hydrological data collected was daily flow for the Modjo River at Mojo flow station.

3.4.1.1. SWAT Model Approach

The model setup involved:(1) data preparation, (2) sub basin discretization, (3) HRU definition, (4) parameter sensitivity analysis, (5) calibration and uncertainty analysis. The required spatial data sets Projected to the same projection called WGS 1984_UTM Zone 37 N, which is the transverse Mercator projections for Ethiopia, using steps such as DEM setup, stream definition, outlet and inlet definition, watershed outlets selection and definition and calculation of sub basin parameters. For the stream definition the threshold based stream definition option was used to define the minimum size of the sub basin. The SWAT interface allows the user to fix the number of sub basins. The spatially distributed data (GIS input format) needed for the SWAT interface includes the Digital Elevation Model (DEM), soil data, and land use data. Data on weather and flow used for prediction of water balance and calibration purposes respectively using GIS 10.4. The Land use/Land cover spatial data was reclassified into SWAT land cover/plant types. The SWAT codes for the different categories of land cover/land use was fed manually on the map as per the inputs prepared by SWAT format the following seven main basic steps were done

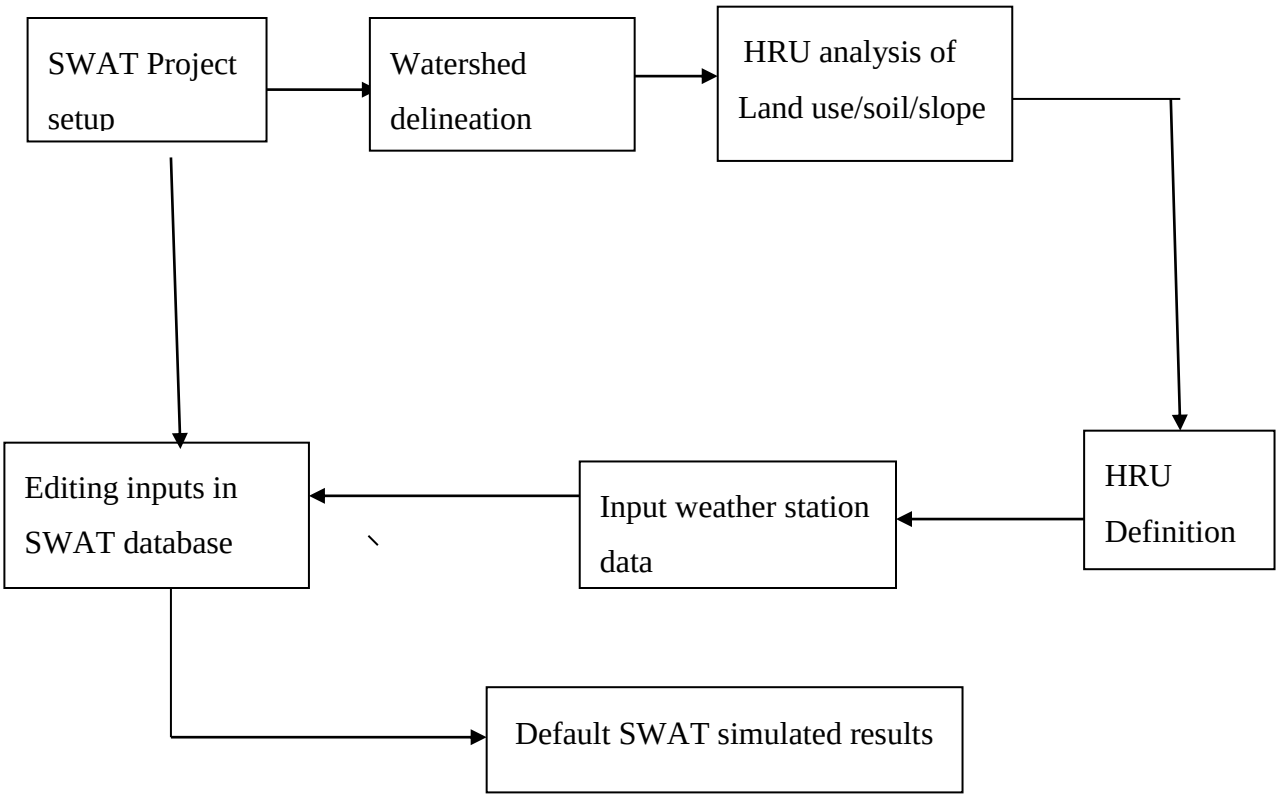

Figure 3.6 Summarized flow SWAT model chart

3.4.1.2 Watershed delineation

QSWAT used digital elevation model (DEM) data to automatically delineate the watershed into several hydrological connected sub-watersheds. The first step in the watershed delineation was loading the properly projected DEM. To reduce the processing time of the GIS functions, a mask will create over the DEM around the study area. Then a poly line stream network dataset will burn in to force SWAT sub-basin reaches to follow known stream reaches. Burning-in a stream network improves hydrological segmentation, and sub-watershed delineation. After the DEM grid load and the stream networks superimpose, the DEM map grid processed to remove the non-draining zones. The initial stream network and sub-basin outlets defined based on drainage area threshold approach. The interface lists a minimum, maximum and suggested threshold area. The smaller the threshold area, the more detail the drainage network delineate by the interface but the slower the processing time and the larger memory space required. In this study, defining of the threshold drainage area was done by successive re-run of the stream and outlet definition routine from the suggested to the minimum are until known smaller streams was created

(http://www.brc.tamus.edu/swat**)**.

3.4.1.3 Importing Weather Data

Weather data used in a watershed simulation was imported in order to provide the moisture and energy inputs that control the water balance and determined the relative importance of the different components of the water cycle. The weather data required by SWAT consist of daily precipitation, maximum/minimum temperature, solar radiation, wind speed and relative humidity. In dbase format the climatic input variables imported together with their weather location and based on data availability.

3.4.1 4. Hydrologic Response Unit Analysis

Hydrologic response units (HRUs) were lumped land areas within the sub-basin that are comprised of unique land cover, soil and management combinations. HRUs enable the model to reflect differences in evapotranspiration and other hydrologic conditions for different land covers and soils. The runoff is estimated separately for each HRU and routed to obtain the total runoff for the watershed. This increases the accuracy in flow prediction and provides a much better physical description of the water balance. The land use and the soil data in a projected shape file format loaded into the SWAT interface to determine the area and hydrologic parameters of each land-soil category simulated within each sub-watershed. After the land use SWAT code assigned to all map categories, calculation of the area covered by each land use and reclassification was done. The land slope classes also integrated in defining the hydrologic response units. The DEM data used during the watershed delineation was also used for slope classification. The multiple slope classification operation was preferred over the single slope classification as the sub-basins have a wide range of slopes between them. Based on the suggested min, max, mean and median slope statistics of the watershed, five slope classes (0- 3, 3-8, 8-15, 15-30 and 30-50%) were applied and slope grids were reclassified **(**MOA, 2005**).**

After their classification of the land use soil and slope grids overlay operation was performed **(**http://www.brc.tamus.edu/swat).

Table 3.5 slope classes (MOA, 2005)

slope classes	Range (%)
Flat or almost flat	0-3
Gently sloping	3-8
Sloping	8-15
Moderately steep	15-30
Steep	30-50

3.4.1.5Sensitivity analysis

As watershed processes are influenced by a large number of parameters, sensitivity analysis was performed using the Sequential Uncertainty Fitting (SUFI-2) algorithm to identify the key parameters that affect stream flow for calibration. Within SUFI-2 the global sensitivity analysis (was performed after iteration).An approach which considers the sensitivity of one parameter in relation to other parameters under consideration was used to determine the sensitive parameters in this study (Abbas pour, 2012).The t-stat which gives a measure of the sensitivity of a parameter and the p-value, the significance of the sensitivity of that parameter were used to rank the various parameters considered to influence stream flow. However, these parameters vary from one watershed to the other depending on prevailing geomorphologic characteristics and activities existing in a watershed and therefore cannot assume generalization status. In initializing the sensitivity analysis, the parameters taken and the final parameters were selected based on test statics. Following sensitivity analysis, model calibration was done using the selected most sensitive parameters.

3.4.1.6. Calibration and Validation of SWAT model

The complex processes occurring in watersheds coupled with the uncertainty inherent in hydrologic modeling parameters, inputs and measured data requires that the hydrologic models be calibrated and validated to minimize predictive errors(http://dx.doi.org/10.1029/2007wr006609) One of the most widely accepted algorithm; the Sequential Uncertainty Fitting (SUFI-2)which operates based on the Latin Hypercube sampling procedure was used to calibrate and validate (http://dx.doi.org/10.1016/j.jhydrol.2006.09.014.) A split sample procedure using monthly stream flow data from Modjo stream gauge for the period 1998-2005 and 2006-2010 were used for

calibration and validation the first year taken for warming up the model before calibration and validation processes.

The SUFI-2 algorithm was operationalzed within the SWAT calibration and Uncertainty Procedure (SWATCUP) environment. As suggested by (Abbaspour et al., 2007) several model simulations were executed with a minimum of 500 simulations in each run. Following each run, simulated results were compared with observed variables of interest and the performance of the model in simulating the observed variable judged against four objective functions. The choice of an objective function is dictated by the object of any particular study and hence there is no objective function that is universally applicable to all situations (Abbaspour et al.2004) In this study however, efficiency measures including the Nash-Sutcliffe (NSE) (Abbaspour et al.,2004) the coefficient of determination (R^2) (Setegn et al. 2008) percent bias (PBIAS) (Moriasi et al.2007) [and RMSE-observations standard deviation ratio(RSR)) (Moriasi et al.2007) were used to evaluate the performance of the model. The performance of SWAT was evaluated using statistical measures to determine the quality and reliability of predictions when compared to observed values. Coefficient of determination (R^2) and Nash-Sutcliffe simulation efficiency (ENS) were the goodness of fit measures used to evaluate model prediction. The R^2 value is an indicator of strength of relationship between the observed and simulated values. The Nash-Sutcliffe simulation efficiency (ENS) indicates how well the plot of observed versus simulated value fits to the 1:1 line. If the measured value is the same as all predictions, ENS is 1. If the ENS is between 0 and 1, it indicates deviations between measured and predicted values. If ENS is negative, predictions are very poor, and the average value of output is a better estimate than the model prediction (Nash and Sutcliffe, 1970).

$$NSE = 1 - \frac{\sum_{i=1}^{n}(Oi-Si)^2}{\sum_{i=1}^{n}(Oi-O)^\wedge 2} \text{-----------------------------------Eqn 3.1}$$

$$R^2 = [\frac{\sum_{i=1}^{n}(Oi-Si)(Si-S)}{\sum_{i=1}^{n}(Qi-O)^\wedge 2)^\wedge 05(\sum_{i=1}^{n}(Si-S)^\wedge 2)^\wedge 0.5}]^\wedge 2 \text{----------------------} Eqn\ 3.2$$

$$\text{PBIAS}= \frac{\sum_{i=1}^{n}(Oi-Si)*100}{\sum_{i=1}^{n}Oi} \text{-----------------------------------Eqn3.3}$$

$$\text{RSR}=\frac{\sqrt{\sum_{i=1}^{n}(Oi-Si)^\wedge 2}}{\sum_{i=1}^{n}(Oi-O)^\wedge 2} \text{-----------------------------------Eqn3.4}$$

where;

Oi = observed variable, Si = simulated variable, O = mean of observed variable, S = mean of simulated variable, n = number of observations under consideration Based on the values of the performance parameters above, the following guideline table for a performance rating of a general watershed simulation model is set up (Moriasi et al,2007).

Table 3.6 Model performance rating based on the range of values for RSR, NSE and PBIAS

Performance rating	RSR	NSE	PBIAS (%)
Very good	$0.00 \leq RSR \leq 0.5$	$0.75 < NSE \leq 1.00$	PBIAS$\leq \pm 1.00$
Good	$0.5 <$ RSR ≤ 0.6	$0.65 < NSE \leq 0.75$	$\pm 10 \leq PBIAS < \pm 15$
Satisfactory	$0.60 < RSR \leq 0.70$	$0.50 \leq NSE \leq 0.65$	$\pm 15 \leq PBIAS < \pm 25$
Unsatisfactory	RSR> 0.70	$NSE < 0.50$	PBIAS≥ 25

4. Results and Discussion

4.1 Climate Projection

4.1.1 Comparison between observed climate Data of the Stations

To see the relation among the stations' temperature and precipitation values, inter comparison of the stations' data was carried out. The data from 1980 to 2010 were averaged over a monthly period to calculate correlation coefficients of the stations.

The correlation involved four stations for precipitation, maximum and minimum temperature. As shown in table 4.1, the average monthly precipitation correlation analysis among the stations resulted in correlation coefficient ranging from 0.983-0.995 .This shows presence of a good agreement among stations 'for precipitation. The correlation of the other stations for precipitation with that of Debrezeyit station specifically showed very high values ranging from 0.987-0.992

Table 4.1 The average monthly precipitation simple correlation analysis

stations	Mojo	Ejere	Debrezeyit	Chefe
Mojo	1	0.983	0.987	0.976
Ejere		1	0.992	0.995
Debrezeyit			1	0.994
Chefe				1

Similarly the correlation analysis of the average monthly temperature resulted in correlation coefficients ranging from 0.163 to 0.995 for maximum temperature, and from 0.814 to 0.992 for minimum temperature This still shows a strong relation among the temporal trends of temperature across the stations with the exception of maximum temperature with R^2 value of 0.163 between Mojo and Ejere. Like the precipitation, the correlation between the other stations' minimum and maximum temperature with that of Debrezeyit station showed a very good correlation coefficient ranging from 0.184 to 0.995 for average maximum temperature, and from 0.814 to 0.981 for average minimum temperature values.

Table 4.2 The average monthly maximum and minimum temperature correlation analysis

	Average monthly maximum temperature				Average *monthly minimum temperature*			
stations	1	2	3	4	1	2	3	4
Mojo(1)	1	0.163	0.995	0.410	1	0.814	0.981	0.803
Ejere(2)		1	0.184	0.950		1	0.827	0.992
Debrezeyit (3)			1	0.400			1	0.814
Chefe(4)				1				1

Hence, Debrezeyit station can be taken as representative station for the climate variables including average monthly precipitation, maximum temperature, and minimum temperature. The average temperature differences from the base-period values (deltas) and the average monthly precipitation change factors (precipitation multipliers) developed for this station can then be applied for the other stations too.

4.1.2 Predictor Variables Selection

The best correlated predictor variables selected for precipitation, maximum temperature and minimum temperature are listed in Table 4.3.The precipitation showed a better correlation with ncepp500af.dat and ncepp850af.dat for the Debrezeyit station The correlation of maximum temperature with the predictor variables were ncepp850af.dat, ncepp500af.dat and nceptempaf.dat strong common for all stations and for minimum temperature common for all stations were nceptempaf.dat, ncepp850af.dat and ncepshumaf.dat

4.1.3 Calibration and Validation

The calibration was carried out from 1980-2001 for twenty-two years and the data from 2002-2010 were used for model verification. It was better than when compared with earlier research works such as Dile,(2009) in which 8 years (1990-1997) data was used for calibration and 4 (1998-2001) years of data was used for model verification and Zeray,(2006) used 15years (1981-1995) and 5years (1996-2000) of data for calibration and validation respectively The model develops a better

multiple regression equation parameters for the maximum and minimum temperature than the precipitation. This is mainly due to the conditional nature of precipitation

Table 4.3 selected predictor variables for the predictands (precipitation, maximum and minimum temperature at Debrezeyit stations0

Station name	Precipitation	Maximum Temperature	Minimum Temperature
Debrezeyit	ncepmslpaf.dat	ncepmslpaf.dat	ncepmslpaf.dat
	ncepp500af.dat	ncepp500af.dat	ncepp850af.dat
	ncepp850af.dat	ncepp850af.dat	ncepr850af.dat
	ncepshumaf.dat	nceptempaf.dat	ncepshumaf.dat

In conditional models, there is an intermediate process between regional forcing and local weather (e.g., local precipitation amounts depend on wet and dry day occurrence, which in turn depend on regional–scale predictors such as humidity and atmospheric pressure) (Wilby and Dawson 2004).

Twenty ensembles of synthetic daily weather series generated using NCEP-reanalysis data for the verification of the calibrated model. The mean of the 20 ensembles of maximum temperature and minimum temperature values gave a better R^2 values, inferring that future projections would also be well replicated. The precipitation verification showed that the calibrated model couldn't able to replicate the independent data set. This is due to complicated nature of precipitation processes and its distribution in space and time. Climate model simulation of precipitation has improved over time but is still a problematic (Bader et al., 2008). Thorpe (2005) also added that rainfall predictions have a larger degree of uncertainty than those for temperature. This is because rainfall is highly variable in space and the relatively coarse spatial resolution of the current generation of climate models is not adequate to fully capture that variability. The summarized monthly values of the observed precipitation, maximum temperature and minimum temperature *vs* the corresponding modeled values are shown in Figure 4.1, Figure 4.2, and Figure 4.3 respectively.

These results show that the simulated maximum temperature has better agreement with the observed results than the other two variables.

Table 4.4 calibration statistics of monthly precipitation, maximum and minimum temperature

R^2		
Predictand	unconditional	conditional
Precipitation	0.306	0.385
Maximum Temperature	0.68	
Minimum TEMPRATURE	0.46	

The simulation of precipitation showed relatively lesser agreement as compared to the maximum temperature. However the result is acceptable due to the fact that precipitation is a conditional process, Conditional processes like precipitation are dependent on other intermediate processes like on the occurrence of humidity, cloud cover, and/or wet-days. Unconditional processes like temperature; however, are not regulated by other intermediate processes. In addition, as indicated in the SDSM manual (Wilby and Dawson 2004), local temperatures are largely determined by regional forcing whereas precipitation series display more "noise" arising from local factors. Hence, larger differences can be observed in precipitation ensemble members than that of temperature. As compared to some similar downscaling results of earlier studies (e.g. Wilby 2005), these results are acceptable. On the other hand, the minimum temperature simulation shows a poor agreement with the observed one. Even though it is difficult to exactly point out the reason behind, this may be due to the inferior data quality used for the comparison purpose.

Validation was done based on 9 year simulation from 2002 to 2010. Here also 20 ensembles (runs) of daily values were generated and the average of these ensembles was taken for the comparison. The validation statistics for all the three predictand variables are shown in table 4.5The correlation coefficients that were found during the calibration step are more or less maintained during the validation step too, even better agreements are found here. However, the agreement of the simulated minimum temperature with the observed one remains poor but good for that of precipitation and maximum temperature

Table 4.5 validation statistics of monthly precipitation, maximum and minimum temperature

R^2		
predictand	unconditional	Conditional
Precipitation (condtional)	0.33	0.34
Maximum Temperature	0.69	
Minimum TEMPRATURE	0.49	

.

a) Percipitation

As can be seen in figure 4.1, SDSM is able to simulate all except the extreme precipitation events like for the month of December. The model underestimates the farthest values in both extremes and keeps more or less an average event. This lack of replicating the extreme values was also observed by Wilby (2005) and he described it as "*the model is less skillful at replicating the frequency of events*

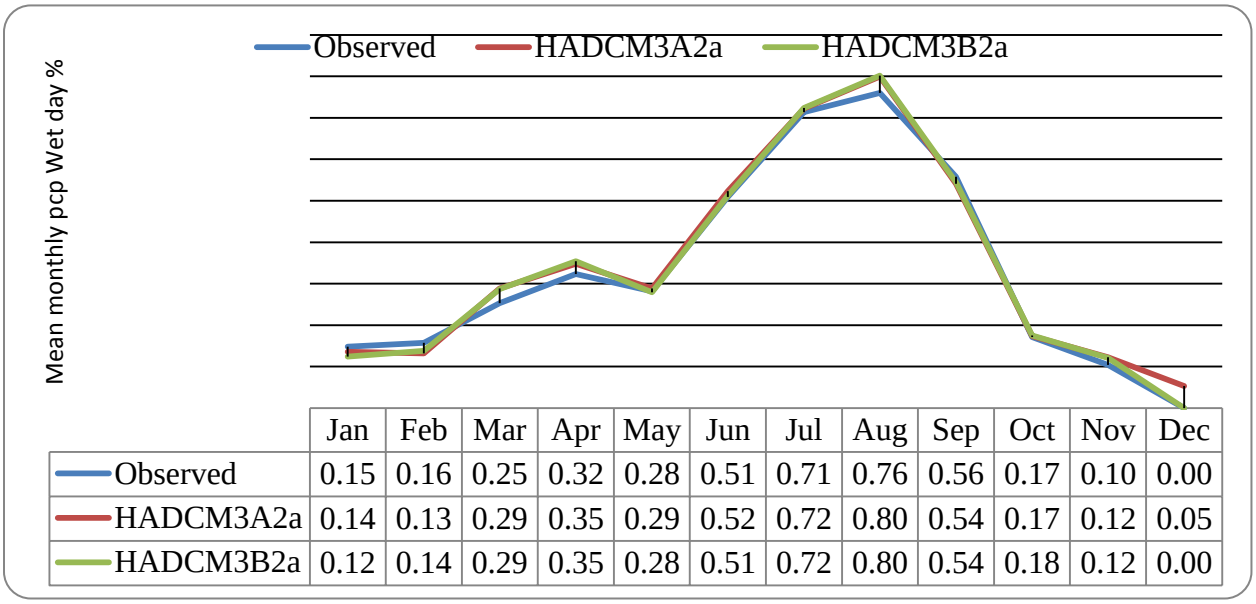

	Jan	Feb	Mar	Apr	May	Jun	Jul	Aug	Sep	Oct	Nov	Dec
Observed	0.15	0.16	0.25	0.32	0.28	0.51	0.71	0.76	0.56	0.17	0.10	0.00
HADCM3A2a	0.14	0.13	0.29	0.35	0.29	0.52	0.72	0.80	0.54	0.17	0.12	0.05
HADCM3B2a	0.12	0.14	0.29	0.35	0.28	0.51	0.72	0.80	0.54	0.18	0.12	0.00

Figure 4.1 Mean daily precipitation wet period percentage for Debrezeyit station A2a and B2a

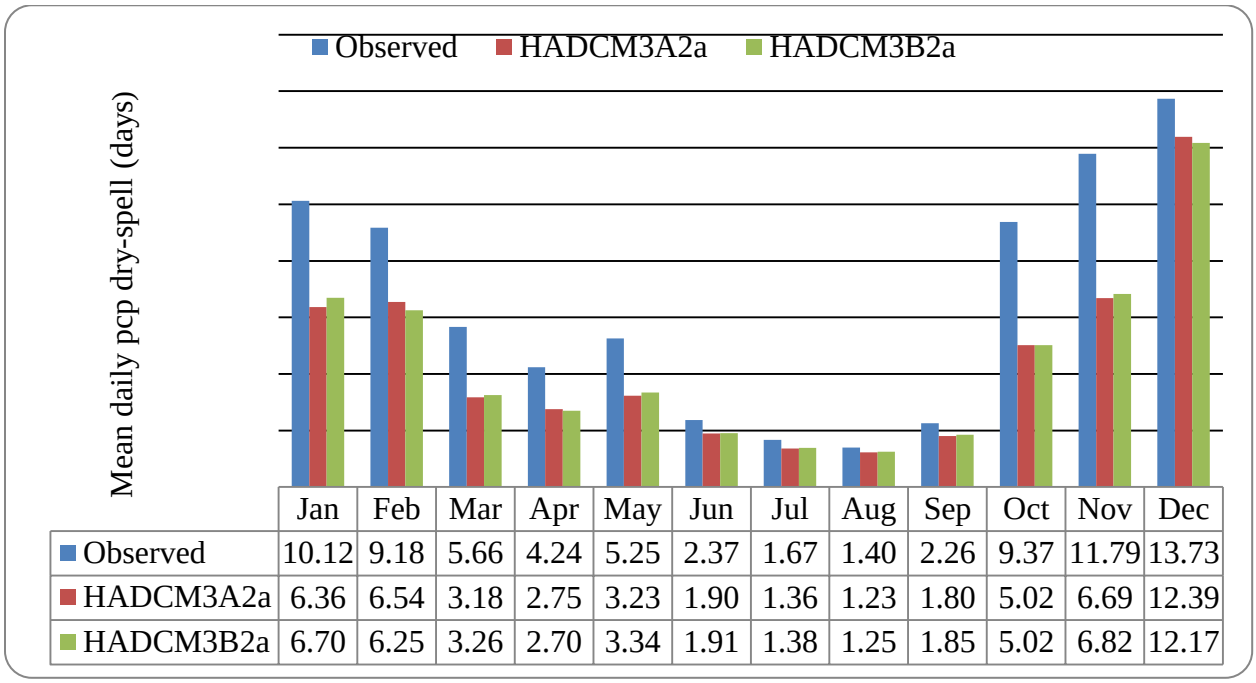

	Jan	Feb	Mar	Apr	May	Jun	Jul	Aug	Sep	Oct	Nov	Dec
Observed	10.12	9.18	5.66	4.24	5.25	2.37	1.67	1.40	2.26	9.37	11.79	13.73
HADCM3A2a	6.36	6.54	3.18	2.75	3.23	1.90	1.36	1.23	1.80	5.02	6.69	12.39
HADCM3B2a	6.70	6.25	3.26	2.70	3.34	1.91	1.38	1.25	1.85	5.02	6.82	12.17

Figure 4.2 Mean daily precipitation dry-period for Debrezeyit station A2a and B2a

b)Minimum Temprature

The monthly minimum temperature downscaled forA2aandB2ascenario in the baseline period

Shown in Figure 4.3

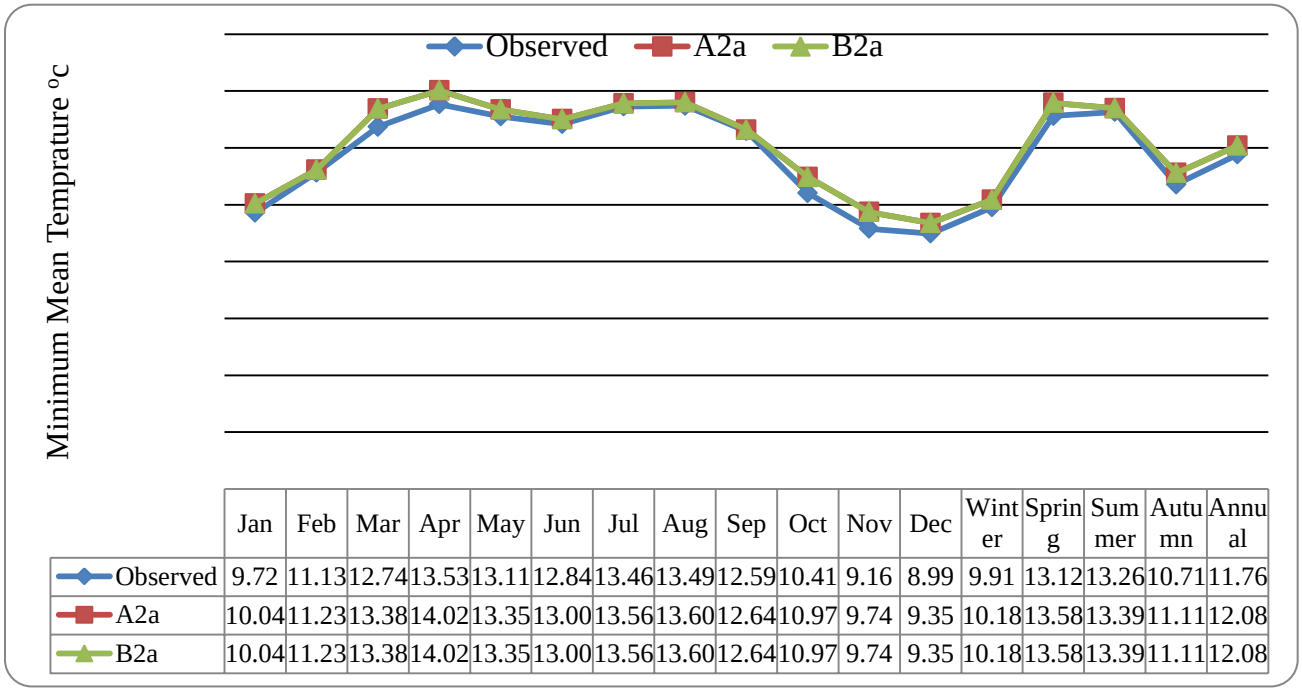

	Jan	Feb	Mar	Apr	May	Jun	Jul	Aug	Sep	Oct	Nov	Dec	Winter	Spring	Summer	Autumn	Annual
Observed	9.72	11.13	12.74	13.53	13.11	12.84	13.46	13.49	12.59	10.41	9.16	8.99	9.91	13.12	13.26	10.71	11.76
A2a	10.04	11.23	13.38	14.02	13.35	13.00	13.56	13.60	12.64	10.97	9.74	9.35	10.18	13.58	13.39	11.11	12.08
B2a	10.04	11.23	13.38	14.02	13.35	13.00	13.56	13.60	12.64	10.97	9.74	9.35	10.18	13.58	13.39	11.11	12.08

Figure 4.3 Observed and Downscaled Mean Monthly Minimum temperature for Debrezeyit station

The variability of monthly minimum temperature observed value is well preserved in the down scaled value from May to October other months and the variance is slightly higher than the down scaled value but the general trend for observed and down scaled values shows similar pattern

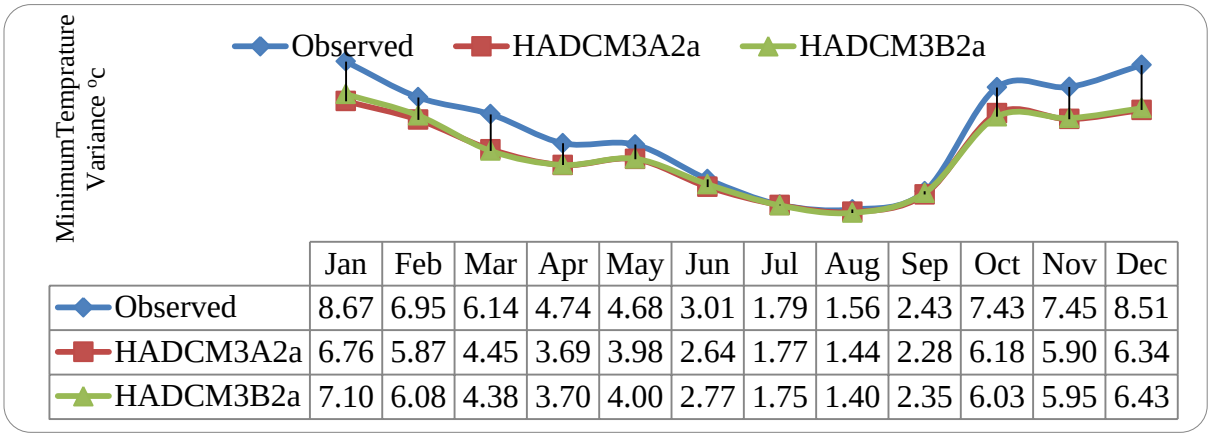

	Jan	Feb	Mar	Apr	May	Jun	Jul	Aug	Sep	Oct	Nov	Dec
Observed	8.67	6.95	6.14	4.74	4.68	3.01	1.79	1.56	2.43	7.43	7.45	8.51
HADCM3A2a	6.76	5.87	4.45	3.69	3.98	2.64	1.77	1.44	2.28	6.18	5.90	6.34
HADCM3B2a	7.10	6.08	4.38	3.70	4.00	2.77	1.75	1.40	2.35	6.03	5.95	6.43

Figure 4.4 Minimum temperature variance modeled vs. observed

c) Maximum Temperature

The monthly maximum temperature downscaled for A2a and B2a scenario in the baseline period Shown in figure 4.5

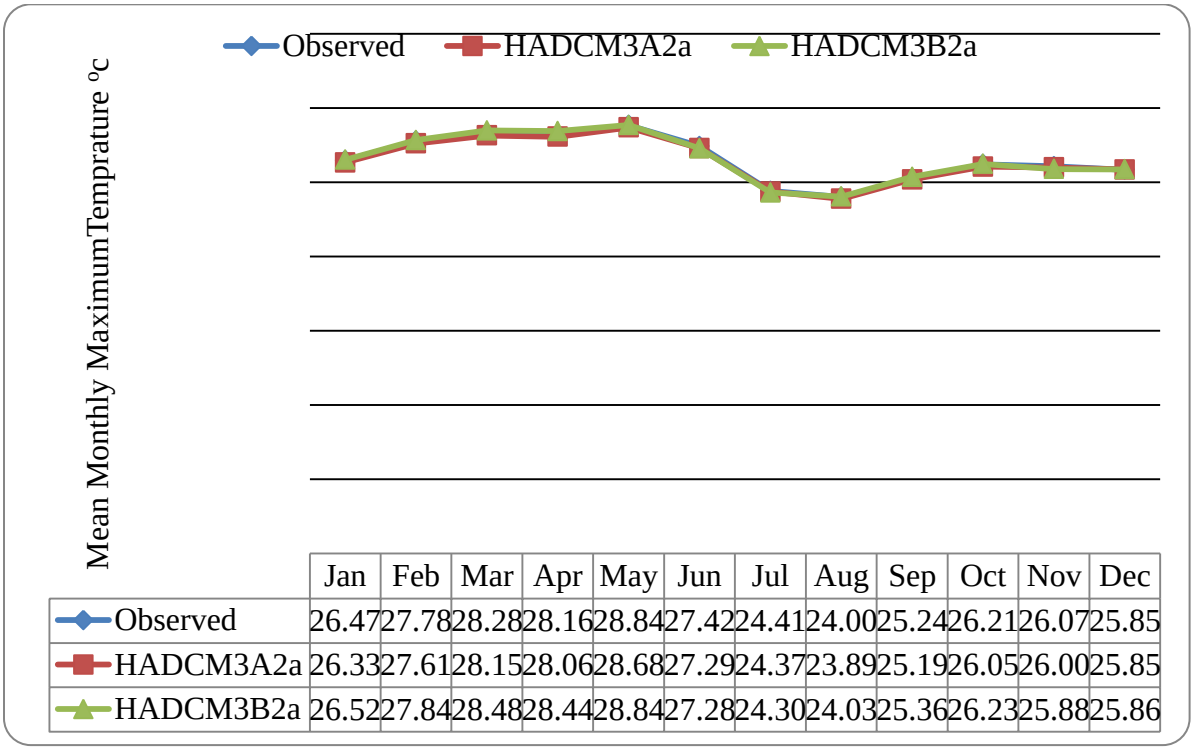

	Jan	Feb	Mar	Apr	May	Jun	Jul	Aug	Sep	Oct	Nov	Dec
Observed	26.47	27.78	28.28	28.16	28.84	27.42	24.41	24.00	25.24	26.21	26.07	25.85
HADCM3A2a	26.33	27.61	28.15	28.06	28.68	27.29	24.37	23.89	25.19	26.05	26.00	25.85
HADCM3B2a	26.52	27.84	28.48	28.44	28.84	27.28	24.30	24.03	25.36	26.23	25.88	25.86

Figure 4.5 Observed and Downscaled Mean Monthly maximum temperature for Debrezeyit station

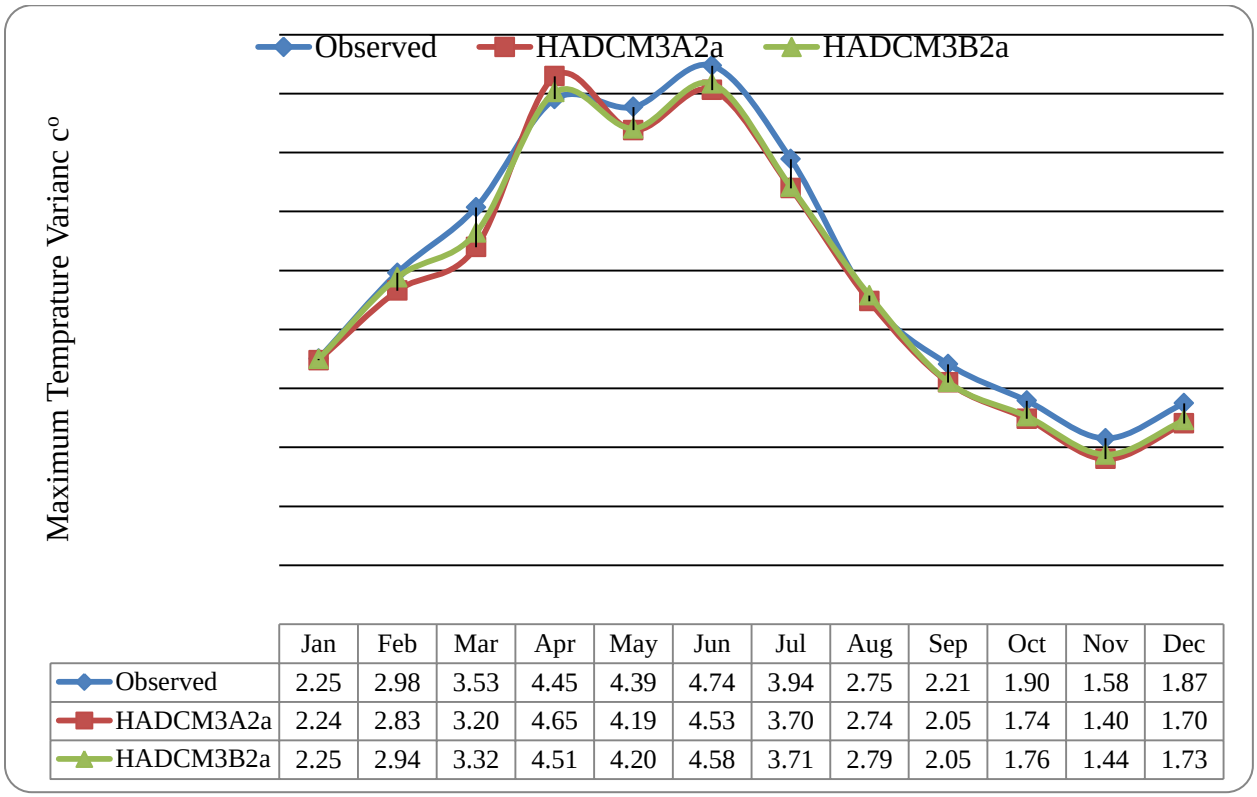

	Jan	Feb	Mar	Apr	May	Jun	Jul	Aug	Sep	Oct	Nov	Dec
Observed	2.25	2.98	3.53	4.45	4.39	4.74	3.94	2.75	2.21	1.90	1.58	1.87
HADCM3A2a	2.24	2.83	3.20	4.65	4.19	4.53	3.70	2.74	2.05	1.74	1.40	1.70
HADCM3B2a	2.25	2.94	3.32	4.51	4.20	4.58	3.71	2.79	2.05	1.76	1.44	1.73

Figure 4.6 Maximum temperature variance modeled vs. observed

The variability of monthly maximum temperature of observed value is well preserved in the months of Jan, February, April, June, July and August ,in the other months it shows slightly higher values than the down scaled values shows similar pattern Generally it is easily seen from the graphs that SDSM able to replicate the maximum, minimum temperature and precipitation values.

4.1.4 Scenario Generation

Predictors from HadCM3 experiment for the period 1961-2099 were used to downscale the present and future climate forcing. The calibrated model was then used for the scenario generation from 2011 to 2099. The scenario generator produces 20 ensembles of synthetic weather series and the mean of the ensembles was used here in the analysis. The generated scenario was divided in to three 30 years of data ranges based on the recommendation of the WMO.As the 2020s, from (2011-20400; 2050s, from (2041-2070) and 2080s, from (2071-2099).The generated scenarios were shown individually for each predictand as below. All the comparisons in the following analysis were done with respect to the baseline period (1980-2010), shows in the figures 4.7and 4.8.

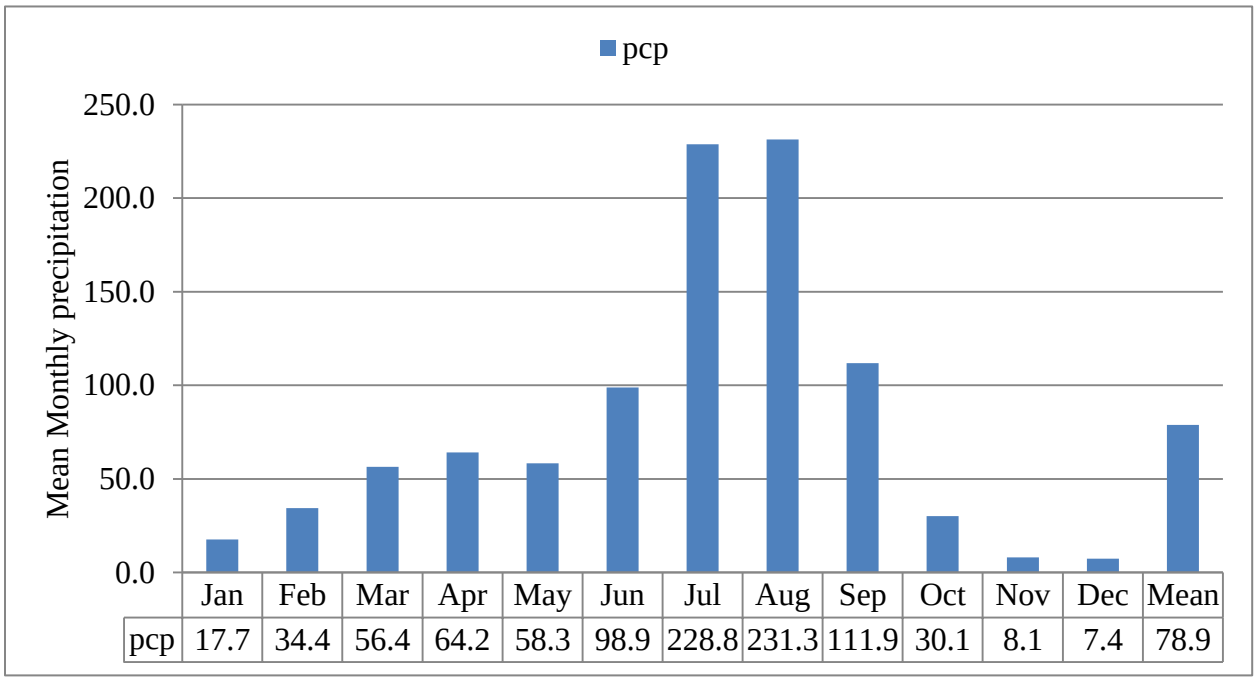

	Jan	Feb	Mar	Apr	May	Jun	Jul	Aug	Sep	Oct	Nov	Dec	Mean
pcp	17.7	34.4	56.4	64.2	58.3	98.9	228.8	231.3	111.9	30.1	8.1	7.4	78.9

Figure4.7 Mean monthly precipitation for base line period Debrezeyit Station (1980-2010)

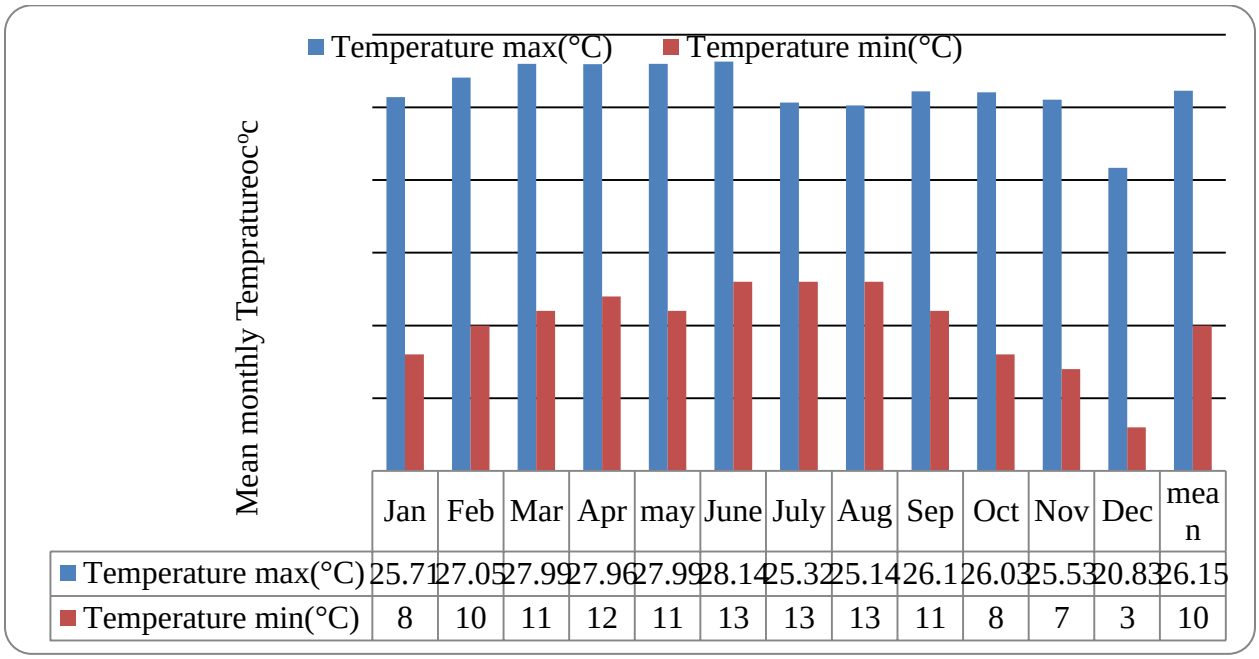

	Jan	Feb	Mar	Apr	may	June	July	Aug	Sep	Oct	Nov	Dec	mean
Temperature max(°C)	25.71	27.05	27.99	27.96	27.99	28.14	25.32	25.14	26.1	26.03	25.53	20.83	26.15
Temperature min(°C)	8	10	11	12	11	13	13	13	11	8	7	3	10

Figure 4.8 Mean monthly maximum and minimum temperature for the base periods Debrezeyit station (1980-2010)

4.1.4.1 Precipitation

The precipitation projection exhibited a decrease in annual mean precipitation in the 2020s, the 2050s and 2080s. As can be seen in Figure 4.9 in 2020s there may be a decrease in precipitation

for both scenarios (A2a and B2a).In 2020s the A2a and B2a scenarios showed an annual mean precipitation decrease up to 6.8 % and2.4 % respectively. In 2050s the decrease in annual mean precipitation may reach up to 10.8% for the A2a scenario and 6.3 % for the B2a scenarios respectively. In the 2080s, the average annual precipitation amount may reduce by 3.64% in A2a scenario and 3.16 % for the B2a scenario. . As shown in figure 4.10 and4.11 in 2020s, the increase in monthly mean precipitation from the month of September up to January and from May to June show a decrease in both A2a and B2a scenarios. In the 2050s, the decrease in monthly mean precipitation from June to November and an increase from December to May in the A2asenario while in the B2a scenario decrease from January to October and an increase from November to May. In 2080s, an increase in mean monthly precipitation from September to June except the month February and decrease in months July, august and February in the scenario A2a and in the B2a scenario an increase from September up to January, and March to June .a decrease in the months July, August and February. Generally the mean monthly rainfall distribution down scaled from SDMS shows almost similar pattern for most future time periods With work of deBoor,(2007) which describes the impact of climate change on rainfall pattern in Ethiopia high land. As he indicated in his out put the mean monthly rain fall decrease in May, June and July and increase September, October and November with respect to the base line period.

As described in IPCC Third Assessment Report (McCarthy et al.., 2001), the projected future change in mean seasonal rainfall in Africa are less well defined. The diversity of African climates, high rainfall variability make the prediction of future climate difficult at sub regional and local scales. Under intermediate warming scenarios, rainfall is predicted to increases in December-February and decrease in June-August in parts of East Africa. With a more rapid global warming scenarios large areas of Africa would experience change in December-February or June-August rain fall that exceed natural variability. With reference to this study rainfall will also experience an increase at June and decrease at August for most parts of the future time the rain fall variation in December-February shows increases.

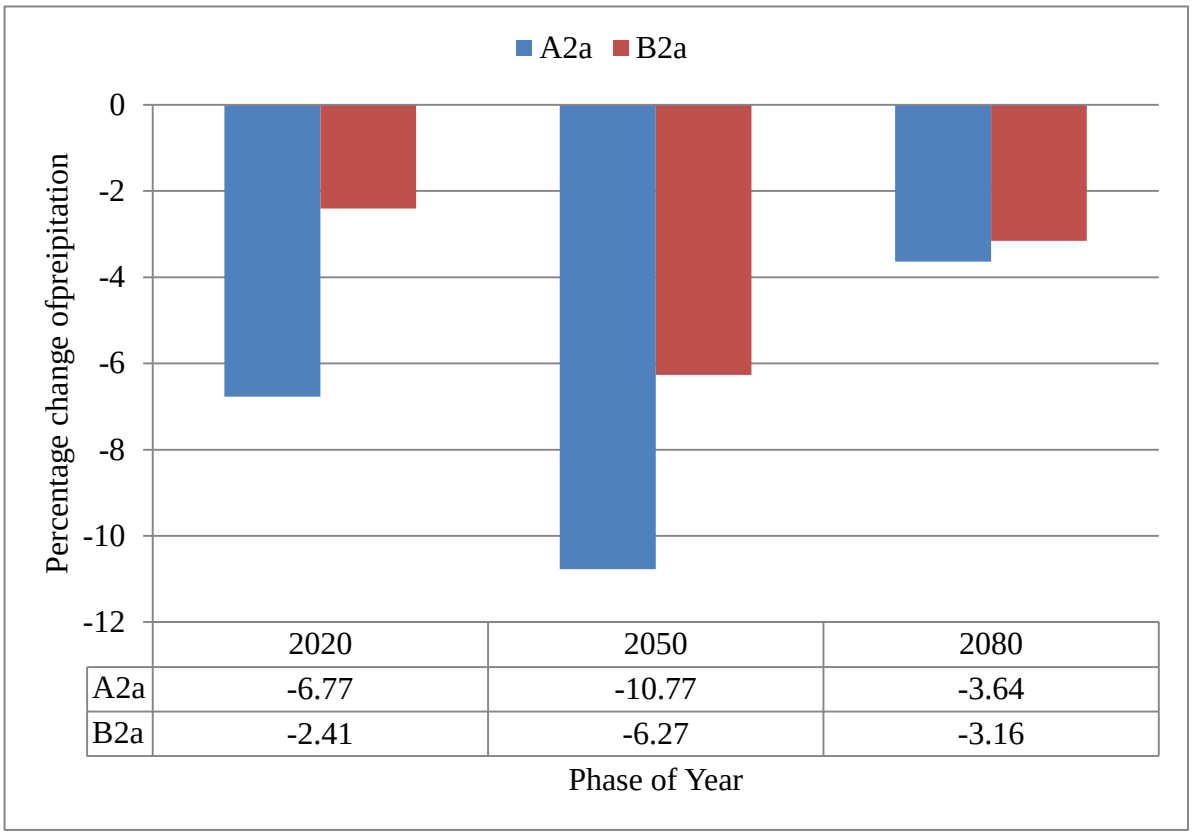

	2020	2050	2080
A2a	-6.77	-10.77	-3.64
B2a	-2.41	-6.27	-3.16

Figure 4.9 Change in percentage of annual precipitation compared with baseline period for A2A &B2a scenarios

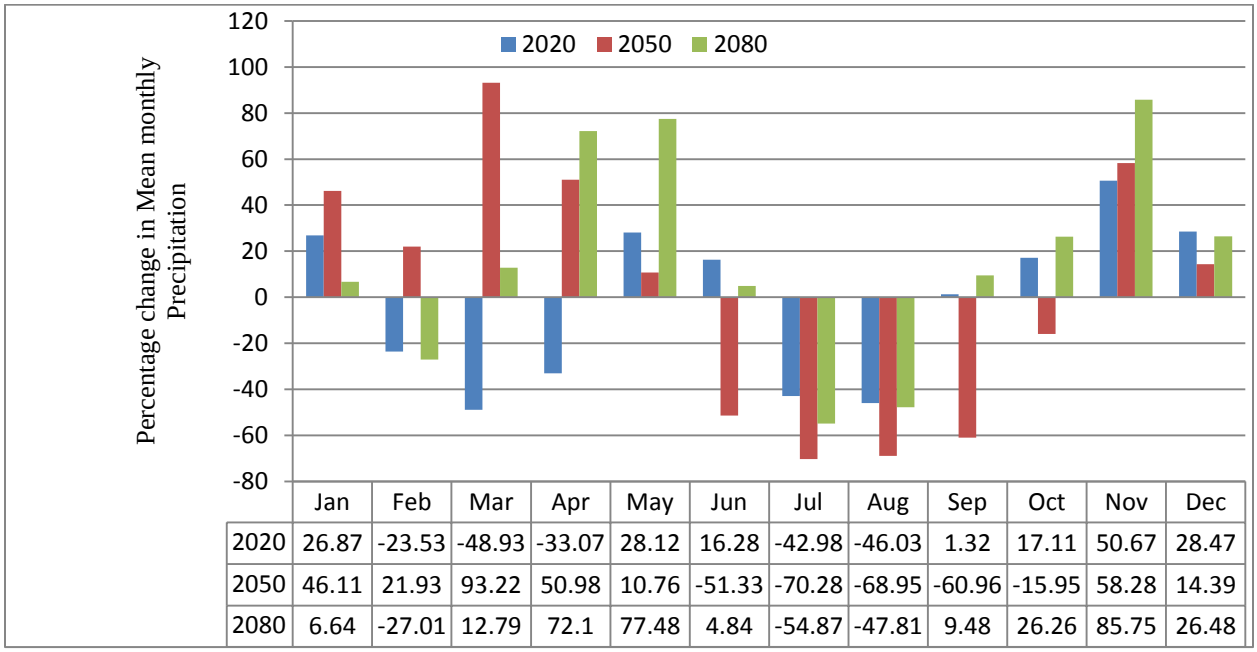

	Jan	Feb	Mar	Apr	May	Jun	Jul	Aug	Sep	Oct	Nov	Dec
2020	26.87	-23.53	-48.93	-33.07	28.12	16.28	-42.98	-46.03	1.32	17.11	50.67	28.47
2050	46.11	21.93	93.22	50.98	10.76	-51.33	-70.28	-68.95	-60.96	-15.95	58.28	14.39
2080	6.64	-27.01	12.79	72.1	77.48	4.84	-54.87	-47.81	9.48	26.26	85.75	26.48

Figure 4.10 Change of percentage monthly mean precipitation compared with baseline period for A2a scenario

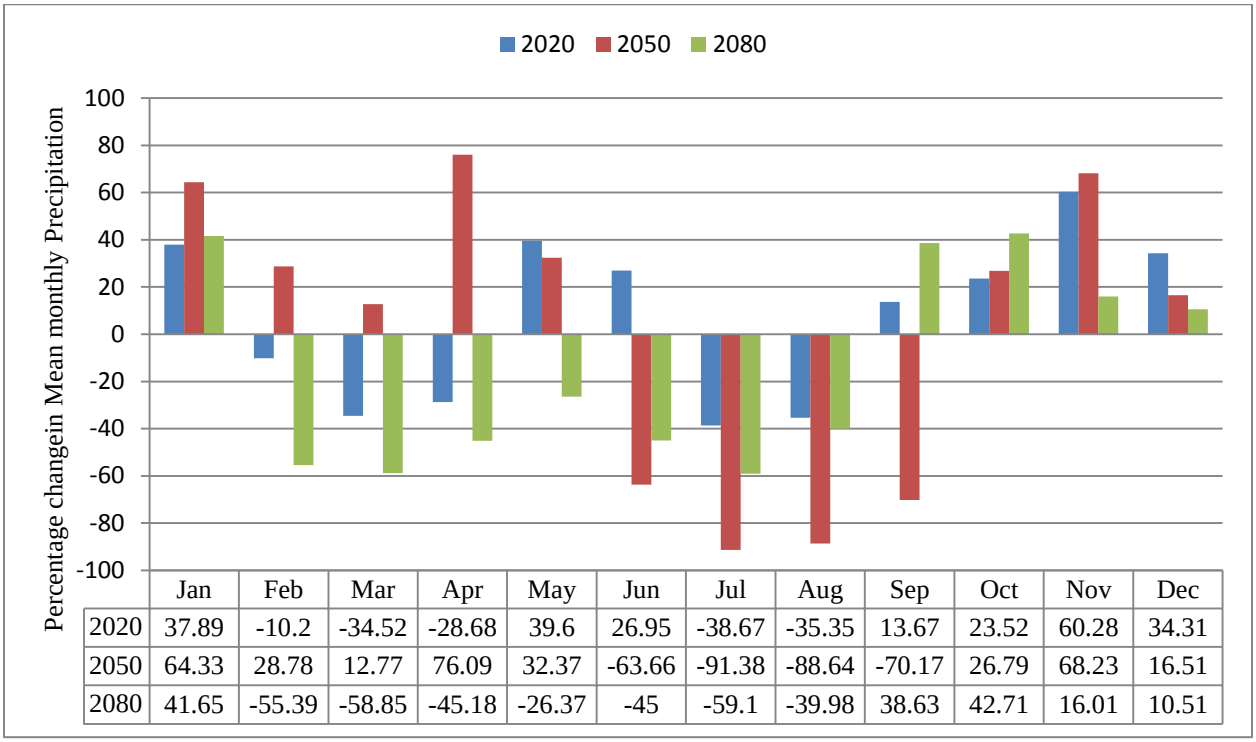

	Jan	Feb	Mar	Apr	May	Jun	Jul	Aug	Sep	Oct	Nov	Dec
2020	37.89	-10.2	-34.52	-28.68	39.6	26.95	-38.67	-35.35	13.67	23.52	60.28	34.31
2050	64.33	28.78	12.77	76.09	32.37	-63.66	-91.38	-88.64	-70.17	26.79	68.23	16.51
2080	41.65	-55.39	-58.85	-45.18	-26.37	-45	-59.1	-39.98	38.63	42.71	16.01	10.51

Figure 4.11 Mean monthly percentage change of precipitation compared with base line period (1980-2010) B2a scenario

As shown in the Figure 4.10 and4.11) there may be a decrease in precipitation in Kiremit (June, July August and September) season in the next 90 years for both scenarios. There may also be a corresponding increase in precipitation amount in Belg season (February, March, April &May for the next 90 years (2050s and 2080s for A2asenario and 2050 for B2a. Kiremit (wet season) and Belg (less rainy season) are the cropping seasons in Ethiopia. Hence this study can give us an insight on the possible impact of climate change on the agriculture and other users in the study area.

4.1.4.2 Mean Maximum Temperature

The maximum temperature scenario generation showed that there may be an increase in mean maximum temperature from September to December and other months show decreases in the 2020s for A2a and an increases from May to January other months show decreases in the2020s for B2a both two scenario show mean increases by 0.64 .and 0.6 respectively. However, 2050s there may be an increase in temperature in the months of October to February and May for A2a and increases from October to March for B2a other months for both scenarios show a decreases. Generally their total mean temperature for both scenarios show incensement by1.03 and 1.06 respectively The change in monthly mean maximum temperature ranges between -1.2 in June and +4.7 in December (2020s), and -2.4 in June and +8.3 in December (2050s) and -0.89 in March and +5.9 in December for the A2a scenario; and between -0.52 in February and+4.9 in December (2020s) and 2.2 in June and+7.8 in December (2050s)and1.3 in March and +5.4 for the B2a

scenario. Seasonally, a pronounced increase in mean maximum temperature is observed in the Bega (dry season) and Kiremit (June beginning rainy season). The monthly change in mean daily maximum temperature from the baseline period is shown in Figure 4.12 &4.13

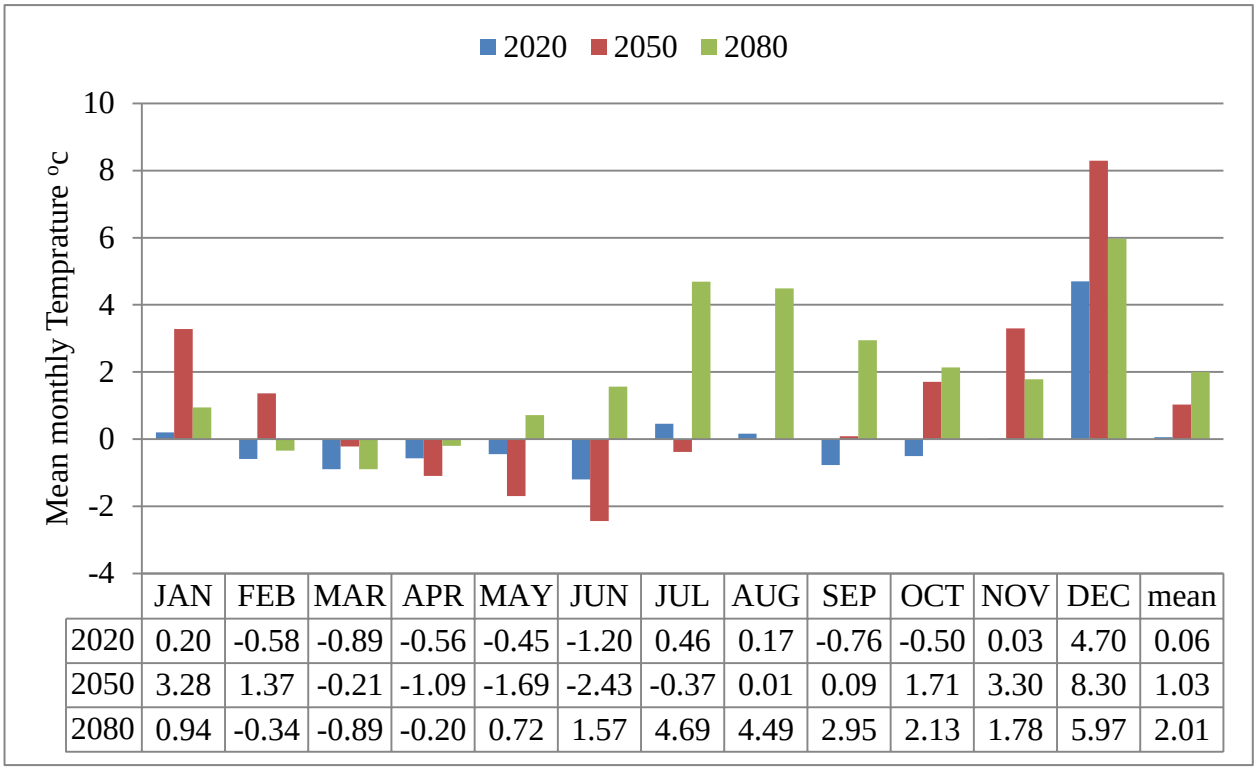

	JAN	FEB	MAR	APR	MAY	JUN	JUL	AUG	SEP	OCT	NOV	DEC	mean
2020	0.20	-0.58	-0.89	-0.56	-0.45	-1.20	0.46	0.17	-0.76	-0.50	0.03	4.70	0.06
2050	3.28	1.37	-0.21	-1.09	-1.69	-2.43	-0.37	0.01	0.09	1.71	3.30	8.30	1.03
2080	0.94	-0.34	-0.89	-0.20	0.72	1.57	4.69	4.49	2.95	2.13	1.78	5.97	2.01

Figure 4.12 Mean monthly maximum temperature compared with base line period (1980-2010) A2a scenario

The overall analysis (2011-2099) of the mean maximum temperature showed that there may be an increasing in both scenarios (A2a and B2a). It is observed that there may also be an increase of mean maximum temperature by 1.03℃/decade mean and 1℃/decade mean for A2a (2011-2099) and B2a (2011-2099) scenarios respectively

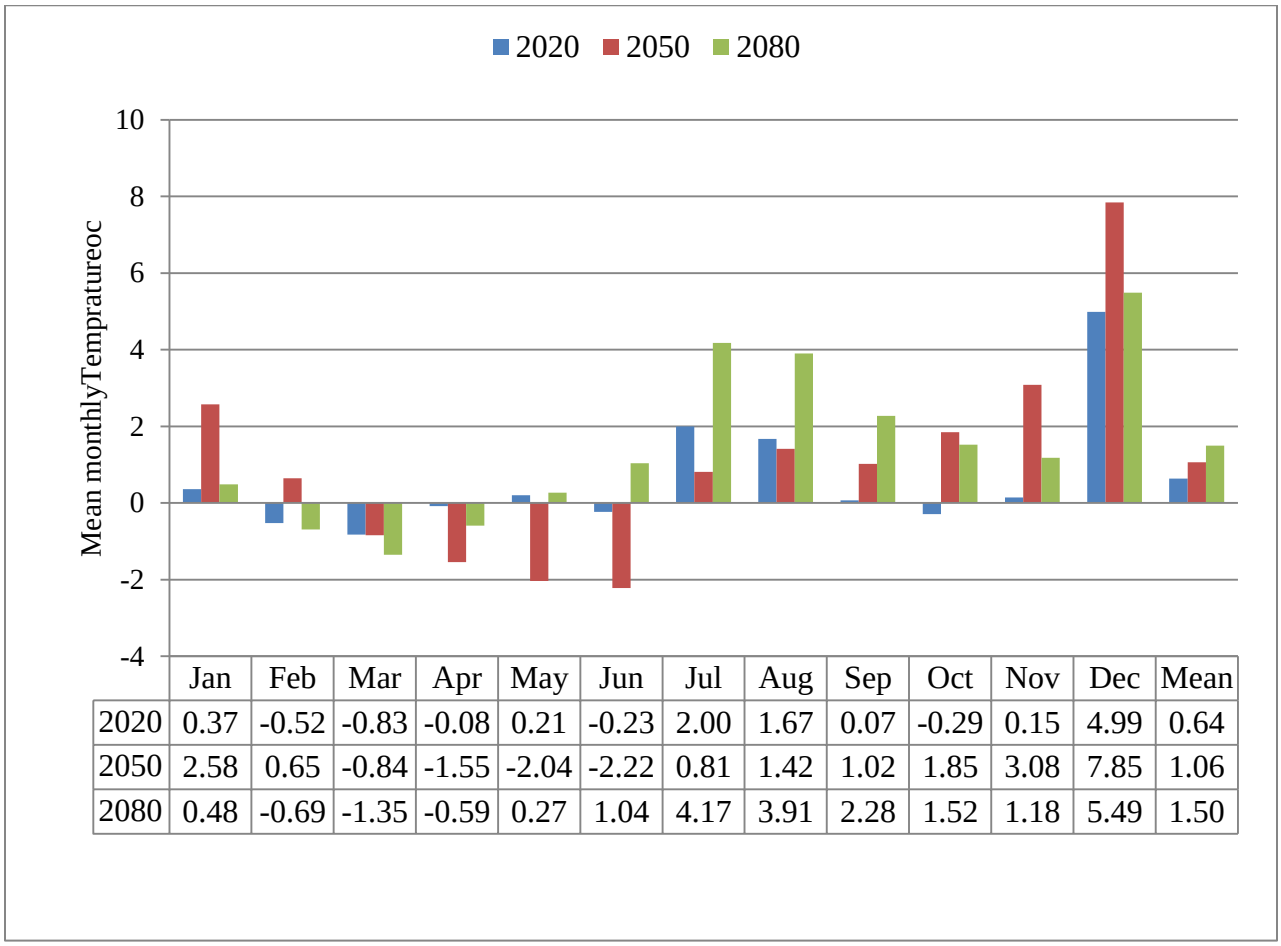

	Jan	Feb	Mar	Apr	May	Jun	Jul	Aug	Sep	Oct	Nov	Dec	Mean
2020	0.37	-0.52	-0.83	-0.08	0.21	-0.23	2.00	1.67	0.07	-0.29	0.15	4.99	0.64
2050	2.58	0.65	-0.84	-1.55	-2.04	-2.22	0.81	1.42	1.02	1.85	3.08	7.85	1.06
2080	0.48	-0.69	-1.35	-0.59	0.27	1.04	4.17	3.91	2.28	1.52	1.18	5.49	1.50

Figure 4.13 Mean monthly maximum temperature compared with base line period (1980-2010) B2a scenario

4.1.4.3 Minimum Temperature

The annual mean minimum temperature trend in three periods may be increasing as compared to the baseline period for both scenarios. In 2020s the monthly mean minimum temperature ranges -0.95^{o}c in March and +2.7^{o}c in December (A2a) and -0.86^{o}c in August and 2.5^{o}c in December for (B2a),and in 2050s -4.1^{o}c in June and +6.1 ^{o}c in December (A2a) and-4.7 ^{o}c in July and+6.2 ^{o}c in December (B2a) And in 2080s it ranges -2.2 ^{o}c in March and +3.7 ^{o}c in November (A2a) and-2.1 ^{o}c in march and+3.5 ^{o}c in December (B2a) .

The projected minimum and maximum temperature in all future time horizons is within the range projected by IPCC (2007) which indicate that the average temperature will be risen by 0.45minimum and 1.06 maximum, towards the end of this century

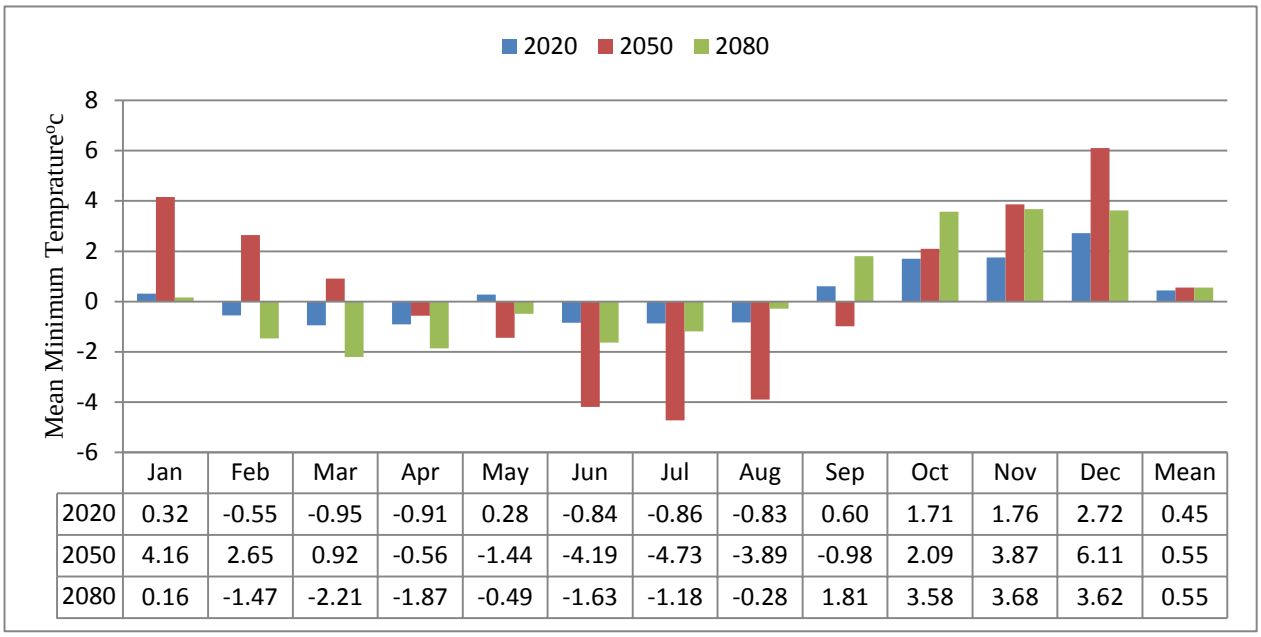

	Jan	Feb	Mar	Apr	May	Jun	Jul	Aug	Sep	Oct	Nov	Dec	Mean
2020	0.32	-0.55	-0.95	-0.91	0.28	-0.84	-0.86	-0.83	0.60	1.71	1.76	2.72	0.45
2050	4.16	2.65	0.92	-0.56	-1.44	-4.19	-4.73	-3.89	-0.98	2.09	3.87	6.11	0.55
2080	0.16	-1.47	-2.21	-1.87	-0.49	-1.63	-1.18	-0.28	1.81	3.58	3.68	3.62	0.55

Figure 4.14 Mean monthly minimum temperature compared with base line period (1980-2010) A2ascenario

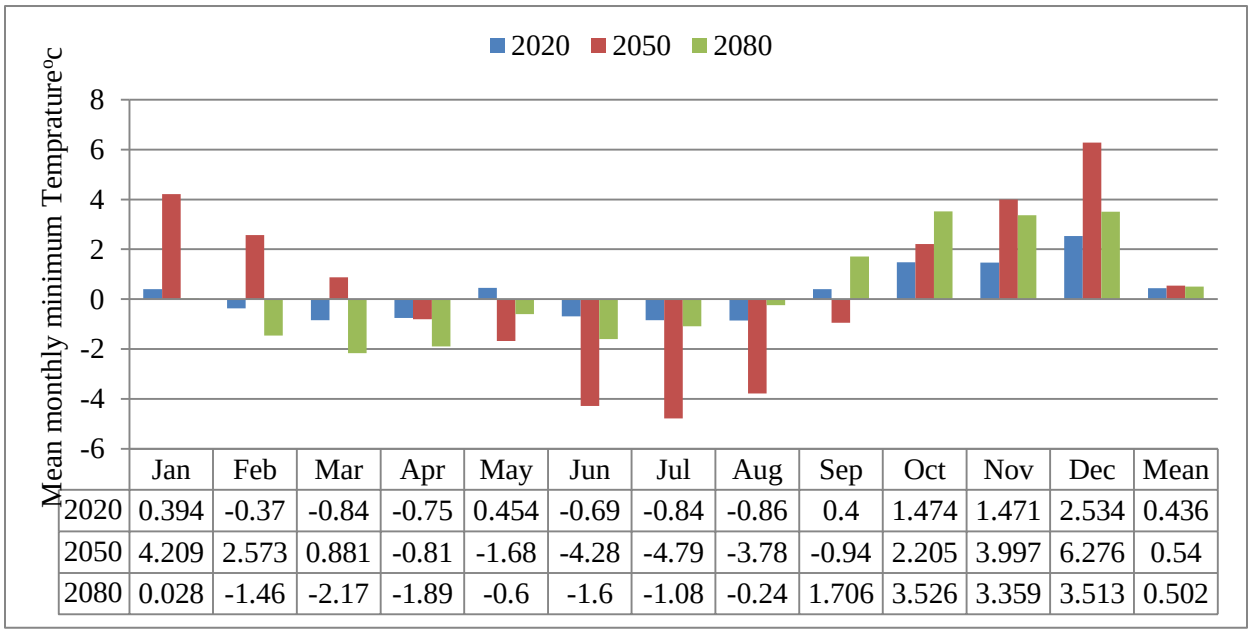

	Jan	Feb	Mar	Apr	May	Jun	Jul	Aug	Sep	Oct	Nov	Dec	Mean
2020	0.394	-0.37	-0.84	-0.75	0.454	-0.69	-0.84	-0.86	0.4	1.474	1.471	2.534	0.436
2050	4.209	2.573	0.881	-0.81	-1.68	-4.28	-4.79	-3.78	-0.94	2.205	3.997	6.276	0.54
2080	0.028	-1.46	-2.17	-1.89	-0.6	-1.6	-1.08	-0.24	1.706	3.526	3.359	3.513	0.502

Figure 4.15 Mean monthly minimum temperature compared with base line period (1980-2010) B2a scenario

4.2 Hydrological Modeling

4.2.1 Simulation for Modjo sub basin

. The watershed delineation of the area gave minimum, maximum and mean elevations in the basin of 1790, 3060, and 2170.51m above sea level respectively. The area coverage by each land use type is presented in Table 4.6.

Table 4.6 Land use types and their areal coverage at Modjo sub basin

Land use/land cover types and area of watershed			
land use code	Area(watershed)		Description of code
	Km^2	%	
TEFF	1518.61	89.22	EragrostisTeff
DWHT	95.41	5.61	Durum Wheat
URBN	48.91	2.87	Residential
WATR	0.067	0.000009	Water
WETN	3.29	0.19	Wetland- Non-Forested
RNGB	35.88	2.11	Range-Brush
Total	1702.15	100	

Most of the area in the watershed is covered by Teff at lower part and durum wheat at higher part

The majority of the land was covered by soil type Vertic cambisols and Eutric Vertisols .The SWAT result for the soils' area coverage in the watershed is shown in Table 4.7

SWAT slope computation using the DEM data indicated that 38.6% of the watershed has a slope of less than 3% and 41.5% of the watershed have a slope less than 8%., 12.5% of watershed has

Table 4.7 Soil type and area coverage

Soil type	Area coverage ha	% coverage of area	Description of Code
ANm	8.41	0.001	Molic Andosols
CMv	72423.21	42.55	Vertic cambisols
LPq	3290.17	1.93	Lithic Leptosols
LVh	148.02	0.09	Haptic Luvisols
LVx	9095.90	5.34	Chromic Luvisols
PHl	12239.73	7.19	Luvic Phaezems
VRe	73010.26	42.89	Eutric Vertisols

Table 4.8 Slope classes and area coverage

Slope classes	Range %	Area coverage	
		Ha	%
Flat or almost flat	0-3	65695.7	38.6
Gently sloping	3-8	70554.4	41.5
Sloping	8-15	21230.5	12.5
Moderately steep	15-30	9609.8	5.6
Steep	30-99.9	3125.3	1.8
Total		170215.7	100

less than15 %,5.6% of the water shed has less than 30% and 1.8.% of the water shed is above 30% slope.

4.2.2 Sensitivity Analysis

The results of the sensitivity analysis gave the degree of sensitivity of parameters and the parameter bound which was important for auto-calibration activities. Alpha Bf, and GwDelay were the most sensitive parameters which has effect on base-flow contribution while Cn2, Esco and Ch_N2, were among the most sensitive parameters which has effect on the surface runoff. From 18 parameters, the ten most sensitive parameters selected for calibration, their ranking and description is shown in Table 4.9

Table 4.9 Sensitive parameter ranking and final auto- calibration result

No	Parameter	Parameter value	Min value	Max value
1	CN2.mgt	85.87	35.00	98.00
2	ALPHA_BF.gw	0.50	0.00	1.00
3	GW_DELAY.gw	215.85	30.00	450.00
4	GWQMN.gw	0.38	0.00	2.00
5	SOL_Z(..).sol	2261.77	0.00	2966.25
6	EsCO.hru	0.85	0.00	1. 00
7	CH_N2.rte	0.24	-0.01	0.30
8	SOL_AWC(..).sol	0.56	0.00	1.00 00
9	SURLAG.bsn	5.74	0.05	24.00
10	EPCO.hru	0.04	0.00	1.00
11	GW_REVAP.gw	0.15	0.02	0.20
12	SOL_K(..).sol	505.00	0.00	2000.00
13	CH_N1.sub	2.18	0.01	30.00
14	CH_L2.rte	3.70	-0.05	500.00
15	RCHRG_DP.gw	0.31	0.00	1.00
16	SLSUBBSN.hru	67.05	10.00	150.00
17	CH_K1.sub	162.75	0.00	300.00
18	SOL_BD(..).sol	1.67	0.90	2.50

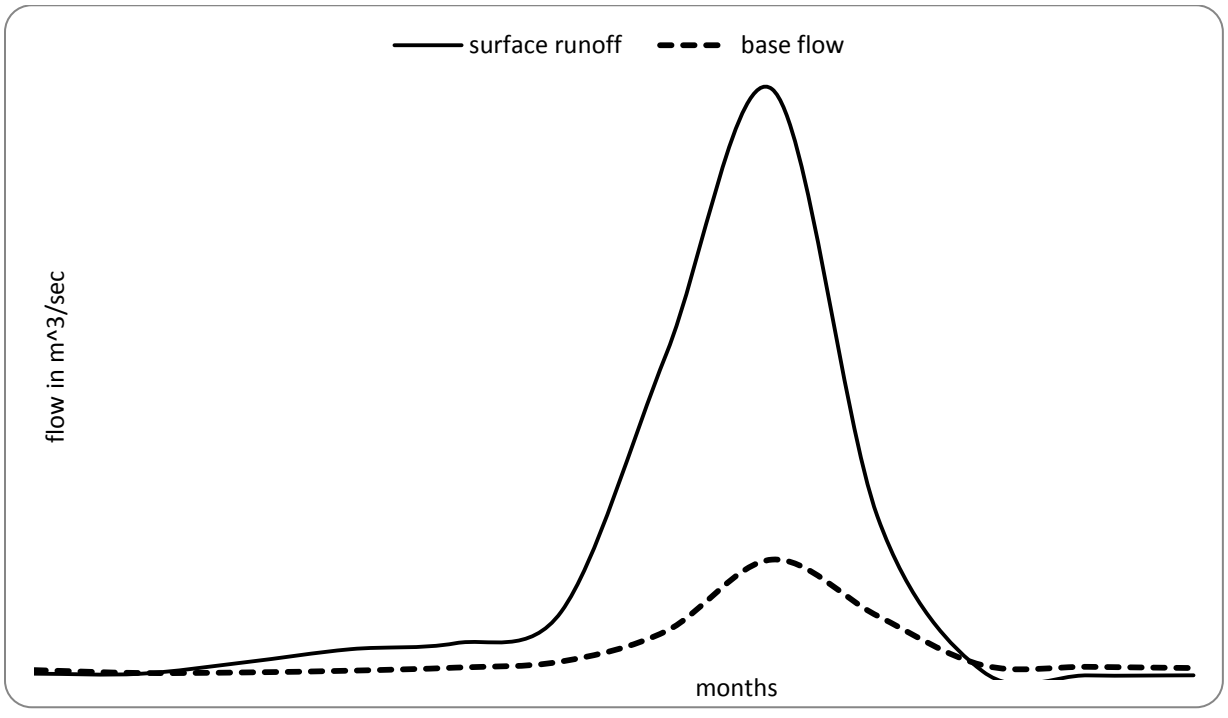

Figure 4.16. base flow separation observed flow vs observed base flow

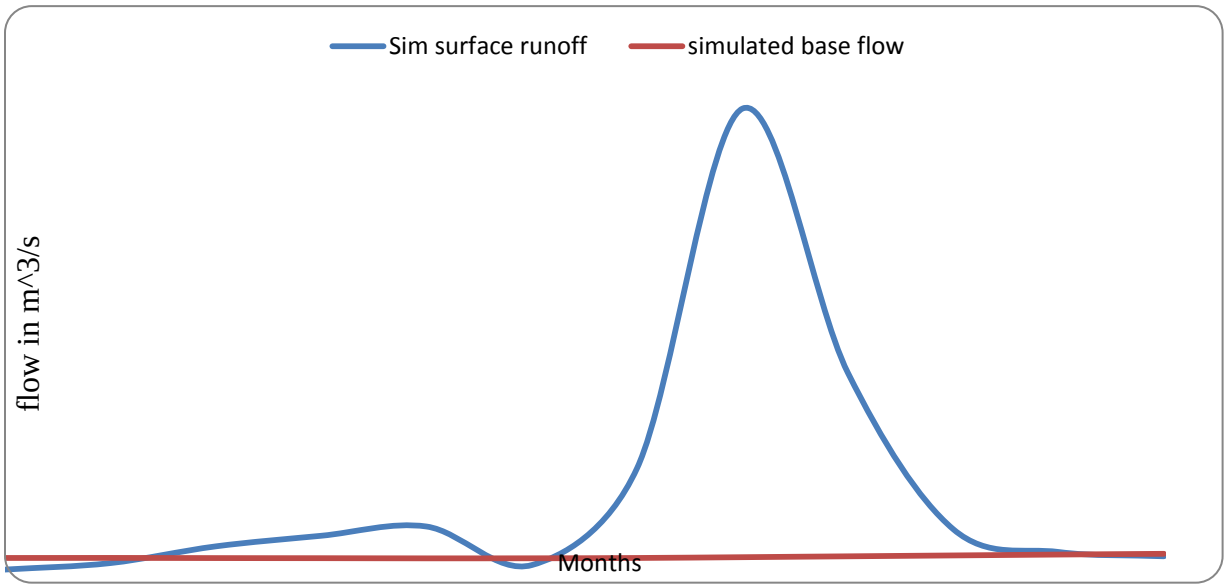

Figure 4.17. Base flow separation simulated v simulated base flow

4.2.3 Model Calibration

The calibration of the model was performed for seven years (1998 to 2005), 1998 was taken for warming period using the flow data at Modjo flow station. The performance of the model was evaluated using R^2, NSE, RSR and PBIAS statistical measures for calibration. After calibration the R^2 = 0.7 1, RSR=0.55 NSE=0.70 and PBIAS=11.5 Santhi et al. (2001) stated that efficiency values greater than or equal to 0.50 are considered adequate for SWAT model application. Hence, it is observed that SWAT exhibited strong performance in representing the hydrological conditions of the watershed It can be seen from flow hydrograph (figure 4.18) that the simulated flows almost replicate the observed flows except peak values are slightly overestimated during 2001, 2002 and 2003 .This may be due to precipitation data given as an input to the model or gauged flow used for the calibration. However, the overall flow trend is well simulated by the model; especially in such cases of the study area where rainfall has temporal variability is quite significant

Table 4.10 calibration parameter ranking and final auto- calibration result

parameter	Fitted value	Min value	Max value
CN2.mgt	-0.12	-0.20	-0.09
ALPHA_BF.gw	0.88	1.00	0.97
GW_DELAY.gw	211.31	30.00	316.65
GWQMN.gw	0.05	0.02	0.05
SOL_Z(..).sol	2261.76	0.00	2966.25
EsCO.hru	0.08	0.00	0.13
CH_N2.rte	0.08	-0.01	0.25
SOL_AWC(..).sol	0.22	0.00	0.46
SURLAG.bsn	2.81	0.05	4.06
EPCO.hru	0.19	0.00	0.26

.

Table 4.11 Calibration and Validation period statistics for measured and simulated flow at Modjo flow station

Period	Total Observd m^3/s	Total simulated m^3/s	Average observed m^3/s	Average Simulated m^3/s	NSE	PBIAS %	RSR	R^2
Calibration (1999-2005)	835.5	979.4	119.4	139.9	0.7	51.1	0.55	0.71
Validation (2007-2010	250.9	246.6	62.7.	61.6	0.52	52	0.6	0.51

. The two rainfall seasons, Kiremt and Belg, which contribute the largest share of the total rainfall, are well explained by the simulated result. So SWAT proved to perform well in simulating the flows of Mojo Sub watershed.

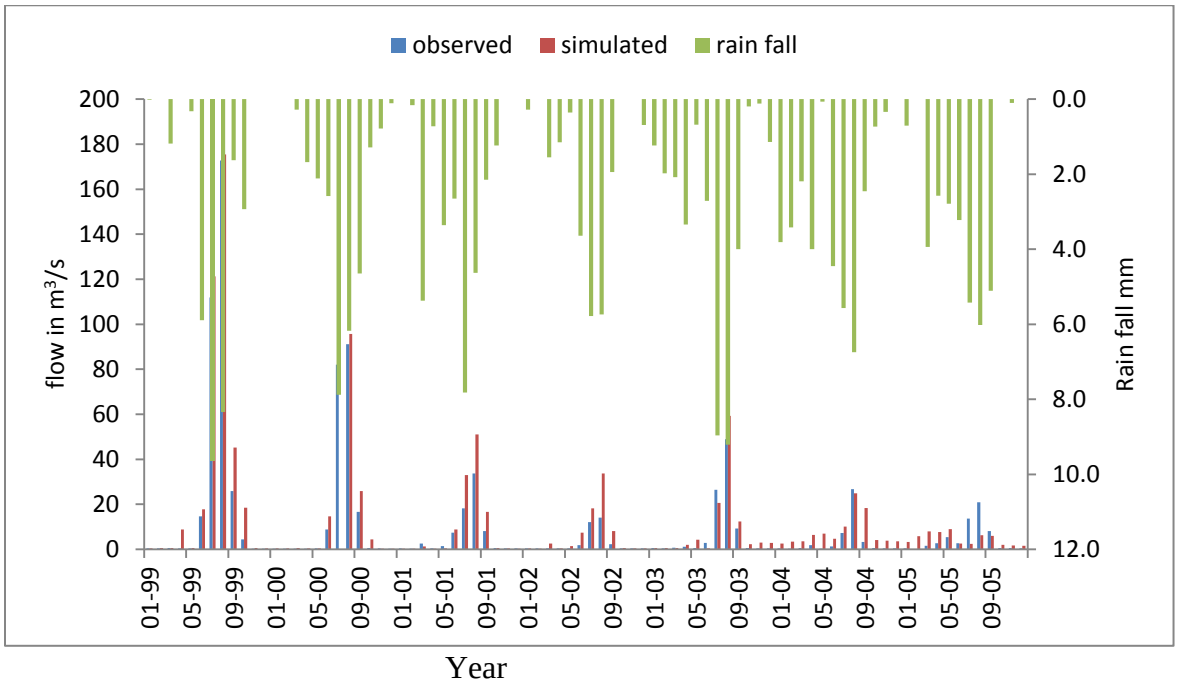

Figure 4.18 Observed and simulated flow hydrograph for the calibration period (1999-2007)

4.2.4 Model Validation

The validation of the model at the Modjo station gauging station was done for an independent data set of five years from 2006 to 2010.with one year warming period (2006) .The figure 4.18 shows that the model replicated the observed flows well. However, it couldn't able to catch the peak flows. Table 4.8 shows the validation statistics of the simulated flow. The R2 was found to be 0.51, which shows it is slightly in good correlation with the gauged flow. This ensures that the simulated flow followings the same trend with the gauged flow in the time serious Even though the model overestimated the flow at the end of 2007, before middle of 2008 and start of middle 2010, and the overall trend of the flow is well simulated by the model. ..

Both the R^2 and NS values fulfilled beyond the minimum requirement of $R^2 > 0.5$ and ENS > 0.5, recommended by Santhi et al (2001). These results show that the model has again simulated the flow well resulting

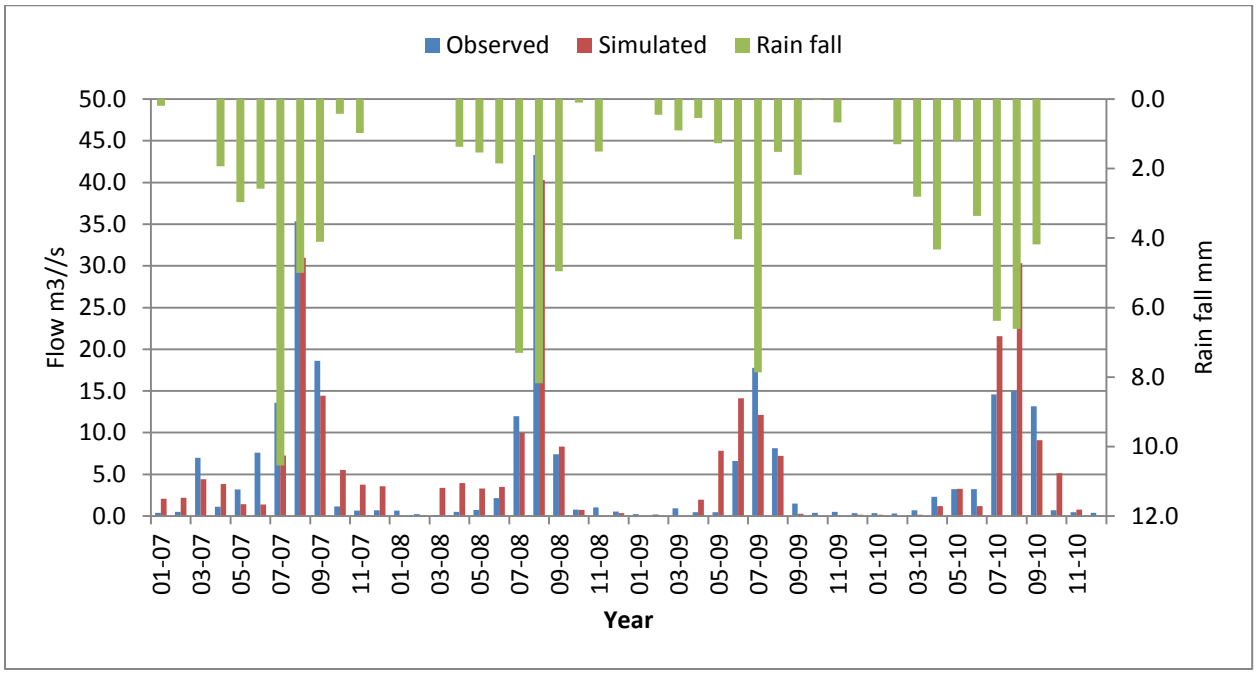

Figure 4.19 Observed and simulated flow hydrograph for the validation period (2007-2010)

4.3 Impact of Climate Change on the Flow Volume

The impact of climate change on flow volume was analyzed on a monthly, seasonal and annual basis.

4.3.1 Impact on Monthly Flow Volume

The impact of climate change was analyzed taking the 1980-2010 river flow as the baseline flow against which the future flows for the 2020s, 2050s and 2080s were compared. Precipitation, minimum and maximum temperature were the climate change drivers considered for the impact assessment. The inputs for the change in precipitation, maximum and minimum temperature are discussed in section 4.1.4. The monthly percentage change in flow volume in both scenarios for the period 2020s, 2050s and 2080s are presented in Figure 4.21 and Figure 4.22. In the 2020s for the A2a scenario, the flow volume may show a decrease for all the months except December. In this period the total decrease may reach up to 63.28% and an increase up to 109.5% in December monthly flow volume may be expected. Increase in flow volume may be observed in months which showed an increase in monthly precipitation for five months and other months show increase in precipitation.

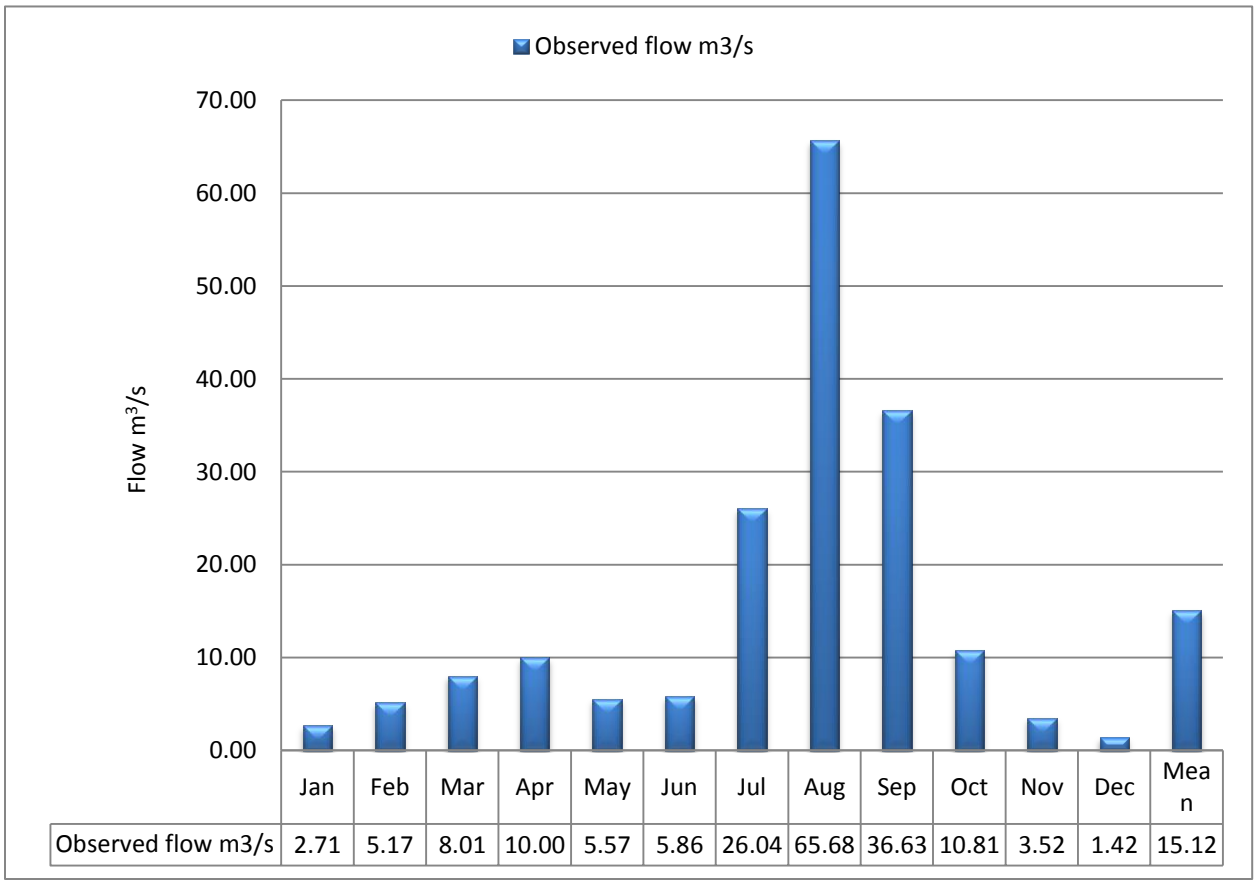

	Jan	Feb	Mar	Apr	May	Jun	Jul	Aug	Sep	Oct	Nov	Dec	Mean
Observed flow m3/s	2.71	5.17	8.01	10.00	5.57	5.86	26.04	65.68	36.63	10.81	3.52	1.42	15.12

Figure 4.20 Mean monthly flows of Mojo river base period data (1980-2010)

. and decrease in flow However, the decrease in flow volume may be due to increment of evapotranspiration (Figure 4.25) and other uncertainties like land use change. In the 2020s for B2a scenario, all decrease the same as the A2a scenario of 2020s may be observed except in December. and the decrease in total period monthly flow volume is expected to reach up to 81.5% as indicated in figure 4.22.

In 2050s for A2a scenarios, the increase in precipitation is reflected in an increase in flow volume and a decrease in precipitation is reflected in a decrease in flow volume but in January, February, March and, April in these months a decrease in inflow while increase precipitation it may from the period (season), catchment and land use change other uncertainties .and at June an increase in inflow while decrease precipitation the reason may from catchment and ground water lag time. In 2050 for B2a both decrease and increase in inflow volume may reach less than one percent near to zero .In 2080s for the A2a scenario an decrease in flow volume in all months except May and June may be increase observed. The decrease in monthly flow volume may reach up to 88.62%.in

August months and May ,June July August March and February that may show increase and decrease in precipitation also show in inflow but January,April,September October,Novenber and December may show increase in precipitation while decrease in inflow

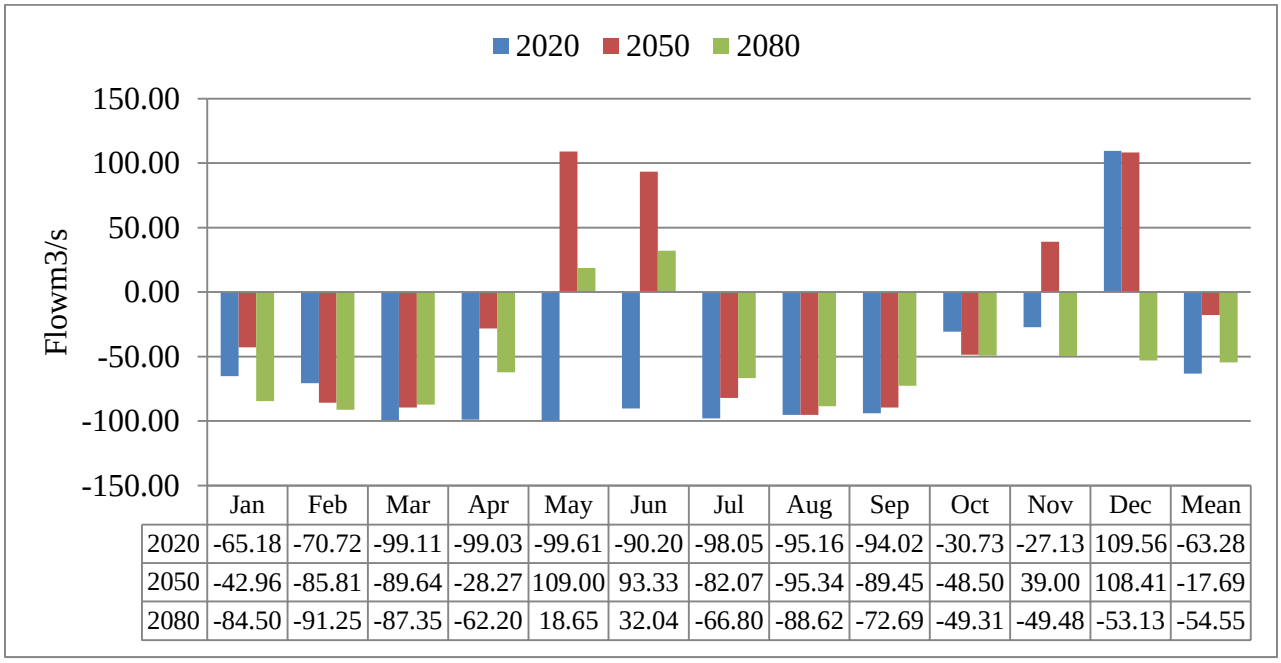

	Jan	Feb	Mar	Apr	May	Jun	Jul	Aug	Sep	Oct	Nov	Dec	Mean
2020	-65.18	-70.72	-99.11	-99.03	-99.61	-90.20	-98.05	-95.16	-94.02	-30.73	-27.13	109.56	-63.28
2050	-42.96	-85.81	-89.64	-28.27	109.00	93.33	-82.07	-95.34	-89.45	-48.50	39.00	108.41	-17.69
2080	-84.50	-91.25	-87.35	-62.20	18.65	32.04	-66.80	-88.62	-72.69	-49.31	-49.48	-53.13	-54.55

Figure 4.21 Monthly percentage change in flow volume for A2a scenario for the periods 2020, 2050 and 2080 against the base flow volume comparison by using scenario

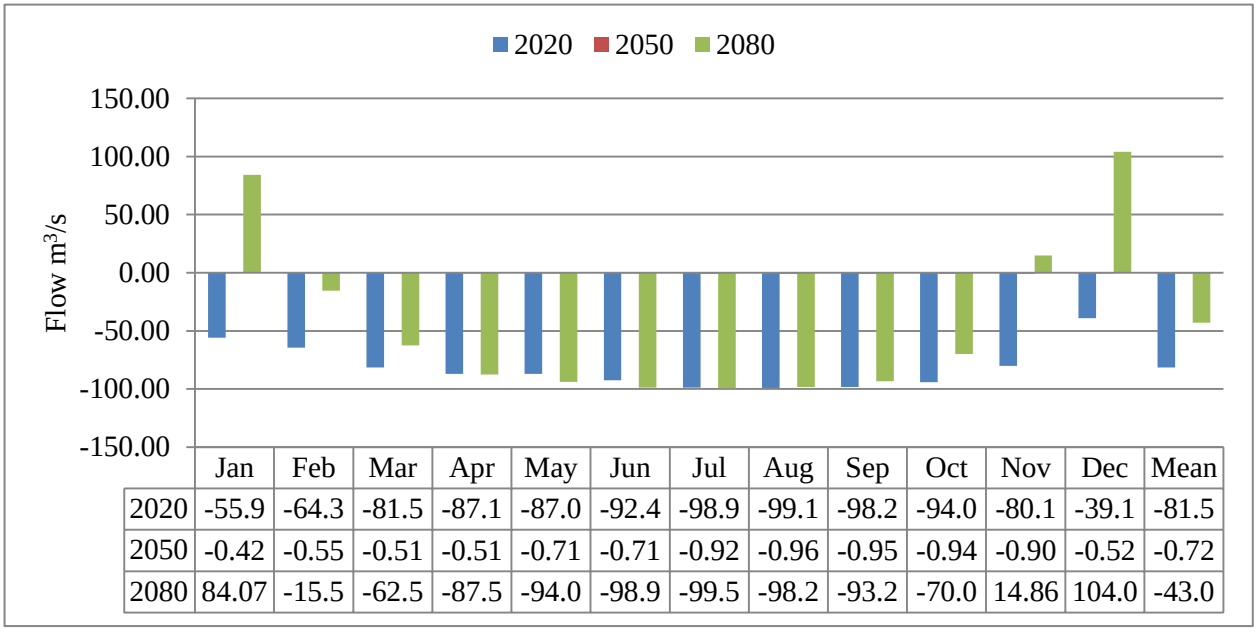

	Jan	Feb	Mar	Apr	May	Jun	Jul	Aug	Sep	Oct	Nov	Dec	Mean
2020	-55.9	-64.3	-81.5	-87.1	-87.0	-92.4	-98.9	-99.1	-98.2	-94.0	-80.1	-39.1	-81.5
2050	-0.42	-0.55	-0.51	-0.51	-0.71	-0.71	-0.92	-0.96	-0.95	-0.94	-0.90	-0.52	-0.72
2080	84.07	-15.5	-62.5	-87.5	-94.0	-98.9	-99.5	-98.2	-93.2	-70.0	14.86	104.0	-43.0

Figure 4.22 Monthly percentage change inflow volume for B2a scenario for the periods 2020,2050 and 2080 against the baseline flow volume comparison by using scenario

4.3.2 Impact on Seasonal and Annual Flow Volume

In this section, the impacts climate change on the seasonal and annual flow volume are presented so as to foresee its consequence on the socio-economic condition of the area. As discussed in the section 2.3, there are three seasons in the study area: Kiremit (rainy and

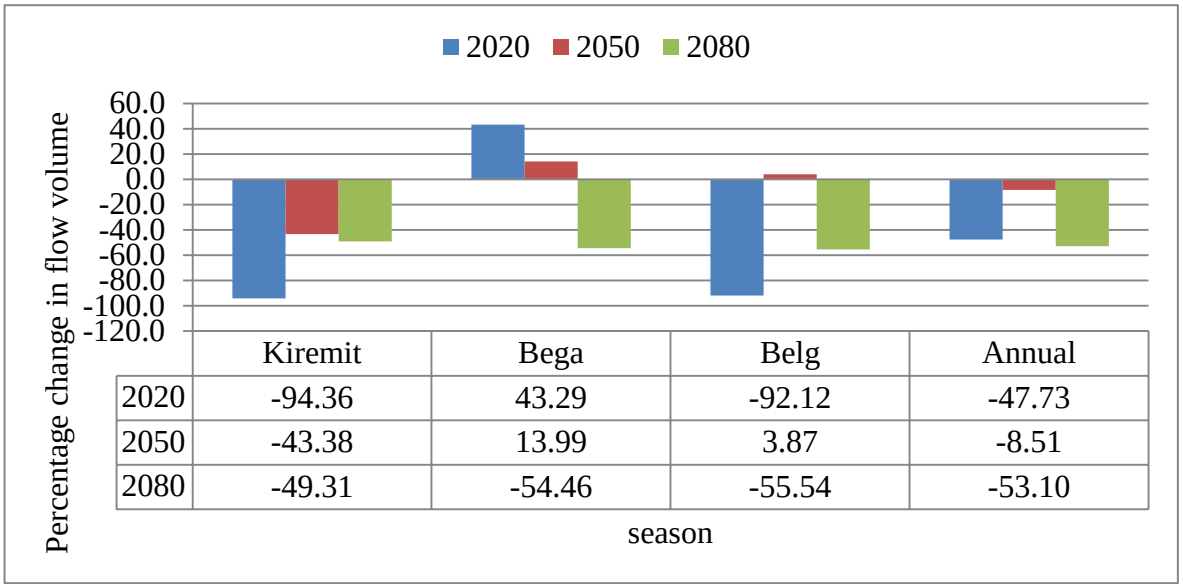

	Kiremit	Bega	Belg	Annual
2020	-94.36	43.29	-92.12	-47.73
2050	-43.38	13.99	3.87	-8.51
2080	-49.31	-54.46	-55.54	-53.10

Figure 4.23 percentage changes in seasonal and annual flow volume in respect to base line climate A2a

cropping season), Belg (small rain season) and Bega (dry season). Figure 4.23 and Figure 4.24 exhibit the implication of climate change on the river flow in these seasons.forA2a and B2ascenario In flow volume for the next periods .kiremit (2020,2050 and2080) -94.36,-43.38 and -49.31 in A2a respectively and -97.21 (2020) and -97.51 (2080) and negligible in 2050 for B2a scenario and Belg seasons may decrease -92.12 and-80.03 in 2020 for A2a and B2a scenario respectively, ,in 2050 may +3.87for A2a and negligible for B2a and for 2080 -55.54 and -64.94 in A2a and B2a respectively that expected to show the larger share in decreased flow volume for both scenario and in Bega season may a decrease in 2080 for A2a by -54.46 , in B2a may decrease -- 67.33 in 2020 and negligible for 2080s while for A2a in 2020 and 2050 may increase by+43.29 and +13.99 respectively when observe annual flow for both scenarios (2020,2050 2080) may decrease by-47.73,-8.51 and-53.10 respectivelyin.A2a scenario and -81.52,negligible and -30.33 respectively in B2a scenario.

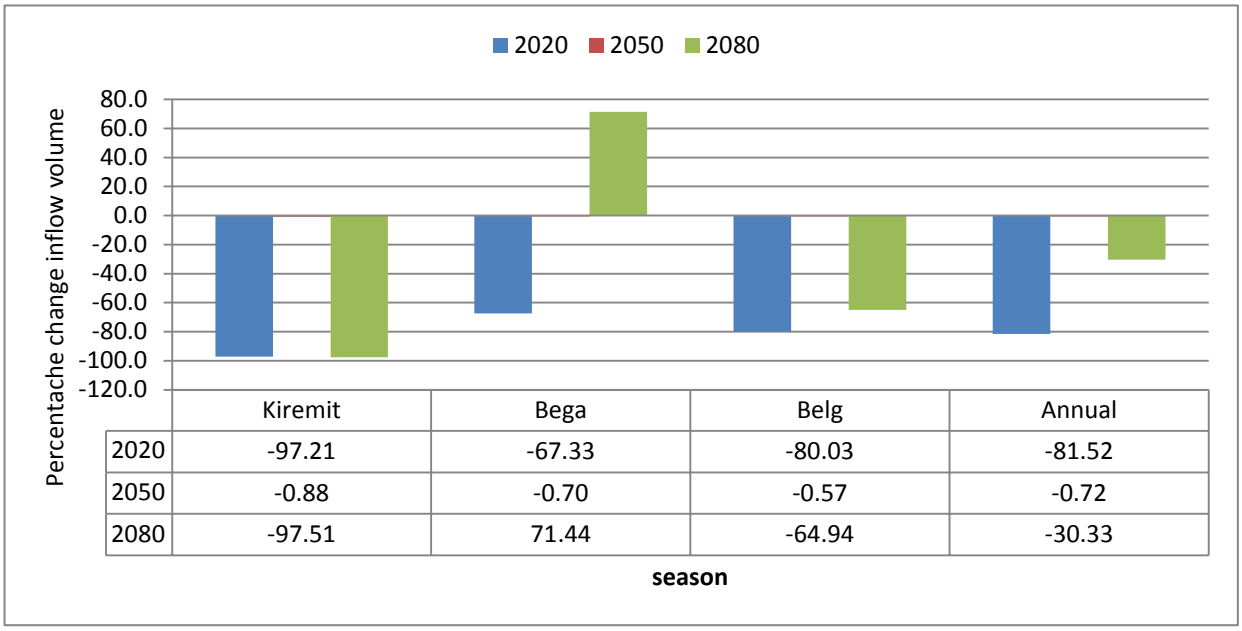

	Kiremit	Bega	Belg	Annual
2020	-97.21	-67.33	-80.03	-81.52
2050	-0.88	-0.70	-0.57	-0.72
2080	-97.51	71.44	-64.94	-30.33

Figure 4.24 Percentage change in seasonal and annual flow volume in respect to baseline climate B2a scenario

The overall change in precipitation monthly and seasonally), increase in temperature and increase in evapotranspiration results in reduction in inflow in the sub basin. And the evapotranspiration may increase from SWAT output result shown in fig 4.25

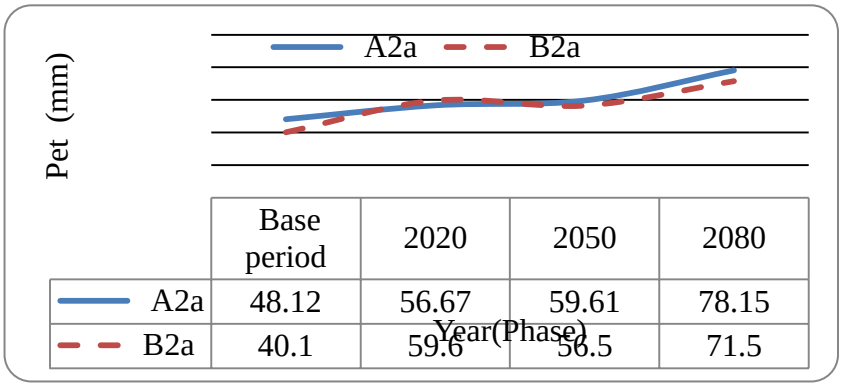

	Base period	2020	2050	2080
A2a	48.12	56.67	59.61	78.15
B2a	40.1	59.6	56.5	71.5

Figure

4.25 Trends of annual potentials Evapotranspiration at Modjo sub basin compared with observed A2a and B2a scenario

5 Conclusions and Recommendations

5.1 Conclusions

Nature and especially climate is not easy to be exactly forecasted even with the advanced technologies of the21st century. Human beings are still including the climate variables, where extreme events of floods and droughts keep on claiming many lives all over the world. Hence, attempts should continue to at least accommodate, if not prevent, ourselves from the enormous danger in the future. Studies like this, which focus on likely future climate change scenarios and their impact on sectors like water are essential. As understanding the problem is part of the solution, grasping the level of impact is a prerequisite to propose adaptation measures that can reduce the damage. Hence, the impact of climate change on Modjo watershed water availability was carried out to address part of the global problem. Therefore, according to the forecast, the average annual maximum temperature may be increased in the future by 1.03 °C /decade mean and 1°C/decade mean for A2a and B2a scenarios in 2020s, 2050s and 2080s, respectively. The mean annual minimum temperature will also be increased by 0..44 °C and 0.44°C in 2020s, and by 0.55°C and 0.54 °C for cases of A2a and B2a scenarios in 2050s respectively. In 2080s it will also increase by 0.55°C and 0.5for A2a and B2a scenarios respectively The precipitation projection exhibited a decrease in annual mean precipitation in the 2020s, the 2050s and 2080s. As can be seen in 2020s there may be a decrease in precipitation for both scenarios (A2a and B2a). In 2020s, the A2a scenario showed an annual mean precipitation decrease up to 6.8 % and B2a showed a decrease up to 2.4%. In 2050s the annually mean precipitation decrease may reach up to 10.77% in A2a scenario and 6.3 % for the B2a scenario. In the 2080s, precipitation decrease may reach up to3.64 % in A2a scenario and 3.16 % for the B2a scenario. Result of hydrological model calibration and validation indicated that the SWAT model simulates the stream flow considerably well for the study area. The model performance for calibration and validation process and resulted in R^2=0.71during calibration, R^2=0.51 during validation. Climate change impact on flow volume of Modjo sub basin was analyzed on a monthly, seasonal basis. The composed changes of increasing and decreasing in precipitation, (all scenario periods annually decrease), increasing in temperature and increase in evapotranspiration result in reduction in inflow of the river. For both A2a and B2a emissions scenarios it is expected to be an average annual reduction in flow volume for the next 90 years. The change ranges from for A2a -8.51%-to -47.73% and from -30.33% to-81.52% for B2a scenarios

5.2 Recommendation

- This study was done in a limited time and resource. Hence the results of this study should be taken as a starting point for further studies and the study is based on single GCMs and two emission scenarios. Downscaled scenarios using other GCM models running the same experiment may likely produce slightly different, but equally plausible results .-Hence, it is often recommended to apply different GCMs and emission scenarios so as to make comparison between different models as well as to explore a wide range of climate change scenarios that would result in different hydrological impacts. Hence this work should be extended in the future by including different GCMs and emission scenarios.
- In this study, downscaling of the large scale variables was done at four meteorological stations and it was assumed that this change will be applicable to other similar which has similar altitude and temperature stations as well. However, it is recommendable if climate change assessment will be done downscaling large scale variables at each station found in the study area if data is available.
- The model simulations considered only future climate change scenarios assuming all other things constant. But change in land use scenarios, soil, management activities and other climate variables will also contribute to surface runoff therefore it is better if one may consider these changes for future climate change predictions.

6. References

Abadi and Kassa Journal of Environment and Earth Science www.iiste.orgISSN 2224-3216 (Paper)

Abbaspour, K.C. (2012) SWAT-CUP-2012.SWAT Calibration and Uncertainty program A User Manual. Swiss Federal Institute of Aquatic Science and Technology, Dübendorf

Abbaspour, K.C., Yang, J., Maximov, I., Siber, R., Bogner, K., Mieleitner, J., Zobrist, J. and Srinivasan, R. (2007) Modeling Hydrology and Water Quality in the Pre-Alpine/Alpine ThurWatershedUsingSWAT.*JournalofHydrology*,**333**, 413430 .http://dx.doi.org/10.1016/j.jhydrol.2006.09.014

Abbaspour, K.C., Johnson, C.A. and van Genuchten, M.T. (2004) Estimating Uncertain Flow and Transport Parameters Using a Sequential Uncertainty Fitting Procedure. *Vadose Zone Journal*,**3**,13401352./10.2174/1874378100802010049http://dx.doi.org/10.2136/vzj2004.1340

Abdela.M Kemal Mohammed (2013) The Effect of Climate Change on Water Resources Potential of Omo Gibe Basin, Ethiopia, Dissertation (Dr.-Ing) Munchen University, Germany

Arc SWAT user web site: http:// www.brc.tamus.edu/swat/arcswat.html

Arnold, J.G. Allen, P.M, and Bernhardt, G.1993.*A comprehensive surface-groundwater flow model*, Journal of Hydrology 142: 47-69pp

Arnold, J.G., Allen, P.M. Muttiah, R. and Bernhardt, G., 1995. *Automated base flow separation and recession analysis techniques.* Ground Water vol 33(6): 1010-1018pp .

Baeda,A.P .M.Ahlonsou, E., Ding, Y.,and Schim el, D., 2001. *The Climate System, an Overview.* In: Climate Change 2001: The Scientific Basis. Contribution of Working Group I to the Third Assessment Report of the Intergovernmental Panel on Climate Change, [(eds.), Houghton, J.T., Ding, Y., Griggs, D.J., Noguer, M., van der Linden, P.J., Dai, X., Maskell, K., and Johnson, C.A.], Cambridge University Press, Cambridge, United Kingdom and New York, NY, USA, 881pp.

Bergkamp, G., Orlando, B., and Burton, I. (2003) Change: *Adaptation of Water Management to Climate Change*. International Union for Conservation of Nature and Natural Resources,Gland& Cambridge.

Beyene T, Lettenmaier DP, Kabat P, (2010) Hydrological impacts of climate change on the Nile River Basin: Implications of the (2007) IPC scenarios. Climate Chang 100: 433–461.

doi:10.1007/s10584-009-9693-0.

Busuioc, A., Chen, D., and Hellstrom, C. 2001 *Performance of Statistical downscaling Models in GCM validation and regional climate change estimates:* application for Swedish Precipitation International Journal of Climatology.

Carter, T.R., (2007).General *Guideline on the use of scenario data for Climate Impact and Adaptation Assessment* Finnish Environmental Institute, Helsinki, Finland.

Crane RG, Hewitson BC (1998) Doubled CO2 precipitation changes for the Susquehanna basin: down-scaling from the genesis general circulation model. Int J Climatol 18:65–76

Cubasch, U., Meehl, G.A., Boer, G.J., Stoufer, R.J., Dix, M., Noda, A., Senior, C.A., Raper, S., and Yap, K.S., (2001). *Projections of future climate change.* Climate Change 2001: The Scientific Basis. Contribution of Working Group I to the Third Assessment Report of the Intergovernmental Panel on Climate Change, [(Eds.), Houghton, J. T., Ding, Y., Griggs, D. J. Noguer, M., van der Linden, P.J., Dai, X., Maskell, K., and Johnson, C. A.], Cambridge University Press, 525-582.

CCIS (2008) Frequently asked questions. SDSM background. http://www.cics.uvic.ca/scenarios/index.cgi?More_Info-SDSM_Background. Accessed 21 Dec 2014

Conway D, Hulme M (1996) The impacts of climate variability an future climate change in the Nile basin on water resources i J Water ResourDev12:261280.doi:10.1080/07900629650169.

Cunderlik, M. J. 2003: Hydrologic model selection fort the CFCAS project: *Assessment of Water Resources Risk and Vulnerability to Changing Climatic Conditions*, Project Report I University of Western Ontario, Canada.

Deressa.TT, Hassan RM, Ringler C, Alemu T, Yesuf M (200) Determinants of farmers' choice o adaptation methods to climate change in the Nile Basin of Ethiopia. Glob Environ Chang 19: 248–255.doi:10.1016/j.gloenvcha.2009.01.002

Dibike, Y. B. and Coulibaly, P., (2005): *Hydrologic impact of climate change in the Saguenay Watershed, comparison of downscaling methods and hydrologic models*, J. Hydro., 307(1–4)

Dile YT, Berndtsson R, Setegn SG (2013) Hydrological Response to Climate Change for Gilgel Abay River,in the Lake Tana Basin Upper Blue Nile Basin of Ethiopia.

PLoSONE8 (10):e79296.doi:10.1371/journal.pone.0079296

Dilnesaw. A.C, 2006 Modeling of Hydrology and Soil Erosion of Upper Awash River Basin PhD Thesis, University of Bonn: 233pp

Dixon, RK, Smith J, Guill S (2003) Life on the edge vulnerability and adaptation of African ecosystems to global climate change. Mitig Adapt Strateg Glob Chang 8:93–113, 2003

Teso. E, Tena Alamirew and Megersa Olumana Predicting Runoff Yield using SWAT Model and Evaluation of BoruDodota Spate Irrigation Scheme, Arsi Zone, Southeastern Ethiopia,(2014)

First, 2001: Initial National Communication of Ethiopia to the United Nations *Framework Conviction on Climate Change (UNFCCC).Report* of the Federal Democratic Republic of Ethiopia, Ministry of Water Resources, National Metrological Services Agency.

Fischer G, Shah M, Tubiello FN, van Velhuizen H (2005) Socio economic and climate change impacts on agriculture: an integrated assessment, 1990-2080. Philos Trans R Soc Lond B Biol Sci 360:2067–2083. doi:10.1098/rstb.2005.1744. PubMed: 16433094.

Ethiopian Economic Association (EEA).(2008).Climate Change and Development Adaptation Measures. Economic Focus, 11(1) Addis Ababa, Ethiopia.

Gates WL, Boyle JS, Covey C, Dease CG, Doutriaux CM, Drach RS, Florino M, Gleckler P, Hnilo JJ, Marlais SM, Phillips TJ, Potter GL, Santer BD, Sperber KS, Taylor KE, Williams DN (1999) *An overview of the results of the Atmospheric Model Inter comparison Project (AMIP I).*

Gibson CC, Ostrom E, Ahn T (2000) The concept of scale and the human dimensions of global change: a survey. Ecol Econ 32: 217–239.doi:10.1016/S0921-8009(99)00092-0.

Giorgi F, Mearns LO (1991) Approaches to the simulation of regional climate change: a review .Rev Geophys 29:191–216

Gleick P (1991) The vulnerability of runoff in the Nile basin to climatic changes Environ Prof 13: 66–73

Green .W. H and Ampt ,G. A., 1911. *Studies on soil physics: 1. the flow of air and water through soils*. J. Agric. Sci. 4: 11-24.

Haan, C.T., Johnson, H.P., Brakensiek, D.L. 1982*Hydrologic modeling of small watersheds* ASAE 533 p.

Hailemariam, Kinfe, 1999. *Impact of Climate Change on the Water Resources of Awash River Basin, Ethiopia*, Climate Research, International and Multidisciplinary Journal, Vol. 12

Haileyesus Belay. 2011. Evaluation of Climate Change impacts on hydrology on selected catchments of Abbay Basin, Master thesis, Addis Ababa University

Hargreaves, G.LHargreaves, G.H., and Riley, J.P., (1985). *Agricultural benefits for Senegal River basin. J i*rrig. And Drain. Engr; 111(2): 113-124.

Hayashi A, Akimoto K, Tomoda T, Kii M (2012) Global evaluation of the effects of agriculture and water management adaptations on the water-stressed population. Mitig Adapt Strateg Glob Chang 18:591–618

Henok, S, (2013). Impact of Climate Change on Hydrological Response: A Case Study on Agula Catchment, Eastern Zone, Tigray

Hewitson BC, Crane RG (1996) Climate downscaling: techniques and application. Clim Res 7:85–95

Hooghoudt. S.B.1940 Bijdrage tot de kennis van enige natuurkundige gootheden van de grond.Versl.Landbouwkd.Onderz.46:515-707.

http://cerawww.dkrz.de/IPCC_DDC/IS92a/HadleyCM3/Readme.hadcm3)

IP CC (Inter governmental Panel on Climate Change). 2001. The *Data Distribution Center*, DDC,

http://ipcc-ddc.cru.uea.ac.uk/ [Accessed 15 May 2009]

IPCC AR4 Inter governmental Panel on Climate Change Fourth Assessment Report, (2007).

IPCC: *Climate change 2007*: synthesis report (htt://www.ipcc.ch/pdf). [Accessed 20 June 2008]

IPCC (Inter governmental Panel on Climate Change).1996.*ClimateChange1995*.The Science of Climate Change. Contribution of Working Group I to the Second Assessment Report of the Inter governmental Panel on Climate Change, [(Eds.) Houghton, J.T., Ding, Y., Griggs, D.J., Noguer, M., van der Linden, P.J., Dai, X., Maskell, K., and Johnson, C.A.] , Cambridge University Press, Cambridge and New York, 572 pp.

IPCC-TGICA, 2007: *General Guidelines on the Use of Scenario Data for Climate Impact and Adaptation Assessment*, Version 2, Prepared by T.R. Carter on behalf of the Inter governmental Panel on Climate Change Task Group on Data and Scenario Support for Impact and Climate Assessment, pp66

IPCC (2012) IPCC special report on managing the risks of extreme events and disasters to advance climate change adaptation. http://ipcc-wg2gov/SREX/

Jenkins GS, Barron EJ (1997) Global climate model and coupled regional climate model Simulations over the eastern United States: GENESIS and RegCM2 simulations. Global Planet Change 15:3–32

Kim U, J.J Kaluarachchi, & V.U Smakhtin, 2008: *Climate Change Impacts on Hydrology and Water Resources* of the Upper Blue Nile Basin, Ethiopia, IWMI RR 126

Knox J, Hess T, Daccache A, Wheeler T (2012) Climate change impacts on crop productivity in Africa and South Asia. Environ Res Lett 7:034032

Koch, F, Griensven, A, Uhlen brook, S, Tekleab, S, Teferi, E, (20120) The Effects of Land use Change on Hydrological Responses in the Choke Mountain Range (Ethiopia) - A new Approach Addressing Land Use Dynamics in the Model SWAT

Lahmer W.B, Pfutzner and A. Becker, 2001: *Assessment of land use and climate change impacts on The Meso scale*, Phys chem. Earth 26(7-8) pp. 565-57.

Lenhart,T., Eckhardt, K.,Fohrer, N., Frede, H.G., 2002.*Comparison of two different approaches of sensitivity analysis.* Physics and Chemistry of the Earth 27 (2002), Elsevier Science Ltd., 645– 654pp.

MearnsL.O. M. Hulme, T.R. Carter, R. Leemans, M. Lal, and P. Whetton, (2001).Climate Scenario Development. In: Climate Change 2001: The Scientific Basis. Contribution of Working Group I to the Third Assessment Report of the Intergovernmental Panel on Climate Change [Houghton, J.T., Y. Ding, D.J. Griggs. Noguer, P.J. van der Linden, X. Dai, K. Maskell, and C.A. Johnson (eds.)].Cambridge University Press, Cambridge, United Kingdom and New York, NY USA,881pp.

Ministry of Agriculture (2005) participatory integrated watershed planning and implementation Manual

Monteith (1965) Evaporation and the environment. In: XIXth symposium of the Society of Experimental Biologists Swansea on the state and movement of water in living organisms. Cambridge University Press, Cambridge

Moriasi, D.N., Arnold, J.G., van Liew, M.W., Bingner, R.L., Harmel, R.D. and Veith, T.L. (2007) Model Evaluation Guidelines for Systematic Quantification of Accuracy in watershed Simulations. *Transactions of the ASABE*,**50**,885900.http://dx.doi.org/10.13031/3

Murphy J (1999) An evaluation of statistical and dynamical techniques for downscaling local

climate. J Clim 12:2256–2284

Nakicenovic N, Alcamo J, Davis G, De Vries B, Fenhann J, Gaffin S, Gregory K, Grubler A, Jung TY, Kram T (2000) Special report on emissions scenarios: a special report of working group III of the Intergovernmental Panel on Climate Change. Pacific Northwest National Laboratory, Richland, WA (US), Environmental Molecular Sciences Laboratory (US)

Neitsch S.L.ArnoldJ.G.Kiniry, J.R., Srinivasan, R., and Williams, J. R., 2002. Soil *and Water Assessment Tool (SWAT) User's* Manual, Version 2000, Grassland Soil and Water Research Laboratory, Black land Research Center, Texas Agricultural Experiment Station, Texas Water Resources Institute, Texas Water Resources Institute, College Station, Texas, 472pp

Neitsch S.L., J.G. Arnold, J.R. Kiniry, J.R. Williams, 2005: *Soil and Water Assessment Tool (SWAT) Theoretical Documentation*, Version 2005, Grassland Soil and Water Research Laboratory, Agricultural Research Service, Black land Research Center, Texas Agricultural Experiment Station

Palmer, R. N., Clancy, E., Rheenen, N. T. Van, and Wiley, M. W., (2004) The Impacts of Climate Change on the Tualatin River Basin Water Supply: An Investigation into Projected Hydrologic and Management Impacts, Report. Department of Civil and Environmental Engineering, University of Washington

Priestley, C. H. B., R. J. Taylor (1972). On the assessment of surface heat flux and evaporation using large-scale parameters, Mon.*Weather.Rev.100, 81-92.*

Rockstrom J, Falkenmark M, Karlberg L, Hoff H, Rost S, Gerten D (2009) Future water availability for global food production: the potential of green water for increasing resilience to global change WateResourceRes5:W00A12.doi:10.1029/2007WR006767

Rockstrom JM, Lannerstad M, Falkenmarkt M (2007) Assessing the water challenge of a new green revolution in developing countries. PNAS 104(15):6253–6260

Sangrey.D.A..K.O.Harrop-Williams,and J.A.Klaiber.1984.Predicting ground water response to precipitation. ASCE J.Geotech.Eng.110 (7):957-975.

Santhi, C. Arnold, J.G., Williams, J.R., Dugas, W.A., Srinivasan, R., and Hauck, L.M., 2001. *Validation of the SWAT Model on a Large River Basin with Point and Non point Sources,*

Journal of the American Water Resources Association, Vol. 37,No. 5, 1169-1188pp.

Smedema. L K.O and D.W Rycrft. 1983. Land drainage- Planning and design of agricultural drainage systems. Cornell University Press Ithica.N.Y.

Setegn, S.G., Srinivasan, R. and Dargahi, B. (2008) Hydrological Modeling in the Lake Tana Basin, Ethiopia Using SWAT Model. *The Open Hydrology Journal*, **2**, 49-62. http://dx.doi.org

SWAT user web site; http://www.brc.tamus.edu/swat/soft_baseflow.html

Taylor & Francis Web site a http://www.taylorandfrancis.com

TheHadCM3predictorvariablesfortheA2aandB2aexperiments,availableat:http://www.cccsn.ca/Download Data/HadCM3_Predictors-e.html [accessed on 10 Dec., 2010]

ThorpeA.J.,2005 ClimateChangePrediction:AchallengingscientificproblemInstituteofPhysics,[online]4Apr.,availableathttp://www.iop.org/activity/policy/Publications/file_4147.pdf [accessed 4 April 2009]

UNEP (2005) Handbook on Methods for Climate Change Impact Assessment and Adaptation Strategies.

Venetis, C.1969.Astudyoftherecessionofunconfinedaquifers.Bill.Int.Assoc.Sci.HVDROL.14(4):119-125

Von Storch H, Zorita E, Cubasch U (1993) Downscaling of global climate change estimates in to regional scales: an application to Iberian rainfall in wintertime. J Clim 6(1161):1171

Wilbanks TJ, Kates RW (1999) Global change in local places: how scale matters. Clim Chang 43: 601–628. doi:10.1023/A:1005418924748

Wilby.R.L.Conway.D.andJones.P.D.2002.ProspectsfordownscalingSeasonalprecipitation Variability using conditioned weather generator parameters. Hydrological process. 16.1215- 1234

Wilby R. L, and Dawson, C.W. August 2004.Using SDSM Version 3.1.*A decision support on The assessment of regional climate changeimpacts*.UserManual:67pp

Wang, Y., Leung, L. R., McGregor, J. L., Lee, D. K., Wang, W. C., Ding, Y., and Kimura, F. (.2004)"Regional climate modeling: progress, challenges, and prospects." Journal of the

Meteorological Society of Japan, 82, 1599–1628.

Wilby R .L and, Dawson C .W 2007 Using SDSM version 4.1 SDSM 4.2; A decision support tool for the assessment of regional climate change impacts. User Leics. LE11 3TU, UK.

Wilby, R., Charles, S., Zorita, E., Timbl, B., Whetton, P., and Means, L. (2004) *Guidelines for use of Climate Scenarios Developed from Statistical Downscaling Methods*.

Wilby, R. L., and Wigley, T. M. L. 1999 *Precipitation Predictors for Downscaling: Observed and General Circulation Model Relationships*. International Journal of Climatology

World Bank (2006) Managing Water Resources to Maximize Sustainable Growth A Country Water Resources Assistance Strategy for Ethiopia. World Bank report no 36000-E Washington USA 91pp

World Bank (2010) World Development report 2010: Development and climate change The International Bank for Reconstruction and Development / The World Bank Washington US 399pp/

World Bank, 2012a, *Linking Gender, Environment, and Poverty for Sustainable Development: A Synthesis Report on Ethiopia and Ghana*

Xu, C.Y., (2000): *Modeling the effect of climate change on water resources in central Sweden, Water resources Management*. 14(3) pp. 177-189

Zeray L., 2006. A Climate Change Impact on Lake Ziway Watershed water availability Ethiopia, MSc Thesis, Cologne, Germany

APPENDIX A List of Tables

Table A.1 Summery of Future Temperature minimum scenario generation

Temperature Minimum													
	Jan	Feb	Mar	Apr	may	June	July	Aug	Sep	Oct	Nov	Dec	Mean
H3A2a 2020	0.32	-0.55	-0.95	-0.91	0.28	-0.84	-0.86	-0.83	0.60	1.71	1.76	2.72	0.45
H3B2a 2020	0.39	-0.37	-0.84	-0.75	0.45	-0.69	-0.84	-0.86	0.40	1.47	1.47	2.53	0.44
H3A2a 2050	4.16	2.65	0.92	-0.56	-1.44	-4.19	-4.73	-3.89	-0.98	2.09	3.87	6.11	0.55
H3B2a 2050	4.21	2.57	0.88	-0.81	-1.68	-4.28	-4.79	-3.78	-0.94	2.20	4.00	6.28	0.54
H3A2a 2080	0.16	-1.47	-2.21	-1.87	-0.49	-1.63	-1.18	-0.28	1.81	3.58	3.68	3.62	0.55
H3B2a 2080	0.03	-1.46	-2.17	-1.89	-0.60	-1.60	-1.08	-0.24	1.71	3.53	3.36	3.51	0.50

Table A.2 Summery of Future Perception scenario generation

precipitation													
	Jan	Feb	Mar	Apr	may	June	July	Aug	Sep	Oct	Nov	Dec	Mean
H3A2a 2020	0.74	0.88	0.94	1.38	2.39	3.69	4.14	4.01	3.65	2.58	1.42	0.73	2.21
H3B2a 2020	0.80	1.01	1.19	1.48	2.59	4.04	4.50	4.57	4.11	3.15	1.64	0.82	2.49
H3A2a 2050	3.21	3.30	3.09	2.96	2.42	1.67	1.27	1.71	1.84	1.56	1.77	2.60	2.28
H3B2a 2050	4.25	4.25	4.13	3.67	2.50	1.15	0.64	0.86	1.07	1.18	1.78	3.38	2.40
H3A2a 2080	0.68	0.50	0.91	1.48	1.49	2.01	3.33	4.54	4.73	4.50	3.51	1.75	2.45
H3B2a 2080	0.81	0.62	0.79	1.03	1.08	1.79	4.07	5.40	4.89	4.23	3.14	1.76	2.47

Table A.3 Summery of Future Temperature minimum scenario generation

Temperature Minimum													
	Jan	Feb	Mar	Apr	may	June	July	Aug	Sep	Oct	Nov	Dec	Mean
H3A2a 2020	-0.32	-0.55	-0.95	-0.91	0.28	-0.84	-0.86	-0.83	0.60	1.71	1.76	2.72	0.45
H3B2a 2020	-0.39	-0.37	-0.84	-0.75	0.45	-0.69	-0.84	-0.86	0.40	1.47	1.47	2.53	0.44
H3A2a 2050	-4.16	-2.65	-0.92	-0.56	-1.44	-4.19	-4.73	-3.89	-0.98	2.09	3.87	6.11	0.55
H3B2a 2050	-4.21	-2.57	-0.88	-0.81	-1.68	-4.28	-4.79	-3.78	-0.94	2.20	4.00	6.28	0.54
H3A2a 2080	-0.16	-1.47	-2.21	-1.87	-0.49	-1.63	-1.18	-0.28	1.81	3.58	3.68	3.62	0.55
H3B2a 2080	-0.03	-1.46	-2.17	-1.89	-0.60	-1.60	-1.08	-0.24	1.71	3.53	3.36	3.51	0.50

Table A.4 Summery of Future Perception scenario generation

precipitation													
	Jan	Feb	Mar	Apr	may	June	July	Aug	Sep	Oct	Nov	Dec	Mean
H3A2a 2020	0.74	0.88	0.94	1.38	2.39	3.69	4.14	4.01	3.65	2.58	1.42	0.73	2.21
H3B2a 2020	0.80	1.01	1.19	1.48	2.59	4.04	4.50	4.57	4.11	3.15	1.64	0.82	2.49
H3A2a 2050	3.21	3.30	3.09	2.96	2.42	1.67	1.27	1.71	1.84	1.56	1.77	2.60	2.28
H3B2a 2050	4.25	4.25	4.13	3.67	2.50	1.15	0.64	0.86	1.07	1.18	1.78	3.38	2.40
H3A2a 2080	0.68	0.50	0.91	1.48	1.49	2.01	3.33	4.54	4.73	4.50	3.51	1.75	2.45
H3B2a 2080	0.81	0.62	0.79	1.03	1.08	1.79	4.07	5.40	4.89	4.23	3.14	1.76	2.47

Table A.5 Summery of Future Temperature maximum scenario generation

Temperature Maximum													
	Jan	Feb	Mar	Apr	may	June	July	Aug	Sep	Oct	Nov	Dec	Mean
H3A2a 2020	-0.20	-0.58	-0.89	-0.56	-0.45	-1.20	0.46	0.17	-0.76	-0.50	0.03	4.70	0.06
H3B2a 2020	-0.37	-0.52	-0.83	-0.08	0.21	-0.23	2.00	1.67	0.07	-0.29	0.15	4.99	0.64
H3A2a 2050	-3.28	-1.37	-0.21	-1.09	-1.69	-2.43	-0.37	0.01	0.09	1.71	3.30	8.30	1.03
H3B2a 2050	-2.58	-0.65	-0.84	-1.55	-2.04	-2.22	0.81	1.42	1.02	1.85	3.08	7.85	1.06
H3A2a 2080	-0.94	-0.34	-0.89	-0.20	0.72	1.57	4.69	4.49	2.95	2.13	1.78	5.97	2.01
H3B2a 2080	-0.48	-0.69	-1.35	-0.59	0.27	1.04	4.17	3.91	2.28	1.52	1.18	5.49	1.50

Table A.6 Rainfall, Minimum & Maximum Temperature

	Jan	Feb	Mar	Apr	may	June	July	Aug	Sep	Oct	Nov	Dec	mean
Rainfall (mm	17.7	34.4	56.4	64.2	58.3	98.9	228.8	231.3	111.9	30.1	8.1	7.4	78.9
Temperature max(°C	25.71	27.05	27.99	27.96	27.99	28.14	25.32	25.14	26.10	26.03	25.53	20.83	26.15
Temperature min(°C)	8	10	11	12	11	13	13	13	11	8	7	3	10

Appendices B; List of Figures

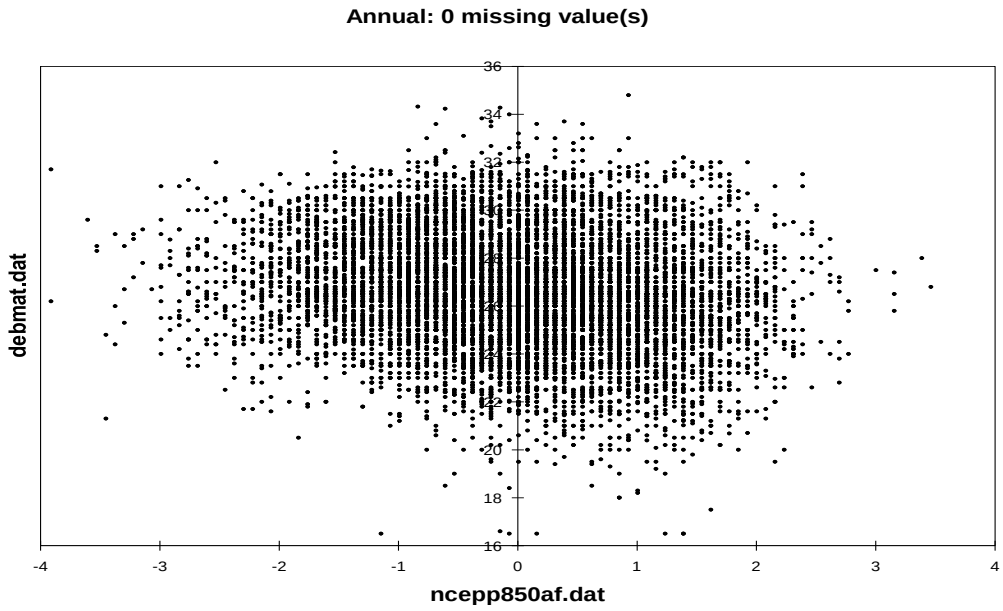

Ncepp850afPredictor variable selection by using scatter plot (Debrezeyit maximum temperature)

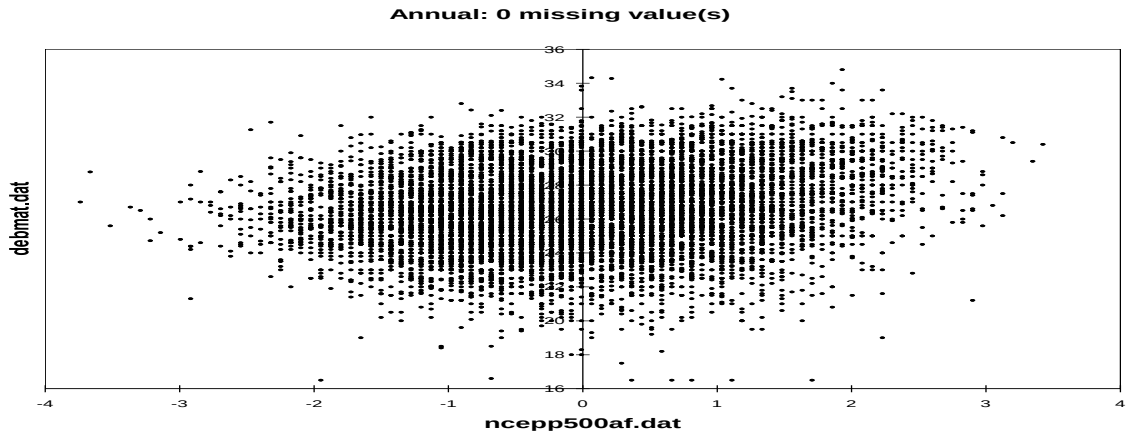

Ncepp500afPredictor variable selection by using scatter plot (Debrezeyit maximum temperature)

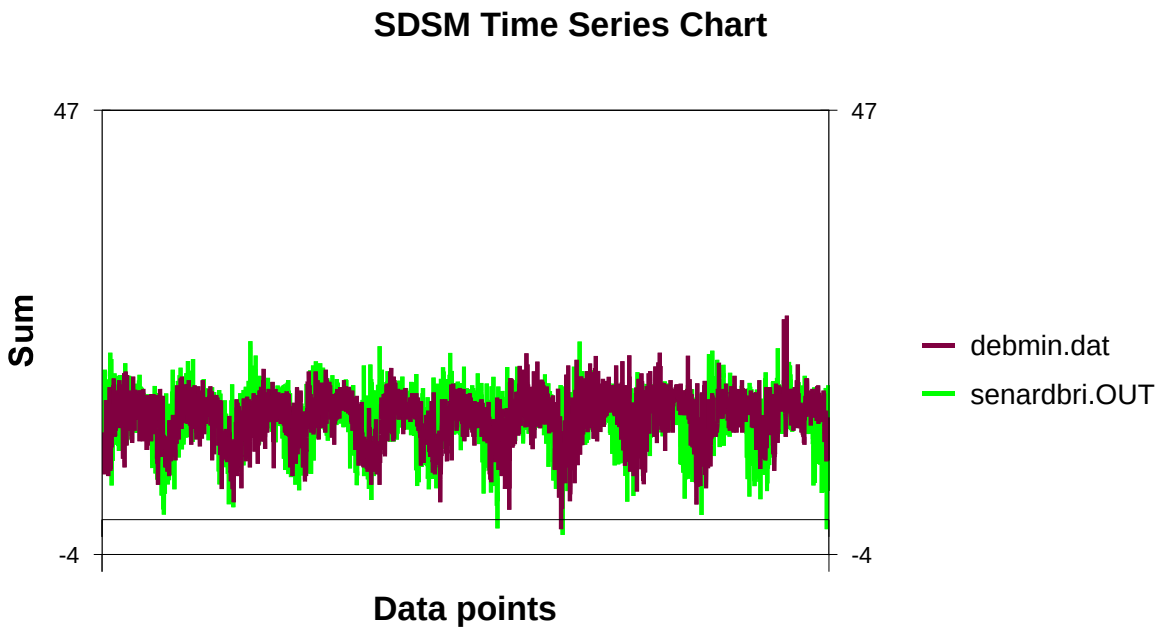

Time series chart for Debrezeyit minimum temperature